Topological Order in Spin Liquids with Chirality

Zur Erlangung des akademischen Grades eines
DOKTORS DER NATURWISSENSCHAFTEN
von der Fakultät für Physik des
Karlsruher Instituts für Technologie

genehmigte

DISSERTATION

von

Dipl.-Phys. Burkhard Scharfenberger

aus Neustadt a.d. Weinstraße

Referent: Prof. Dr. Peter Wölfle, TKM

Korreferent: Prof. Dr. Alexander Shnirman, TKM

Datum der Prüfung: 14. Juli 2011

Acknowledgments

A little learning is a dangerous thing,
drink deep or taste not of the Peirean spring.

– Alexander Pope

Let me in these first lines express my gratitude to all who supported me in my effort to attain a physics doctorate.

First, I want to thank Prof. Peter Wölfle. On the one hand, for giving me the opportunity to pursue a PhD in physics at the TKM but moreover, for always being forthcoming with his help, even on short notice.

A great debt of gratitude I owe to Martin Greiter. The three years of collaboration brought many profound and enligntening conversations about physics, the world and everything else. This time has made him a friend to me as much as a supervisor.

A big 'thank you!' goes also to Ronny Thomale, without whose active support and seemingly limitless knowledge where of utmost importance to me.

I am furthermore grateful to Prof. Alexander Shnirman for agreeing to co-referee my thesis and for enabling me to stay at the TKM a little while longer.

All the rest of the institute is deserving of my gratitude as well, such a lively, active and stimulating atmosphere is truly something special.

At last, the place of honour I reserve for my parents, for they made it all possible and I shall not forget it.

Contents

1 Introduction

The concept of topological order, where a phase of matter is characterised by a set of global topological invariants instead of local order parameters, has become an intensely studied field in contemporary condensed matter physics. It was first discovered in the $S = 1/2$ chiral spin liquid (CSL) [1], which was motivated by the liquid states proposed to explain the fractional quantum Hall (FQH) effect [2–4].

In this thesis, we study the properities of the CSL and a number of other states and systems which potentially possess topological order.

First, we rewrite the CSL wavefunction in terms of Schwinger boson operators to set up a hierarchy of spin liquid states for spin S, and numerically determine the topological degeneracy for all hierarchy elements with $S \leq 2$. For a spin S liquid state obtained from merging S spin 1/2 CSLs of each chirality we find values of $(S + 1)^2$ for the topological degeneracy. This provides strong evidence that these types of liquids support non-Abelian statistics for $S \geq 2$ while at the same time preserving P and T symmetry. This makes them interesting as trial states for frustrated spin S antiferromagnets, since both share the same symmetries.

A recently introduced extension of entanglement entropy [5, 6] as a tool to probe for hidden topological order is based on entanglement spectra (ES) [7]. In a second line of work, we compute the entanglement spectra of the CSL and another member of the spin liquid hierarchy, the $S = 1$ chirality liquid obtained by merging two CSLs of opposite chirality, as well as those of the groundstates of a frustrated J_1-J_2 antiferromagnetic Heisenberg model for both these spins. In the $S = 1/2$ case we monitor the ES as we change boundary conditions from periodic to cylindrical. As we compare the results of the J_1-J_2 model to the spectrum of the CSL, we find preliminary hints of a topological phase transition in the J_1-J_2 spectrum, which appears to be corroborated by the behaviour of a small chiral perturbation which we add to the Heisenberg hamiltonian. However, it would have to be checked whether the observed effects persist as system size is increased. In case of $S = 1$, where we use cylindrical boundary conditions throughout, the entanglement spectra, although they do show some similar features and there is still a decent overlap, differ in their main characteristic: quantum numbers and weight of the lowest level. However, most likely effects of the small system size of only 4×4 sites, which is limited by fast Hilbert space growth and the reduced symmetry of the cylindrical boundary conditions, are significant. This makes it difficult to draw conclusions for larger systems.

The last part of this thesis is devoted to a tangential idea related to the numerical method of exact diagonalisation. Recently, a method was described [8] which allows the spinon-excitation content of an eigenstate of the Haldane-Shastry model to be read directly off the Young tableaux representing the total spin of the state. Since total momentum is conserved in the HSM, this method can also be used to solve the mathematical problem of finding the eigenvalues of the cyclic permutation on subspaces of the same symmetry contained in product

spaces of fundamental SU(n) representations. We generalize this method to arbitrary higher symmetric representations of SU(n) and show how it can significantly speed up computation of momentum eigenvalues of total SU(n)-spin states.

One of the central goals of condensed matter physics is to find, describe and explain the various phases of matter and transitions between these phases as parameters like temperature, pressure, magnetic or electric field or also couplings between particles are varied. A central pillar of our understanding of phase transitions at finite temperatures is the description in terms of a local order parameter usually connected to a symmetry a system possesses in one phase, but which is broken in the other. This describes such diverse phenomena as transition between a liquid and a (crystaline) solid as well as between different crystal phases, between para- and (anti-)ferromagnet (which can be regarded as (finite temperature) spin liquid and crystal respectively) and Bose-Einstein-condensation-type transitions, *e.g.* the superfluid transition in helium or the normal metal-superconductor transition. Not connected with symmetry breaking but nevertheless described by an order parameter are the gas-liquid-amorphous solid transtions or transitions into mesophases like *e.g.* liquid-crystals. At finite temperatures, phase transitions are driven by temperature fluctuations, but they are possible even at $T = 0$, where it is quantum fluctuations which can drive a system across a quantum critical point as the ground state of its Hamiltonian changes abruptly upon variation of some non-temperature system parameter. These transitions are usually still described with the help of an order paramter, as is the one between superconductor-insulator where the order parameter is cooper-pair density and phase. It was only after the discovery of the fractional Quantum Hall effect (FQHE) in 1982 by Tsui, Störmer and Gossard [2], that this picture of phase-transition $\leftrightarrow$ order parameter had to be complemented by something new. The integer Quantum Hall effect, a quantisation of the off-diagonal conductivity in integer multiples of the conduction quantum e^2/h in strong magnetic fields at low temperatures (first observed by v.Klitzing in 1980 [9]), could be understood in terms of non-interacting electrons occupying orbitals characterized by Landau-level (*i.e.*, energy) and canonical angular momentum quantum numbers. These Landau-levels are highly degenerate: the number of angular momentum states in each is given by the number of Dirac flux quanta $N_\Phi = \Phi/\Phi_0$ permeating the sample. Taking disorder into account, one finds that all but one of these states, which are extended in the clean case, become localized and the observed jumps in conductivity now coincide with the (de)population of the one remaining extended level (each state) at the center of each Landau subband. It soon became clear, however, that a single particle picture is insufficient to explain the appearance of conductivity-plateaus at fractional values of ν, the most prominent ones of which occur at filling fractions $\nu = q/(2p+1)$, with q, p positive integers.

In 1983 Laughlin [3] proposed a very successful class of trial quantum Hall liquid states for filling factors $\nu = 1/m$, with m an odd integer, where close approach of particles is suppressed with power m. Numerical studies including Coulomb interaction between electrons [10] showed an excellent agreement with the exact ground state, but the most convincing aspect of these states was the interpretation of the plateaus in terms of quasi-electron and -hole excitations, which are connected to threading negative or positive flux quanta respectively through the sample. The charge of these quasiparticles is $\pm e/m$ and their (Abelian) statistical phase upon interchange is $\theta = \pm\pi/m$. This can be understood by help of Wilczek's [11, 12] charge-flux-

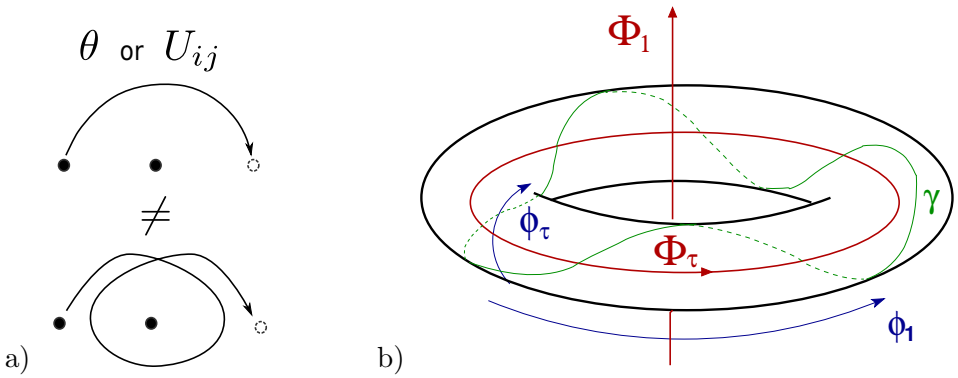

Figure 1.1: Topologically ordered states exhibit exotic quasi-particle statistics, like Abelian (anyonic) or even non-Abelian a) upon local interchange or b) upon winding around non-trivial loops on manifolds of higher genus (¿0)

composite picture and corresponds to the Berry's phase of the many-body wavefunction upon interchange through winding of two excitations. While (direct) observation of the statistics still defies expermentalists' efforts (although schemes have been proposed employing Fabry-Perot-interferrometers to measure the Aharonov-Bohm-phase of a current around quantum dots with a fixed number of quasi-particles [13]), the fractional charge has indeed been observed, first in 1995 in resonant tunneling through a quantum anit-dot [14] which were corroborrated by recent experiments measuring shot noise across quantum point contacts [15].

In 1985 Haldane and Rezayi [16] noticed that demanding periodic boundary conditions for the Laughlin $1/m$ FQH liquids gives an m-dimensional manifold of solutions.

At around the same time, the transverse currents in a quantum Hall sample had been recognized as gapless chiral edge channels where the magnetic fields separates left- and right movers and thus enables dissipationless transport [17, 18].

These two major ideas inspired Wen's [1, 19] paradigm-changing interpretation of fractional quantum Hall liquids as an example of *topological order* (TO): a topologically ordered phase is not characterized by a local order parameter but by topologocical invariants like ground state degeneracy and number of edge-excitations, which cannot change continuously as parameters are varied but rather only through a quantum phase transition. The field took another step forward when it was realized [20] that invariance of a system with a gapped liquid state under Wilson- (magnetic translation) operators implies an intimate connection between topological ground state degeneracy and statistics of quasiparticles.

Besides FQH liquids, Spin liquids are another large class of states exhibiting topological order. There, quantum fluctuations suppress the formation of magnetic or other kinds of local (spin solid) order which would break the continous symmetries, like global SU(2) and translation symmetries. Whereas in the quantum Hall effect as well as the recently found topological insulators, topological order can be detected rather directly via the classification of edge states, the situation is more subtle for spin liquids. While they do not exhibit gapless edge states in general, they still possess hidden topological order emergent through fractionalisation of

quantum numbers and quasiparticle statistics. Spin liquids are possible canditates for as yet unidentified phases in a number of systems, among others the frustrated Kagomé antiferromagnet [21, 22] and J_1-J_2 Heisenberg model of a square-lattice antiferromagnet with next-nearest-neighbour interaction [23]. The relevance to current problems of high interest as well as their accessability by various methods has established spin liquids as a major playground for new developments in field theory and quantum criticality. Apart from field theoretical approaches, there have also been analytical spin liquid solutions to some simple toy models, for instance the non-Abelian liquid found by Yao and Kivelson as the exact ground state of the Kitaev honeycomb model [24, 25]. Another analytically founded example inspired by the Quantum Hall effect is the chiral spin liquid state (CSL) put forward by Kalmeyer and Laughlin [4] as one of the first trial states for high-T_c superconductors. It is essentially a bosonic quantum Hall wavefunction of spin flip operators. Its elementary excitations are spinons which carry $S = 1/2$ but no charge, and which obey half-Fermi statistcs. While the CSL turned out not to be directly relevant to high-T_c superconductors, it was the system in which Wen first established the notion of topological order [1]. Owing to its equivalence to a QH state, the CSL's low energy physics is described by a Chern-Simons effective field theory. An extension of this description leads to other branches in the field of spin liquids, such as the Z_2 spin liquids, which, in addition to spinons, support vison excitations which carry no spin but couple to an additional gauge field with Z_2 symmetry.

The CSL will be highly relevent to us, as we will use it as the building block in one of the major proposals of this thesis: a hierarchy of SU(2) invariant quantum spin liquids. We were able to evaluate numerically the topological degeneracy (TD) of all liquids from this hierarchy with $S \leq 2$, which allows us to infer their statistical properties via the TD-statistics connection mentioned above. An especially interesting example is the $S = 2$ chirality liquid we obtain by 'merging' 2 $S = 1/2$ CSLs of both chiralities each. It is the first example of a spin rotationally invariant spin liquid with non-Abelian excitations which also preserves parity (P) and time reversal (T) symmetries. We establish a connection of hierarchy states obtained from k CSLs of only one type of chirality with the Read-Rezayi k-cluster FQHE liquids [26], which generalize electron pairing as described by the Pfaffian $\nu = 5/2$ state. Using conformal field theory, one can show that these states have a TD of $k+1$ [27]. This leads us to conjecture, that a general hierarchy states with $S \geq 2$ obtained from merging an equal number of CSLs with positive and negative chirality support non-Abelian elementary excitations and, since they are also evidently P and T invariant, we propose them as candidate states for disordered spin S antiferromagnets.

In our numerics we determine the topological degeneracy of our hierarchy states by writing out the wavefunctions for different center-of-mass-zero parameters because it is a more efficient method if one knows the analytic form of spin liquid one wishes to analyze. Another possible way to go is via the entanglement entropy. The entanglement entropy S_A of a subsystem A of a bigger system is the von-Neumann entropy of its reduced density matrix ρ_A. It was shown that for low-dimensional liquid states [5, 6], S_A is not extensive but rather has a leading contribution which scales with the boundary size of A. If A is furthermore not a simply connected region, its entanglement entropy has a system size independent, *i.e.*, topological contribution S^topo[6, 28]. In a recent study of the Pfaffian state on a sphere, Li and Haldane [7]

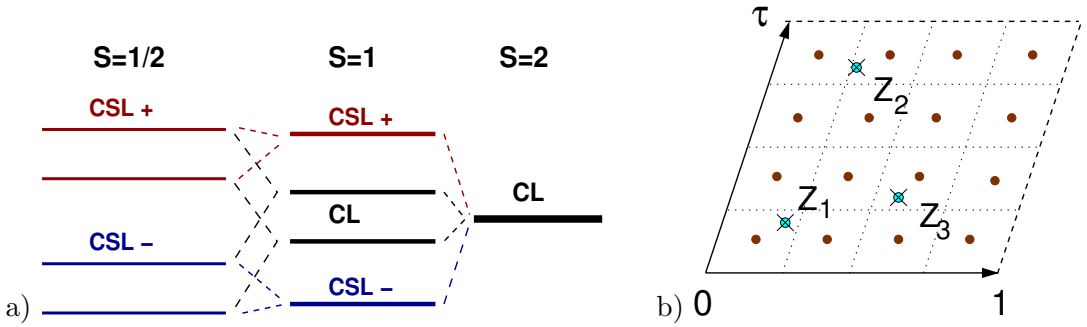

Figure 1.2: a) merging 2 CSLs of each chirality gives a P and T invariant liquid with TD of 9, indicating non-Abelian statistics of the excitations b) to compute this TD numerically we evaluate the analytically known wavefunctions for a sufficient number of randomly chosen points in the principal region

argued that instead of computing only one number from it, the full spectrum of the reduced density matrix itself should provide a more sensitive tool to probe a system for topological order. Since ρ_A can be interpreted as a thermodynamic state of some hamiltonian H at a fictious temperature $T = 1$, the gap between lowest and second lowest level in the entanglement spectrum (ES) reveals the strength of entanglement across the system boundary: a large gap means weak entanglement, with the limit of 'infinite' gap being a simple product state. It has been found that for the Pfaffian state as well as for Abelian FQH liquids on sphere, the angular momentum resolved ES shows a set of low lying levels which can, at least up to finite size distortions, be brought into correspondence with edge states expected from conformal field theoretical calculations [7]. Choosing a different normalistion for the many-body state reveals an 'entanglement gap' between these low lying levels typical for the topologically ordered FQH states and higher 'generic' ones, which is conjectured to remain finite under adiabtic transformation of one state into another if and only if the two states are topologically equivalent [29].

In one of the first entanglement spectrum studies of two-dimensional spin lattices, we use ES to obtain information about the topological properties of frustrated quantum antiferromagnets in comparison to our spin liquid hierarchy states. For this numerical work we implement software to efficiently compute a symmetry (quantum number) resolved entanglement spectrum for spin lattice clusters up to 32 sites, which is easily extensible to larger systems with a more efficient diagonalisation routine.

For some systems, most notably the (geometrically) frustrated Kagomé lattice and the (interaction) frustrated next-nearest-neighbour Heisenberg model at critical coupling $J_1 = 2J_2$, spin liquids are candidates for the as yet unidentified phases (see, *e.g.* , [30]).

In this thesis we present the investigation of a 4×6 lattice cluster of $S = 1/2$ spins and a 4×4 cluster of $S = 1$ spins. The subsystem A was a 4×3 and 4×2 cluster, respectively. As conserved quantum numbers, we thus had the z-component of the total spin on A, S^z_A, as well as the momentum along the edge ($m_A = 0, 1, 2, 3$ in units of $2\pi/4$). For the 4×6 cluster,

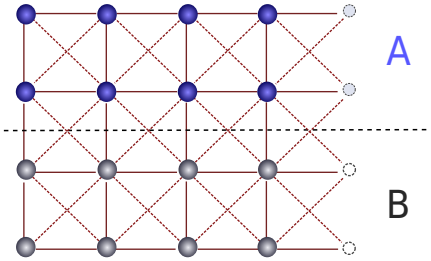

Figure 1.3: we investigate the entanglement spectra spin liquids from our hierarchy and antiferromagnetic next-nearest neighbour Heisenberg groundstates on lattice clusters of $S = 1/2$ and $S = 1$ spins and different boundary conditions

we both wrote down a CSL wave function and determined the groundstate of a J_1-J_2 AF for different values of an effective length parameters. In case of the CSL with quasi-periodic boundary conditions defined on the principal region $P = \{a + ib\tau | a, b \in [0, 1)\}$, $\mathrm{Im}[\tau] > 0$ the natural parameter is $|\tau|$, while for the AF we decreased the coupling strengths between two rows and defined as effective length the ratio of bulk-to-edge coupling. In this process, boundary conditions change from periodic to cylindrical. We know that the CSL must undergo a topological phase transition in the process, as it has topological order on a torus but not on a cylinder. The idea was to compare the entanglement spectra of both systems to find possible evidence of similar behaviour in the Heisenberg model groundstates.

We indeed find that in both cases the lowest-level gap in the ES decreases (but does not close) before approaching its final value in the limit of cylindrical boundary conditions, which is higher than its initial one. In the AF this is accompanied by an increased susceptibility to a chiral perturbation in the vicinity, but not quite at, the position of the gap-peak. We take this as preliminary evidence that a topological phase transition might indeed take place in the AF groundstate. The system is not big enough however, to really enable an analysis analogous to the FQHE states on a sphere that was mentioned above. To be able to say anything more definite, such as whether the ground level gap we observed closes completely, or how it is connected to the entanglement gap from the FQH one would have to repeat the computation for larger systems. We intend to do this as soon as the necessary computational facilities become available.

In the 4×4 spin $S = 1$ lattice cluster, we compared entanglement spectrum and evaluated the overlap of a AF groundstate with the $S = 1$ chirality liquid. We chose this liquid, because it is the first P and T invariant element in the hierarchy and as such shares the symmetries of the Heisenberg hamiltonian. While we find a decent overlap, the entanglement spectra are not very similar. The system is likely affected even more significantly by finite size effects than the 4×6 $S = 1/2$ cluster. Since the subsystem A is a mere 2 rows high it cannot really be said to constitute a 'bulk'. We hope to be able to do the same computation again on larger clusters at some stage in the future.

The third line of work we want to present in this thesis takes a somewhat different direction. In the course of our numerical work, a severe limitation to the method of exact diagonalisation

we employ in studying our systems became obvious once more: Since it does not throw away any information, it is maximally versatile in the range of quantum systems it can, in principle, be applied to. But of course keeping all information means we can only use the physical symmetries of the system to reduce our Hilbert space. In case of the hamiltonians we consider, these are global SU(2) as well as lattice symmetries. While it is not hard to make use of the lattice symmetries in a product basis, doing the same in a total spin basis is a much harder problem, and the state-of-the-art in spin lattice computations is still to use symmetry-reduced product bases. We cannot report here to have solved this problem, but another interesting one which arises in this context is how to determine the eigenvalues (quantum numbers) of said lattice symmetries. The general problem can be solved either by brute-force diagonalisation of the symmetries in a product basis, or more subtly using character theory of finite groups and the fact that all symmetries of a finite lattice cluster of N sites are just elements of the permutation group S_N. In the case of spin chains of fundamental SU(N) spins, where the symmetry operation in question is the cyclic permutation C_N (*i.e.*, translation by one lattice site), the solution of the problem of finding the eigenvalues e^{ip} is automatically contained in the method of extended Young tableaux [8] invented as a way to determine the spinon content of the spectrum of the Haldane-Shastry model. In this thesis, we generalize the method to higher symmetric representations of SU(n), and show how it can be used to significantly speed up computation of momenta in a total (SU(n)-)spin representation.

This thesis is organized as follows. In chapter 2, we review fractional quantum Hall states and the chiral spin liquid derived from them and take a close look at the properties characterising their topological order. In chapter 3, we present the main result of this thesis: the hierarchy of fractional spin liquids we construct with the CSLs as basic building block. chapter 4 is devoted to our entanglement spectrum analysis of the CSL and one other hierarchy state, the $S = 1$ chirality liquid, which we compare to groundstates of next-nearest-neighbour Heisenberg antiferromagnets. In chapter 5, we present the generalisation of the extendend Young tableaux procedure. It allows reading off the eigenvalues of the cyclic permutation directly from the Young tableaux representing a total highest weight subspace of a product space built from arbitrary symmetric representations of SU(n). Finally in chapter 6 we provide a summary of our results, and indicate possible extensions as well as future work required to verify our observations.

2 Topological order

The strongly correlated many-body states invented to describe the fractional quantum Hall Effect (FQHE) led to the discovery of *topological order* (TO): an ordering that cannot be described by a local order parameter associated with a broken symmetry but nevertheless shows invariants like ground state degeneracy, fractional excitations and number of edge states. These are insensitive to smooth changes of parameters and can only be altered by a quantum phase transition, TO may be interpreted as a new paradigm for phases of matter. Far from being confined to the states encountered in the FQHE, topological order and its features emerge in many systems with genuine quantum behaviour. For instance, at the heart of the recently opened field of topological insulators are edge states, charge or spin-current carrying (D-1)-dimensional excitations localised at the boundary of D dimensional topologically ordered systems. Spin liquids are another diverse area where topological phases appear. They have again enjoyed increased interest in the last few years both because of their numerical accessability and in some cases analytical tractability and because they are conjectured to stabilized in some model systems of practical interest, *e.g.* , among others, frustrated quantum magnets. An important example of a spin liquid is Laughlin's chiral spin liquid (CSL) (chirality = broken P and T symmetry). The wave function is essentially that of a bosonic fractional quantum Hall liquid for spin flip operators acting on a Hilbert space spanned by $S = 1/2$ spins. It receives special attention here because it serves as the basic building block for one of the main results we present in this thesis: a hierarchy of topologically ordered liquids with spin $S \geq 1$ per site, which allows to have non-Abelian statistics while restoring P and T symmetry at the same time. We will present its construction and properties of some hierarchy members in the next chapter.

In this chapter, we give an overview of the discovery of TO and its diverse manifestations found to date. We review Laughlin's $1/m$ FQH liquids, the statistics of quasi-particles and its topological degeneracy (TD) on a non-trivial topology. We then introduce the effective field theory description and demonstrate how it describes fractional conductance and (electrical) charge of the quasi-particles. This is followed by an account of the connection between TD and fractional statistics for both Abelian and non-Abelian excitations and a sketch of edge states and topological insulators. Lastly, we review in detail the chiral spin liquid due to Kalmeyer and Laughlin, which, as mentioned, will play a key role in the next chapter.

2.1 Background

Ever since its discovery by Tsui, Störmer and Gossard [2] nearly three decades ago the fractional quantum Hall effect (FQHE) has served as a fertile playground for condensed matter physics and has inspired numerous new concepts. Fractionalisation of quantum numbers is one

example. Even though first recognized in polyacetylene, where the elementary spin excitations were found to carry not $S = 1$, but $S = 1/2$ [31], it was only appreciated as an important and common many-body phenomenon by studying the fractional Quantum Hall liquids proposed as trial states to explain the off-diagonal conduction plateaus. Among the most prominent are the $\nu = 1/m$ states where m is an odd integer, put forward by Laughlin [3] in 1983. Unlike the Landau-levels from the integer QHE, they represent true many-body states, *i.e.*, they do not arise as Slater determinants of single-particle orbitals. The Laughlin FQH liquids are not the exact eigenstates of the Hall-hamiltonian with Coulomb- interaction, yet numerical studies have shown overlaps with true (finite size) groundstates close to 1 [10]. More recently, a very similar low-'energy' part of the entanglement spectrum [7], providing the strongest evidence yet that the $1/m$ states indeed capture the off-diagonal order of the true ground state. Arovas *et al.* [12] applied the idea of charge-flux composites [11] to the FQHE states, identified the quasi- particles and showed that they obey fractional (anyonic) statistics: by adjoining $1/\nu$ flux quanta to one (fermionic) degree of freedom the basic excitations are identified as insertion or removal of a single flux quantum, which carries a charge $\pm e/m$ and exchange phase $\pm\pi/m$. Only much later, in 1990, was fractional statistics generalised to non-Abelian 'phases' when Moore and Read [20] proposed a state with a Pfaffian wave function for the filling fraction $\nu = 5/2$. It describes pairing of electrons and the elementary excitations are Majorana fermions. Braiding of Majoranas effects not only a phasefactor but a rotation within the subspace of fixed quasi particle number.

In 1985 Haldane and Rezayi [16] discovered what was later termed *topological degeneracy* (TD): they noticed that a $1/m$ fractional quantum Hall liquid obeying quasi-periodic boundary conditions acquires a set of m new parameters, the center-of-mass-zeros. The state space obtained upon variation of these parameters is m dimensional and can be understood as the m-fold degenerate ground state of the quantum Hall hamiltonian on a torus. Following an earlier proposal by Girvin [10], Shou-Chen Zhang *et al.*in 1989 were able to derive an effective field theory for the FQHE directly from the microscopic Hamiltonian [32]. It contains a real scalar field $\phi(\boldsymbol{x}, t)$ interpreted as the quasi-particle density coupled to both the real electromagnetic gauge field $A(\boldsymbol{x}, t)$ and another, 'statistical', gauge field $a(\boldsymbol{x}, t)$, the latter appearing as a Chern-Simons topological term. This effective action allows to derive quantization of conductance and vortex solutions for ϕ (this explains why CS actions are called topological).

The other seminal discovery of the 1980's condensed matter physics was high-temperature superconductivity in the cuprates. Among the proposals put forward to describe the electronic state in the copper-oxide planes was the *chiral spin liquid*(CSL) by Kalmeyer and Laughlin [4]. It is modelled upon the earlier fractional QH liquid, but is rewritten for bosonic (localized spin) degrees of freedom. It led the way for a whole new class of spin liquids in two spatial dimensions: spin rotation invariant states with no long range 2-spin correlations which break parity and time reversal, *i.e.*, are chiral. They do however exhibit strong local antiferromagnetic correlations and possess a local order parameter, which on a lattice can be alternatively characterized as a triple product of spin operators from one triangular plaquette or as the Berry's phase picked up when moving a spin around a plaquet [33]. For the square lattice Wen, Wilczek and Zee [33] were also able to give an explicit frustrated spin hamiltonian involving interaction of up to 6 sites which has such a CSL as groundstate.

After Girvin [10] two years earlier had introduced the notion of off-diagonal long range order, known from superconductivity and liquid helium [34], in fractional quantum Hall liquids, and Wen in 1989 [1] discovered the ground state degeneracy of chiral spin liquids on nontrivial topologies, it was Wen and Niu [19] who proposed to unify the observations for CSLs and FQHLs under the paradigm of *topological order*. It denotes a novel class of phases of matter which seemingly cannot be understood in the Landau-Ginzburg framework of broken symmetry with associated local order parameter, like in a ferromagnet or a crystal. Rather, order is manifest in the appearance of invariants of topological nature, like ground state degeneracy, fractional statistics and edge states. The latter are located near the boundary of a system (Hall sample, finite section spin lattice) carrying charge or spin currents, and are topologically protected in the sense that the are stable agains disorder which does not change the topological invariant characterising the bulk state.

In a 1991 paper, Moore and Read [20] proved an intimate connection between the topological ground state degeneracy of a Laughlin type fractional QH liquid on a torus and the statistics of its basic excitations. In essence, they construct an algrebra of operators representing quasi-particle pair creation, subsequent translation by one principal vector and final annihilation (Wilson-line operators) and show that translation operations in the two principal directions do neither commute (phase 0) nor anti-commute (commutation with phase π), but rather incur a phase $\nu\pi$ upon interchange. Diagonalising one of the operators then shows that energy eigenstates must be degenerate in multiples of $1/\nu$ if the hamiltonian is invariant under the translation operation. This holds strictly speaking only in the thermodynamic limit $L \to \infty$ and if all *local* excitations are gapped. Only then is the interaction between quasi-particles purely statistical as otherwise interaction between them would lift the degerneracy by terms of order e^{-L}.

As was already mentioned above, in the same paper, Moore and Read moreover constructed a new liquid state for the filling fraction $\nu = 5/2$, the Pfaffian state, where basic excitations display a non-Abelian Berry's phase. A Pfaffian wave function also appears as the zero-energy solution of the Bogoliubov-deGennes equations of a p+ip superconductor. These states have recently received much attention for their potential to enable topological quantum computing [35]. In such a scheme, the qubits are double-pairs of (Majorana) quasi-particles and single qubit operations are achieved by braiding within pairs (not all single qubit operations are possible however), while two qubit operations could be implemented by braiding between pairs . Since the state of a qubit can only be changed by nonlocal operations it would conceivably be very robust against common types of noise (charge, position).

Non-Abelian statistics make predicting the topological degeneracy somewhat more intricate: there are fewer states in the ground state multiplet than expected. Initially, there was apparently some confusion as to the correct values of the TD in a non-Abelian liquid, and only in 2000 Read and Green [36] were able to give the definitive answer. A clear and intuitive understanding of what causes some states expected from Abelian statistics to be absent in the non-Abelian case was presented by Oshikawa *et al.* [37], termed 'blocking mechanism', only quite recently.

In 1999 Read and Rezayi [26] defined a class of FQH liquids which generalize the Moore-Read pairing state to clusters of k particles. The statistics of elementary excitations are non-Abelian

for all values $k > 1$ and the topological degeneracy was proven by Wen and Zee [27] to be $k + 1$.

In recent times, attention has turned back to spin liquids and spin lattice models as neat model systems to study topological order. One reason may be that fractional Quantum Hall liquids seem to be fairly well understood by now, but more important is probably that liquid states are conjectured to be stabilized in frustrated quantum magnets, where frustration can be introduced via the interaction (*e.g.* next-nearest neighbour Heisenberg) or via the geometry (*e.g.* the Kagomé-lattice). Other branches the field has diversified into are Z_2 spin liquids, where an additional emergent charge $2e$ gauge field reduces gauge freedom from U(1) to $\mathbb{Z}_2$ [38, 39] and algebraic liquids, which are potentially good descriptions of critical phases, as all spin-spin correlators decay algebraically with distance [40].

In some cases, spin models allow studying topological order in an exactly solvable context, as is the case with Kitaev's toric code [41], a Z_2 spin liquid interesting as topologically protected quantum memory and also Kitaev's honeycomb lattice spin model [24], where Yao and Kivelson [25] found a time reversal breaking CSL ground state with non-Abelian vortex excitations and two topologically distinct sectors seperated by a quantum critical point.

A new measure for detecting topological order that the study of spin systems has uncovered is *topological entropy*. It is the scale-invariant part of the von-Neumann entropy of a non-simply connected region on the lattice. Field theoretical considerations [6] as well as a derivation using a string-net condensate on a honeycomb- lattice [28] arrive at the result that the topological entropy is essentially the logarithm of the total *quantum dimension*. This is defined via the scaling of the internal Hilbert space of the quasi particles with their number and for Abelian liquids is simply equal to the topological degeneracy. This also holds for some non-Abelian ones like the Moore-Read state.

2.2 Topological degeneracy and fractional excitations

In this section we want to examine in more detail two of the key features of topological order, the ground state degeneracy and the fractional statistics of fundamental excitations/quasiparticles. We also introduce the topological algebra of flux insertion- and Wilson-loop operators which provide the intimate link between topological degeneracy and statistics. We will consider as examples both fractional FQH liquids, the systems were these notions were first discovered in, and spin liquids, which have moved more into focus in recent times.

2.2.1 Laughlin $1/m$ states

We will first review the origin of the topological degeneracy in the case of the Abelian FQH liquids proposed by Laughlin as trial states for the primary series of plateaus $\nu = 1/m$ with m an odd integer.

In circular gauge with open boundary conditions, the wave function for the $1/m$ state is

$$\Psi_{\text{Laughlin}}[\boldsymbol{z}] = \prod_{i<j}^{N}(z_i - z_j)^m \prod_{j=1}^{N} \mathrm{e}^{-\frac{1}{4l^2}|z_j|^2} \tag{2.1}$$

where z_i are the complex coordinates of the N electrons in the sample and the magnetic length l^2 is the area of one Dirac flux quantum

$$2\pi l^2 B = \Phi_0 \tag{2.2}$$

Since m is odd integer, $\Psi_{\text{Laughlin}}[\boldsymbol{z}]$ is completely anti-symmetric in all coordinates, as is required for fermions. The number of flux quanta N_Φ is related to the number particles via the filling fraction

$$N_\Phi = N/\nu = m\,N \tag{2.3}$$

i.e., there are m times as many flux quanta Φ_0 as particles. If (2.1) is an eigenstate, adiabatic insertion of one flux quantum at, say, the origin leads to another eigenstate because whole flux quanta can be removed via a gauge transformation

$$A_\mu \to A_\mu + \nabla\Lambda(z) \tag{2.4}$$

$$\psi(z) \to \mathrm{e}^{i\frac{e}{c\hbar}\Lambda}\psi(z) \tag{2.5}$$

Here, $\psi(z)$ is a generic single particle orbital and serves to remind ourselves, that a gauge transformation entails a phase-change of the wave functions. Thus the gauge will only lead to periodic boundary conditions if the circular integral over the function Λ effecting the described gauge transformation gives a multiple of 2π. This is the case for

$$\Lambda = -\frac{\Phi_0}{2\pi}\phi. \tag{2.6}$$

in polar coordinates. Computing a closed loop integral around the origin shows that we indeed encircle one Dirac flux quantum and the gauge transformation is thus single valued. On the other hand, by increasing the flux, we insert angular momentum $\hbar$ into the system and therefore expect the occupation numbers of canonical angular momentum states to have changed by 1. This corresponds to an increase of one in the power of any coordinate z_i in Ψ_{Laughlin}, *i.e.*, $z_i^m \to z_i^{m+1}$. Therefore, if we insert the flux at a general position ξ, we get

$$\Psi^{\text{qh}}_{\text{Laughlin}}[\boldsymbol{z},\xi] = \prod_i (z_i - \xi)\,\Psi_{\text{Laughlin}}[\boldsymbol{z}]. \tag{2.7}$$

We identify 2.7 as a state with a quasi-hole excitation at postion ξ. The other kind of quasi-particle for the Laughlin states, quasi-electrons, correspond to the removal of one flux at a position η

$$\Psi^{\text{qe}}_{\text{Laughlin}}[\boldsymbol{z},\eta] = \prod_j \mathrm{e}^{-\frac{1}{4l^2}|z_j|^2} \prod_i (\partial_{z_i} - \eta) \prod_{i<j} (z_i - z_j)^m \tag{2.8}$$

Repeating either process m times, we can create a factor looking like a full fermionic degree of freedom, *i.e.*, a full hole/electron with charge $\pm e$. This motivates a picture of quasiparticles as one flux quantum with an attached charge $\pm e/m$. Creating such a quasiparticle by flux insertion will require a non-continuous change in the electronic pattern and the $1/m$ states thus describe incompressible quantum liquids where both creation of individual quasi-particles as well as pair-creation is gapped. The energy cost is roughly of the order

$$\Delta E_{\text{qp}} = \nu\hbar\omega_c \tag{2.9}$$

per particle.

2.2.2 Statistics of quasiparticles

The flux-charge composites that form the quasiparticles of the Laughlin-liquid acquire phases of $2\pi/m$ upon winding of one around the other which can be understood as the Aharonov-Bohm phase of a charge νe particle encircling a flux Φ_0:

$$2\theta = \frac{1}{m}\frac{e}{c\hbar}\oint(\Phi_0/2\pi)\phi \mathrm{d}\phi$$

therefore the statistical parameter measuring phase change upon interchange of particles is

$$\theta = \frac{\pi}{m}. \tag{2.10}$$

A statistical parameter $\theta = 0$ corresponds to bosons and $\theta = \pi$ to fermions. Because in 3 spatial dimensions all paths are homotopic to a point (in the absence of line-defects), these are indeed all the possibilities that arise there. In two dimensions however, pointlike singularities lead to a nontrivial fundamental group. Therefore particles 'remember' how often they were wound around each other and many-body eigenstates are no longer a representations of the permutation- but rather the *braid group*. For the Laughlin FQH liquid, phases are Abelian and the $1/m$ state are one-dimensional braid-group representations.

2.2.3 Fractional Quantum Hall liquids on a torus

We give a brief account of the origin ot topological degeneracy in FQH liquids. First found in the $1/m$ Laughlin states by Haldane and Rezayi [16] in 1985, it provides the paradigm for topological degeneracy in non-Abelian quantum Hall- as well as spin liquids.

Mapping the Laughlin states onto a torus is equivalent to imposing the quasi-periodic boundary conditions

$$\begin{aligned}\Psi_{\mathrm{Laughlin}}[z_1+1, z_2, \ldots, z_N] &= \mathrm{e}^{i\phi_1}\,\Psi_{\mathrm{Laughlin}}[\boldsymbol{z}]\\ \Psi_{\mathrm{Laughlin}}[z_1+\tau, z_2, \ldots, z_N] &= \mathrm{e}^{i\phi_\tau}\,\Psi_{\mathrm{Laughlin}}[\boldsymbol{z}]\end{aligned} \tag{2.11}$$

on a liquid in the principal region $\mathscr{P} = \{a + b\tau | a, b \in [0,1)\}$ spanned by the 'vectors' 1 and $\tau \in \mathbb{C}$.

To be able to fulfill these conditions, one has to replace factors $z_i - z_j$ by $\vartheta(z_i - z_j|\tau)$, with $\vartheta(z|\tau) = \vartheta_{\frac{1}{2},\frac{1}{2}}(z|\tau)$ the odd Jacobi-theta function (cp. App. A.1), while the gaussian of the droplet has to be replaced by a gaussian with translation symmetry along the real axis and finally we need to introduce a set of $m+1$ new parameters, m 'center-of-mass-zeros' $Z_\nu \in \mathscr{P}$, $\nu = 1 \ldots m$ and a phase shift e^{iK}. The conditions (2.11) then lead to

$$\begin{aligned}\mathrm{e}^{iK}\,(-1)^{N_\Phi} &\stackrel{!}{=} \mathrm{e}^{i\phi_1}\\ \mathrm{e}^{iK\tau}\,(-1)^{N_\Phi}\,\mathrm{e}^{2\pi i\sum_\nu Z_\nu} &\stackrel{!}{=} \mathrm{e}^{i\phi_2}\end{aligned} \tag{2.12}$$

which confines the $m+1$ parameters to an m-dimensional hyperplane.

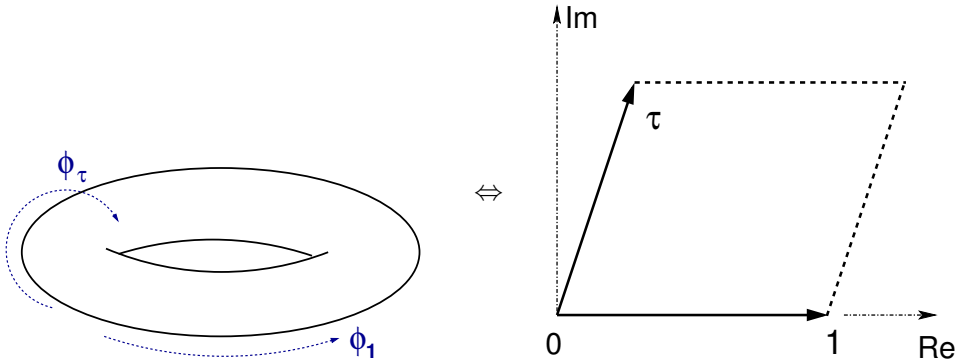

Figure 2.1: A torus topology is equivalent to quasi-periodic boundary conditions where the many-particle wave function acquires 'boundary phases' ϕ_1 and ϕ_τ

In total, the wave function on a torus is

$$\Psi_{\text{Laughlin}}\left[\boldsymbol{z}|\{Z_\nu\},K\right] = \mathrm{e}^{i\,KZ}\prod_{\nu=1}^{m}\vartheta(Z-Z_\nu|\tau)\prod_{i<j}^{N}\vartheta(z_i-z_j|\tau)^m\prod_{j=1}^{N}\mathrm{e}^{-\frac{\pi}{4}(|z_j|^2-z_j^2)}. \tag{2.13}$$

This explains the name of the parameters Z_ν, as they introduce m additional zeros of the many-body wavefunction at the position of the center-of-mass $Z=\sum_j z_j$.

The function space spanned by $\Psi_{\text{Laughlin}}[\boldsymbol{z}|\{Z_\nu\},K]$ as the Z_ν vary over $\mathscr{P}$ is m-dimensional [42] and this is the topological degeneracy. Topological, since its appearance is owed to the non-trivial topology of the torus, and a degeneracy, since one can identify this space as the ground state space of the QH-hamiltonian at a filling $\nu=1/m$ [43, 44] (see also appendix A.4).

The non Abelian Moore-Read wave function invented to describe half filling $\nu=1/2$ looks similar to a Laughlin liquid. In circular, open boundary gauge it reads

$$\Psi_{\text{Pf}} = \text{Pf}\left[\frac{1}{z_i-z_j}\right]\prod_{i<j}^{N}(z_i-z_j)\prod_{j=1}^{N}\mathrm{e}^{-\frac{1}{4}|z_j|^2}. \tag{2.14}$$

Here, the Pfaffian $\text{Pf}\left[\frac{1}{z_i-z_j}\right]$ is defined as the polynomial

$$\text{Pf}\left[\frac{1}{z_i-z_j}\right] = \mathscr{A}\left\{\frac{1}{z_1-z_2}\frac{1}{z_3-z_4}\cdots\frac{1}{z_{N-1}-z_N}\right\} \tag{2.15}$$

where $\mathscr{A}$ denotes antisymmetrisation, in this case over all pairings $1/(z_{2j-1}-z_{2j})$. When one 'toroidalizes' (2.14), the Pfaffian is responsible for an additional 3-fold degeneracy: the z_i being fermionic the denominator is rewritten just like Jastrow-like product $\prod_{i<j}(z_i-z_j)$ using the odd Jacobi theta function $\vartheta(z|\tau)$ from above. Boundary conditions however require the numerator to be replaced by a theta-function $\vartheta_{a,b}(z|\tau)$ as well. Total anti-symmetry dictates one can use any one of the 3 even theta-functions (a,b) equal to $(0,0)$, $(0,1/2)$ or $(1/2,0)$.

2.2.4 Effective field theory

If one is only interested in the low energy behaviour of a system, an effective field theory reformulation of the full Hamiltonian, with short-range, high energy fluctuations integrated out, is a very useful tool. The coarse-graining it implies makes it applicable to dicrete systems like spin lattices as well continuous ones.

The elemetnary excitations of a FQHE state or spin liquid can be described by a complex scalar field $\phi(\boldsymbol{x}, t)$, which is essentially the amplitude of excitations on the ground state. We need to find the Langrange density $\mathscr{L}[\phi, \partial_\mu \phi]$ of its dynamics. It is coupled to the electromagnetic potential A_μ plus in general emergent gauge fields describing particle statistics. Instead of starting from the exact Hamitonian H, more often one uses the theory of invariants to set it up 'empirically', including the only leading order terms invariant under the symmetries of H.

In the following we would like to sketch the effective field theory for the $\nu = 1/m$ (m an odd integer) Abelian states broadly following Zhang *et al.* [32]. The Langrange density at this filling fraction is given by

$$\mathscr{L} = \mathscr{L}_\phi + \mathscr{L}_a + \mathscr{L}_{\text{em}} \tag{2.16}$$

where $\mathscr{L}_{\text{em}} = -\frac{1}{16\pi} F_{\mu\nu} F^{\mu\nu}$ is the usual Maxwell Langrangian for the electromagnetic gauge field A_μ while the other two describe the dynamics of the statistical gauge field a_μ and the coupling of matter to the gauge fields respectively:

$$\mathscr{L}_\phi = \bar{\phi}[i\partial_0 - e(A_0 + a_0)]\phi + \frac{\kappa}{2}\bar{\phi}[i\nabla - e(\boldsymbol{A} + \boldsymbol{a})]^2\phi + s|\phi|^2 - u|\phi|^4 \tag{2.17}$$

$$\mathscr{L}_a = -\frac{e^2 m}{4\pi}\epsilon^{\mu\nu\sigma}\, a_\mu \partial_\nu a_\sigma \tag{2.18}$$

here as in the following, greek indices take values $0, 1, 2$ and $\epsilon^{\mu\nu\sigma}$ is the fully antisymmetric tensor of rank 3. In $\mathscr{L}_\phi$ $s = 2un$ (cp. solution for ϕ below), κ, u are phenomenological parameters and n the electron density. $\mathscr{L}_a$ is a Chern-Simons topological term and describes a statistical flux attached to the quasi particle field. The equations of motion

$$\partial_\nu \frac{\partial \mathscr{L}}{\partial(\partial_\nu a_\mu)} = \frac{\partial \mathscr{L}}{\partial a_\mu}$$

reveal a conserved quasi-particle current j^μ

$$j^\mu = \frac{e^2 m}{2\pi}\epsilon^{\mu\nu\sigma}\partial_\nu a_\sigma \tag{2.19}$$

where $j^0 = \partial\mathscr{L}_\phi/\partial a_0 = e|\phi|^2$ and $j^i = \partial\mathscr{L}_\phi/\partial a_i - \partial_i(\partial\mathscr{L}_\phi/\partial(\partial_i a_i))$ Thus, j^0 is simply the density of quasi-particles and defining the magnetic field associated with the statistical gauge field $b \equiv \partial_1 a_2 - \partial_2 a_1$ the meaning of the 0th equation

$$|\phi|^2 = \frac{em}{2\pi}\, b \tag{2.20}$$

becomes apparent: it describes quasi particles carrying a statistical flux $em/2\pi$, which is confirmed by the explicit vortex solutions for ϕ shown below. The particle current is

$$J^\mu = \frac{\partial \mathscr{L}}{\partial A_\mu} = \frac{e^2}{2\pi\, m}\epsilon^{\mu\nu\sigma}\partial_\nu A_\sigma + \frac{e}{m} j^\mu \tag{2.21}$$

We see that the spatial part J^i is composed of the answer to the electric field $e_j = \partial_j A_0 - \partial_0 A_j$ and the quasi-particle current contribution $e/m\, j^i$:

$$J^i = \sigma_{\mathrm{H}}^{ij}\, e_j + \frac{e}{m}\, j^i \tag{2.22}$$

Here, $\sigma_{\mathrm{H}}^{ij} = \frac{e^2}{2\pi\, m}$ is the Hall conductance and it is now a fraction $1/m$ of the conductance of a filled Landau-level ($\nu = 1$). Note also, that the quasi-particles carry fractional charge e/m in the electromagnetic current (whereas they carried charge e in the quasiparticle current!). Therefore, the addition of the gauge field a_μ governed by the topological Chern-Simons action successfully describes quantisation of conductance in the fractional Quantum Hall effect.

What is the explicit solution for ϕ? The signs in front of parameters $s = 2un$ and u are different, so we do obtain a non-zero solution and in polar coordinates its large distances $r \to \infty$ behaviour is given by

$$\phi(r,\varphi) = \sqrt{n}\, \mathrm{e}^{\pm i\varphi} \tag{2.23}$$

$$a(r,\varphi) = \pm\hat{\varphi}/er \tag{2.24}$$

with $a(r=0,\varphi) = 0$ and $\hat{\varphi}$ the unit-vector in tangential direction. This solution describes a vortex at the origin, which is topological in that the compactness of the phase of the field ϕ gives rise to a winding number around the vortex core.

The total charge carried by a vortex is

$$q_{\mathrm{s}} = \int \mathrm{d}^2x\, J^0 = \frac{e^2}{2\pi\, m}\oint \boldsymbol{a}\mathrm{d}\boldsymbol{r} = \pm\frac{e}{m} \tag{2.25}$$

consistent with (2.22). So we can identify it with the fractionally charged quasi-holes and quasi-electrons given explicitly in (2.7).

2.2.5 Topological algebra and blocking mechanism

In incompressible (gapped) liquids, like the Laughlin- and Moore-Read Pfaffian states, quasi-particle statistics provide a different angle on topological degeneracy. Consider such a liquid on a torus. One can define the following two pairs of operators

F_1:	insert a flux in 1-loop
F_τ	insert a flux in τ-loop
T_1	create quasi-e^--quasi-hole pair, transport one around 1-loop then reannihilate
T_τ	create q-e^--qh pair, transport around τ-loop, reannihilate

T_1, T_τ are the Wilson-line (or loop) operators of the topologically non-trivial cycles. Say, our incompressible quantum Hall liquid has statistical phase $\theta = \pm p/q$, q odd and coprime to p. Then the relative Aharonov-Bohm phase for quasi-particle transport around loop i with or without one additional flux inserted will be just $\exp[\pm 2\pi i\, p/q]$, or in other words we have the commutation relation

$$T_i F_i = F_i T_i \, \mathrm{e}^{2\pi i\, p/q} \tag{2.26}$$

where we fixed the sign of the phase by fixing a sense of circulation and type of quasiparticle transported (*e.g.* always the quasi-electron in direction of the principal vectors $1, \tau \in \mathbb{C}$). Let us use the Wilson-loop operators T_i as our observable to probe the state of the liquid and say we are in an eigenstates $|\alpha_i\rangle$. Then we see that flux insertion brings us to another eigenstate since

$$T_i(F_i\,|\alpha_i\rangle) = \mathrm{e}^{2\pi i\, p/q}\, F_i T_i\,|\alpha_i\rangle = \alpha_i \mathrm{e}^{2\pi i\, p/q} F_i\,|\alpha_i\rangle$$

Thus, the eigenstates $|\alpha_i\rangle$ are in fact phase-states and inserting a flux brings us to a state with a phase increased by $2\pi p/q$:

$$F_i\,|\alpha_i\rangle = |\alpha_i + 2\pi\, p/q\rangle \tag{2.27}$$

Also, we clearly have $F_i^q = 1$, *i.e.*, . inserting q flux quanta leaves the state as it was. This is not a contradiction to the gauge argument from above which we used to construct quasi-hole (and electron) states, since we are not talking about flux *piercing* the torus, but rather flux through its *holes*. Therefore, we can say the quantum Hall hamiltonian is invariant under F_i and we get a q-fold multiplet $|0\rangle, |2\pi p/q\rangle, \ldots, |2\pi p(q-1)/q\rangle$, *i.e.*, a topological degeneracy of q. However, there are two principal directions, and can make the construction shown above for both of them. Does this mean we have a topological degeneracy q^2 with states $\{|\frac{2\pi p}{q} j, \frac{2\pi p}{q} k\rangle\}$, $j, k = 0, \ldots, q-1$? Not necessarily, because T_1 and T_τ need not be independent. If quasi-particle statistics is Abelian, we have in fact

$$T_1 T_\tau = \mathrm{e}^{2\pi i p/q} T_\tau T_1 \tag{2.28}$$

because the sequence of operations $T_1^{-1} T_\tau^{-1} T_1 T_\tau$ corresponds to winding one particle around the other, as is illustrated in Figure 2.2. This implies $T_\tau = F_1$ (and vice versa), therefore the algebras for the two directions are in fact identical. Topological degeneracy is thus only q, as one would expected comparing what we have said here to the example of the (Abelian) Laughlin liquid (where $p = 1$ and $q = m$), where we know from the explicit wave function that the topological degeneracy is m. As mentioned before, this is strictly true only in an infinite system, where world-lines of quasiparticles can be spaced arbitarily far apart, so that interaction between them is purely statisitcal.

If excitations are non-Ablian, the story becomes more involved, as one might imagine. in fact the correct solution was found by Read and Green [36] in a seminal paper as late as 2000. Their calculations are somewhat unaccessible, but Oshikawa *et al.* [37] found a beautifully intuitive explanation, which we want to sketch in the following.

The two algebras spanned by T_1 and T_τ cannot be more than identical, nor more than completely independent, therefore q and q^2 are is still lower and upper bounds respectively for the total topological degeneracy, but non-Abelian statistics will cause identification of

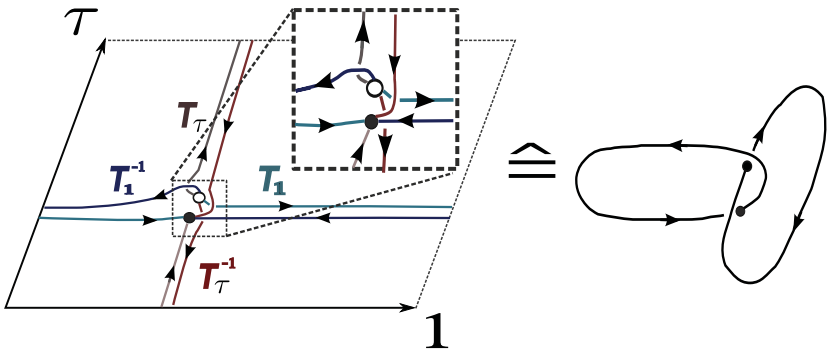

Figure 2.2: The Wilson-operator sequence $T_1^{-1}T_\tau^{-1}T_1T_\tau$ is topologically equivalent to two linked particle loops. They are *not* doubled as the left picture might suggest at first glance, because the ends and start of the paths in 1 and τ direction respectively are joined (*e.g.* . T_τ to T_τ^{-1}) to give a single loop for each principal direction.

some state, while others remain distinct. Take for example the Moore-Read Pfaffian state for half-filling. As stated above and described in detail in [35], pairs of Majorana-fermion excitations span an internal Hilbert-space and braiding of Majoranas rotates the state vector in the subspace of fixed excitation number. Each quasi-particle vortex carries charge $\pm e/2$ and $\pm$half a flux quantum. Therefore we have the relation

$$F_1 = T_\tau^2 \tag{2.29}$$

i.e., transporting a quasiparticle around the loop τ twice will introduce a full flux quantum. Since excitations behave non-Abelian, braiding of quasi-particle b via $T_1T_\tau T_1^{-1}T_\tau^{-1}$ does not result in a simple phase anymore, rather it causes a rotation of the state vector. One can now diagonalise the flux insertion operators. F_1 and F_τ themselves do not commute, but F_1 and F_τ^q do. For the Pfaffian state $q = 2$ and the Abelian exchange phase is $2\pi/4$ and we consider eigenstates $|f_1, f'_\tau\rangle$ with $F_1 |f_1, f'_\tau\rangle = f_1 |f_1, f'_\tau\rangle$, $F_\tau |f_1, f'_\tau\rangle = f'_\tau |f_1, f'_\tau\rangle$. Using the commutation relations between F_i and T_i and T_1 and T_τ^2 we see that we can generate a total of 8 eigenstates by applying powers of T_1 and T_τ:

$$\begin{array}{ll} |f_1, f'_\tau\rangle & T_\tau |f_1, f'_\tau\rangle \\ T_1 |f_1, f'_\tau\rangle & T_\tau T_1 |f_1, f'_\tau\rangle \\ T_1^2 |f_1, f'_\tau\rangle & T_\tau T_1^2 |f_1, f'_\tau\rangle \\ T_1^3 |f_1, f'_\tau\rangle & T_\tau T_1^3 |f_1, f'_\tau\rangle \end{array}$$

Not all of states are allowed however: in defining the Wilson-loops T_i, we said that the particle-hole pair is annihilated after completing the loop. Owing to the non-Abelian statistics, this is not always possible. We create and annihiliate pairs by applying (Dirac) creation/destruction operators $c, c^\dagger$ Expressed in terms of the Majorana-operators of particle and hole they are

$$\begin{aligned} c &= \gamma_\mathrm{p} - i\gamma_\mathrm{h} \\ c^\dagger &= \gamma_\mathrm{p} + i\gamma_\mathrm{h} \end{aligned} \tag{2.30}$$

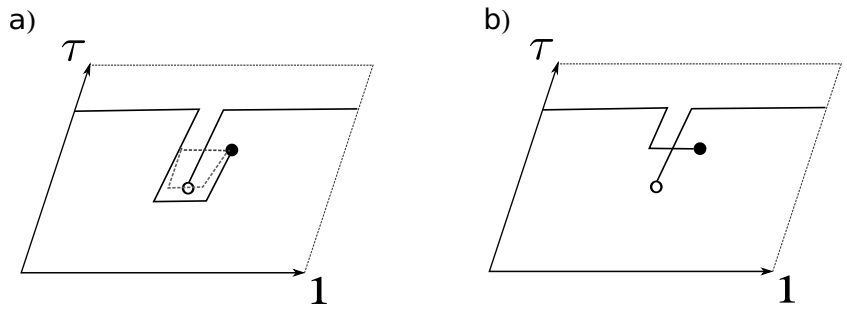

Figure 2.3: Winding the particle of a p-h-pair around the torus in 1-direction, there is the ambiguity in who crosses the branch cut connecting the pair: a) the hole or b) the particle? This has no physical consequences however, as either case implies $c \to c^\dagger$

The key is now that due to the Majorana's non-Abelian statistics, winding, say, the particle p around the torus in 1-direction will change the sign of either γ_p or γ_h and therefore

$$c \overset{\text{winding}}{\longrightarrow} \pm c^\dagger \tag{2.31}$$

i.e., what was the destruction operator before winding turns into a *creation* operator after winding! The sign is of no physical consequence and is simply an artifact of whether we say the particle or the hole passes the branch-cut (see Fig. 2.3). Since the destruction- acts as a creation operator on the (many-body) state after winding it will simply give 0, since the single-particle orbital it acts on is already occupied.

This so called *blocking mechanism* holds for winding either around 1 or τ, and also if we do both. For $T_\tau T_1$, annihilation is still blocked

$$c \xrightarrow{T_1} \pm c^\dagger \xrightarrow{T_\tau} c^\dagger \tag{2.32}$$

whereas one might have hoped that two sign changes cancel out and unblock this state. This can be understood if we realise that we made an implicit assumption: that the boundary conditions are *even* in both directions (++). Looking at figure 2.3, we see that the a Wilson loop leaves a branch cut behind (the line connecting particle and hole), which effectively changes boundary conditions from (++) to (+−). But this means the T_τ operation does not flip the sign of any Majorana operator, thus leaving also c, $c^\dagger$ unchanged.

The total number of states in the algebra is therefore dependent on the boundary conditions:

BC	states blocked	#available
++	$T_1^{2k+1},\ k=0,1,\ T_\tau T_1^l,\ l=0,1,2$	2
+-	$T_1^{2k},\ k=0,1$	6
-+	$T_\tau T_1^{2k},\ k=0,1$	6
- -	$T_\tau T_1^{2k+1},\ k=0,1$	6

The Pfaffian state on a torus falls into one of the latter categories, confirming the topological degeneracy of 6 one also obtains from the explicit wave function.

2.2.6 Z_2 liquids

We would like to state the main features of the Z_2 class of liquids already mentioned before. They were devised to describe a spin rotation- and lattice symmetry-invariant resonating valence bond state on the two dimensional lattice [38].

The idea is to introduce a new scalar field Λ, associated with charge 2 quasi particles, *i.e.*, it transforms like $\Lambda \to \mathrm{e}^{2i\theta}\Lambda$ if the spinons undergo a phase transformation $z_\alpha \to \mathrm{e}^{i\theta} z_\alpha$, and couple it minimally to the electromagnetic gauge field and to the spinon field via a Chern-Simons-like topological term. The first breaks the U(1) gauge symmetry down to $\mathbb{Z}_2$ with the effect of reducing gauge field fluctuations, the latter promotes pairing of spinons into a p-wave singlet state called a vison. The action of such a liquid is

$$S_\Lambda = \int \mathrm{d}^2 r \mathrm{d}t \left[|(\partial_\mu - 2iA_\mu)\Lambda|^2 + s_v|\Lambda|^2 + u_v|\Lambda|^4 - i\Lambda\epsilon^{\alpha\beta} z^*_\alpha \partial_a z^*_\beta + \text{c.c.} \right] \tag{2.33}$$

and similarly for S_z, with 'masses' s_z and u_z where the last term above appears only once and $u_z > 0$ as well as $u_z > 0$. One can give a phase diagram depending on the two 'masses' s_z and s_v of the spinon and vison field respectively as parameters. Only the case $s_z > 0$ and $s_v < 0$ describes a Z_2-liquid phase were gauge symmetry is reduced to $\mathbb{Z}_2$ and the spinon field has no vacuum expectation value and thus preserves spin rotation symmetry.

2.3 Edge states

One of the marks of topological phases are excitations located at the interface between systems with different topological order. It was again the Quantum Hall effect which provided the first example for this phenomenon [17]. In the integer effect, at least while the chemical potential resides between Landau levels, the modes carrying the longitudinal current are 1-dimensional Fermi-liquid states (quantum numbers of charge carriers: momentum k, charge $q = -\mathrm{e}$, renormalized mass m^*) localized near the edges of the sample since all states are localize by disorder in the bulk. The magnetic field separates left and right movers, locating them at opposite sides (*i.e.*, the modes are unidirectional). Being topologically ordered, the fractional QH effect exhibits edge states as well, yet there Wen [18, 45, 46] showed they form in fact a chiral Luttinger liquid. This led to the prediction of a power law tunnelling I-V-curve, which was subsequently indeed observed [47, 48].

The existence of gapless excitations located at the edges is already a consequence of Laughlin's gauge argument: consider an annulus with inner radius r_1 and outer radius $r_2 > r_1$. If we increase the flux through the hole by one flux quantum, only the occupation numbers can have changed and we must have transported charge νe from the inner to the outer boundary. In the thermodynamic limit $r_1, r_2 \to \infty$ the work required for this goes to zero, *i.e.*, the boundary mode involved in the charge transfer has zero-energy.

There is also a field theoretical argument. Integrating out the electrons in the quantum Hall problem we are left with an effective Lagrangian for the gauge field A_μ [18]

$$\mathscr{L}_{\text{eff}} = \frac{\nu e^2}{4\pi} \delta A_\mu \partial_\nu \delta A_\lambda \epsilon^{\mu\nu\lambda} + \frac{1}{4g_1^2}(\delta F_{0i})^2 + \frac{1}{4g_2^2}(\delta F_{12})^2 + \dots \tag{2.34}$$

where δA_μ is the difference of the local gauge potential to a uniform background and $\delta F_{\mu\nu} = \partial_\mu \delta A_\nu - \partial_\nu \delta A_\mu$ is the field strength. The action $S_{\text{bulk}} = \int \mathrm{d}^3 x \mathscr{L}_{\text{eff}}(\delta A_\mu(x))$ is invariant under gauge transformations $A_\mu \to A_\mu + \partial_\mu \Lambda$ only on a compact manifold, like a torus. On, say, a disc however one has

$$S_{\text{bulk}}(\delta A_\mu + \partial_\mu \Lambda(x)) - S_{\text{bulk}}(\delta A_\mu) = \int \mathrm{d}x_0 \mathrm{d}\sigma \frac{\nu e^2}{4\pi} \Lambda \, \delta F_{\sigma 0} \tag{2.35}$$

where σ parametrizes the boundary. Thus, in order to have a total action which is gauge-invariant, one postulates a boundary action S_{bd} satisfying

$$S_{\text{bd}}(\delta A_\mu + \partial_\mu \Lambda(\sigma)) - S_{\text{bd}}(\delta A_\mu) = -\int \mathrm{d}x_0 \mathrm{d}\sigma \frac{\nu e^2}{4\pi} \Lambda \, \delta F_{\sigma 0}. \tag{2.36}$$

This action is generated by a Langrangian depending on the part of the gauge field localized at the boundary $\mathscr{L}_{\text{bd}} = \mathscr{L}_{\text{bd}}(\delta A_\mu(\sigma))$. One can go on to derive the functional form of the boundary action S_{bd} and from this the algebra of the edge-excitations of a QH fluid, but there is a more intuitive way.

Exploiting the fact that FQH and spin liquids are incompressible, one can find an intuitive derivation of the chiral edge states [49]. Assume we have a droplet of (incompressible) fluid with circular boundary localized by a smooth potential. The quantum-Hall conductance σ_H will cause a circular current along the edge as response to the field gradient:

$$\vec{j} = \sigma_H \, \hat{e}_{\text{z}} \times \vec{E}_{\text{bd}}, \quad \sigma_H = \nu \frac{e^2}{h} \tag{2.37}$$

This means electrons are moving along the boundary with the drift velocity $v = Ec/B$, where c is the light velocity. A wave along the edge can be described by a scalar density $\rho(x)$, where x is the coordinate along the edge. A wave packet satisfies the equation of motion

$$\partial_t \rho - v \partial_x \rho = 0 \tag{2.38}$$

where propagation can only happen in the direction determined by the Lorentz force. The energy stored in the wave is

$$H = \int \mathrm{d}x \, \frac{1}{2} e^2 h \rho E = \int \mathrm{d}x \, \pi \nu v \rho^2. \tag{2.39}$$

Taking the Fourier transform this becomes

$$\begin{aligned} \dot{\rho}_k &= ivk \, \rho_k \\ H &= 2\pi \frac{v}{\nu} \sum_{k>0} \rho_k \rho_{-k}. \end{aligned} \tag{2.40}$$

This is just a set of the classical equations of motion $\dot{q} = \partial H/\partial p$, $\dot{p} = -\partial H/\partial q$ if we identify ρ_k as the 'coordinates' with the corresponding canonical momenta $p_k = 2\pi i \rho_{-k}/\nu k$. If we now

canonically quantize the theory, *i.e.*, assume $[q_k, p_{k'}] = i\delta_{k-k'}$, we arrive at

$$\begin{aligned} [\rho_k, \rho_{k'}] &= \frac{\nu}{2\pi} k \delta_{k+k'} \\ k,\, k' &= \text{integer} \times \frac{2\pi}{L} \\ [H, \rho_k] &= v\rho_k \end{aligned} \tag{2.41}$$

This is called a U(1) Kac-Moody algebra. It is essentially a collection of independent harmonic oscillators with dispersion $\hbar\omega_k = vk$ for $k > 0$, reflecting the fact that propagation can happen only in one direction. The level degeneracies for some fixed total momentum are

$k_{\text{tot}}/2\pi/L$	0	1	2	3	4	5	6	...	n
# levels	1	1	2	3	5	7	11	...	$p(n)$

where $p(n)$ is the number of partitions of n into positive integers.

If our quantum Hall fluid supports non-Abelian statistics, this is in fact not the whole story. In that case, we have to supplement (2.41) by a chiral Majorana fermion mode [46], yielding a different total momentum degeneracy spectrum. Therefore, given sufficiently fine momentum resolution, one can distinguish between different topological orders by looking at the edge excitations, which was recently exploited in entanglement spectrum analyses [7, 50] (see also chapter 4).

Topological insulators. —In the case of the Hall-effect it is the magnetic field permeating the sample which imposes a non-trivial topology on the electronic states. But something similar can also happen without external field due to the internal spin-orbit coupling. In that case there is now a correlation between direction of motion and direction of spin polarisation which causes any current through the material to show a net spin-polarisation.

Closely related to this is the new field of *topological insulators* which emerged when in 2005 Kane and Mele [51] realized that spin orbit interaction can create charge or spin carrying states on the boundary of systems which are insulators in the bulk. In their paper they studied monolayer-graphene with spin orbit interaction. The low energy dispersion of clean graphene shows famous Dirac-cones at the K and K' points of the (hexagonal) Brillouin zone. Under the influence of spin-orbit coupling, the dispersion changes from linear to quadratic and the cones become gapped. Kane and Mele were now able to show, that the presence of a boundary, *i.e.*, when the graphene sheet is cut into a semi-infite system or a ribbon, gives rise to gapless propagating modes along the edge which are robust even in the presence of a perturbation, as long as time reversal symmetry is preserved (Figure 2.4).

A year later, in 2006, Bernevig *et al.* [52] proposed a 2D system in which these gapless edge states were indeed observed [53]. Soon after 3 dimensional materials showing topologically insulating behaviour were also discovered [54, 55]. If the boundary, which is a 2D surface there, has a certain orientation with respect to the crystal lattice (*e.g.* (111) in Bi_2Se_3, momentum parallel to the surface is well defined and spin-orbit interaction induces a Dirac-cone like dispersion as long as time reversal symmetry is maintained. Therefore even if the bulk material has a band gap, the surface will support gapless modes.

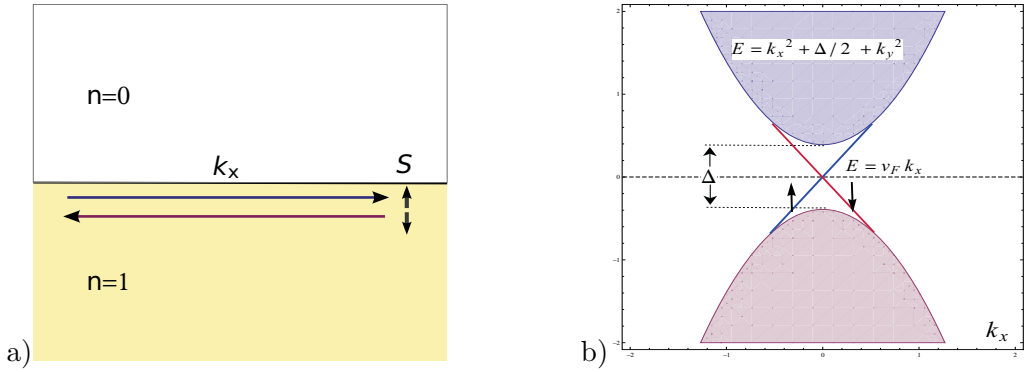

Figure 2.4: a) a two dimensional, semi-infinite topological insulator (n=1 region): spin-orbit interaction induces a band gap in the bulk and a direction dependent spin polarisation. The topology of the bands cannot be smoothly connected to the insulator (n=0 region) without closing the gap. This gives rise to b) excitations lying in the gap between (idealized parabolic) highest occupied and lowest unoccupied band

2.4 Chiral spin liquids

Besides fractional Quantum Hall liquids, spin liquids are another class of system which also exhibit characteristic features of topological order. What makes them attractive for theoretical study is their discrete nature, naturally amenable to numerical investigation and also, the possibilty to find exactly solvable models showing toplogical effects. The recent example for the latter is the Kitaev model [24] of spins on a Honeycomb-lattice with direction-dependent nearest neighbour interactions. The exact, time-reversal breaking groundstate found by Yao and Kivelson [25] supports non-Abelian vortex excitations.

Here however, we want to look more closely at the chiral spin liquid, in particular the spin $S = 1/2$ liquid due to Laughlin [4] which we will use in the next chapter as basic building block for a hierarchy of liquids with a higher spin S per site.

Under a generic spin liquid in two spatial dimensions we want to understand a homogeneous, spin-rotation invariant state on a lattice where all 2-point correlators vanish with increasing separation

$$\langle \hat{\boldsymbol{S}}_{z_i} \hat{\boldsymbol{S}}_{z_i+\Delta z} \rangle \overset{\Delta z \to \infty}{\longrightarrow} 0 \tag{2.42}$$

even at *zero temperature*. This decrease is often exponential, as in the case of the Laughlin liquid [56], but can also obey a power law, like in the *algebraic spin liquids* [40] which are candidates for the multitude of low-lying excitations of a Heisenberg model on the Kagome-lattice. The above definition is meaningful, whether all sites harbour a spin or not. Yet unless explicitly stated otherwise, we will in the following assume all sites to be occupied by (immobile) spins (*i.e.*, like in a Hubbard model at half filling and large U).

What local properties are required by and compatible with (2.42)? Homogeneity implies that spin rotation invariance must not only hold for the total system but also for finite subsystems (of sufficient size). This in turn means there must be strong local anti-ferromagnetic

correlations

$$\langle \hat{\boldsymbol{S}}_{z_i} \hat{\boldsymbol{S}}_{z_i+a} \rangle \gtrsim -1$$

where a is the lattice constant.

2.4.1 The Chiral Spin Liquid (CSL)

Based on an idea by D.H. Lee, Kalmeyer and Laughlin [4] put forward a chiral spin liquid wave function as a trial state for electrons in the CuO planes of high temperature superconducting materials.

A *chiral* spin liquid (CSL), *i.e.*, one which breaks parity (P) and time reversal (T), can be characterised in several ways [33].

For one, a CSL has a nonzero expectation value of the chirality operator, defined as

$$\chi_{ijk} := \hat{\boldsymbol{S}}_i \cdot (\hat{\boldsymbol{S}}_j \times \hat{\boldsymbol{S}}_k) \tag{2.43}$$

where ijk is a triple of neighbouring sites from one triangular plaquet (see Fig. 2.5). Parity or time reversal symmetry would force $\langle \chi_{ijk} \rangle$ to be 0 everywhere, since both change the sign of the triple product (P changes the order $ijk \to ikj$, while T flips the sign of each spin). For the same reason, the combined PT symmetry may be preserved in a chiral spin liquid.

A non-vanishing $\langle \chi_{ijk} \rangle$ can also be interpreted as a nonzero Berry's phase when we transport spins around the triangle ijk. Let $P_{(ijk)}$ be the operator effecting the cyclic permutation (ijk) we have

$$B_{ijk} := \langle P_{(ijk)} \rangle = \langle P_{(ij)} P_{(jk)} \rangle \tag{2.44}$$

$$= \frac{1}{4} \langle (1 + \hat{\boldsymbol{S}}_i \hat{\boldsymbol{S}}_j)(1 + \hat{\boldsymbol{S}}_j \hat{\boldsymbol{S}}_k) \rangle \tag{2.45}$$

and from this one can see that Berry's phase B_{ijk} and chirality χ_{ijk} are directly related through

$$\langle \chi_{ijk} \rangle = -2i \, (B_{ijk} - B_{ikj}). \tag{2.46}$$

This allows the alternative characterisation of a chiral spin liquid as a spin state, where clockwise and counterclockwise spin transport yield *different* Berry's phase.

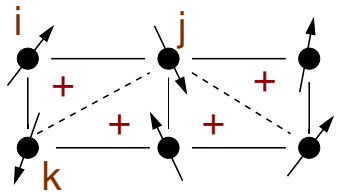

Figure 2.5: Snapshot of a 2×3 patch of a square lattice. The chirality operator (2.43) is defined for sites from one (triangular) plaquet.

As stated, both χ_{ijk} and B_{ijk} are well defined only for fully occupied lattices. Introducing electron creation/destruction operators $c_i, c_i^\dagger$ and using them to express the spin operator as

$$\hat{\boldsymbol{S}}_i = \hbar/2\, c_{i,\tau}^\dagger \vec{\sigma}_{\tau\tau'} c_{i,\tau'} \tag{2.47}$$

where $\vec{\sigma}$ is the vector of Pauli-matrices we can give meaning to it for general fillings, *i.e.*, when some sites are empty (*e.g.* due to doping).

Vanishing two point correlators only indicate absence of 'classical' magnetic long range order. Because of homogeneity, $\chi = 1/N \sum_{(ijk)} \langle \chi_{ijk} \rangle$ is finite and therefore the chiralities must be correlated over arbitrary distances. There are two ways to obtain a state with vanishing χ: relaxing translation- invariance, *e.g.* in a square lattice restricting it to the two sublattices with doubled lattice constant, or, the solution we will pursue in the next chapter, merging $S = 1/2$ chiral spin liquids with opposite chiralities into a liquid with higher spins per site.

2.4.2 CSL wave function

The Laughlin CSL for N spins $S = 1/2$ on a lattice with open boundary conditions can be written as [4]

$$|\psi^{\mathrm{CSL}}\rangle = \sum_{\{z_1,\dots,z_M\}} \psi^{\mathrm{CSL}}[\boldsymbol{z}]\, S^+_{z_1} \dots S^+_{z_M} \, |\downarrow\rangle_N \tag{2.48}$$

where the sum is over all subsets of M sites and $|\downarrow\rangle_N$ denotes the fully spin- down polarized state. The wave function ψ^{CSL} for open boundary conditions is

$$\psi^{\mathrm{CSL}}[\boldsymbol{z}] = \prod_{j=1}^{M} G(z_j) \prod_{i<j}^{M} (z_i - z_j)^2 \prod_{j=1}^{M} \mathrm{e}^{-\frac{\pi M}{2N}|z_j|^2} \tag{2.49}$$

where the product over $G(z_i)$ acts as a gauge, ensuring that ψ^{CSL} is a singlet. On the square lattice with unit lattice constant it is given by $G(z = x + iy) = (-1)^{(x+1)(y+1)}$ but generalises to arbitary lattices as depicted in Figure 2.6 Apart from this, (2.48) is form-equivalent to a bosonic fractional Quantum Hall state in a magnetic field of M/N flux quanta per plaquet:

$$\frac{1}{4l^2} = \frac{\pi}{2}\frac{N_\Phi}{N\,a} \overset{!}{=} \frac{\pi M}{2N} \;\Rightarrow\; B = \frac{M}{N}\Phi_0$$

where l^2 is the magnetic length defined in (2.2).

Just like other $1/m$-Laughlin liquids, the CSL can be mapped onto a torus by help of the odd Jacobi theta function:

$$\psi^{\mathrm{CSL}}_{\mathrm{torus}}[\boldsymbol{z}; Z_0] = \mathrm{e}^{i\,K(Z_0)Z}\, \vartheta(Z - Z_0|\tau)\vartheta(Z - Z_0|\tau) \prod_{i<j}^{M} \vartheta^2(z_i - z_j|\tau) \prod_{j=1}^{M} G(z_j)\, \mathrm{e}^{-\frac{\pi}{2}|z_j|^2 - z_j^2} \tag{2.50}$$

where C is the center of the lattice cluster and Z_0 a center-of-mass-zero parameter needed to ensure quasi-periodicity. In appendix A.2 we investigate the boundary conditions in detail.

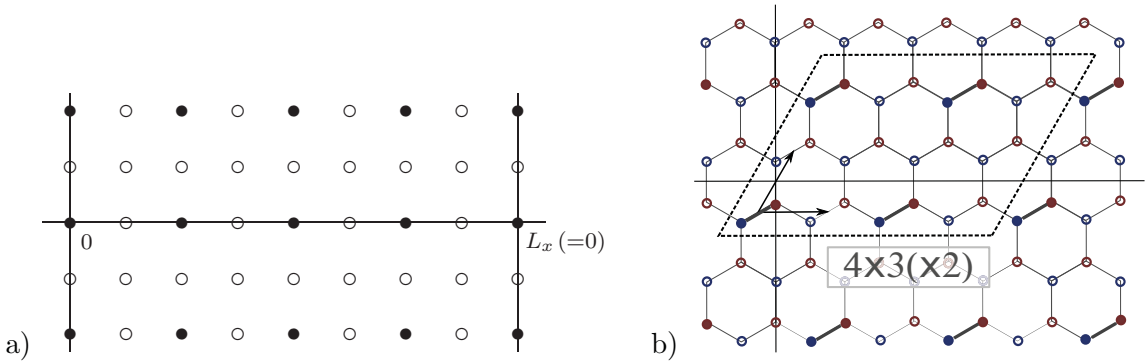

Figure 2.6: The site dependent sign $G(z)$ on the a) square and b) hexagonal lattice. Filled dots represent $G(z) = 1$ circles $G(z) = -1$. On a general lattice $\{n\boldsymbol{a} + m\boldsymbol{b} | n, m \in \mathbb{Z}\}$, spanned by vectors $\boldsymbol{a}$ and $\boldsymbol{b}$, G is given in a similar way $G = (-1)^{(n+1)(m+1)}$

Varying Z_0 in the principal region yields a 2 dimensional functional space, *i.e.*, the topological degeneracy of the $s = 1/2$ CSL is 2.

Spin rotation invariance as well as vanishing correlation follow directly from the same statements for a FQH state. Only translation invariance is broken in the open boundary formulation (2.48), but it will be restored when we write it in periodic boundary conditions. It is a spin singlet and P and T are both broken, as is evident once we realize that both operations correspond to complex conjugation: T because it is anti-unitary and P since in 2 dimensions parity means flipping *one* axis. If we define (2.49) to have chirality '+', P as well as T send ψ_+^{CSL} to ψ_-^{CSL}.

2.4.3 CSL from lowest Landau level

The equivalence of the CSL wave function with a quantum Hall state inspired another way to construct it: it can be rewritten as the product of two lowest-Landau-level wave functions $\phi_{lll} = \prod_{i<j} z_i - z_j \prod_j \exp(-\pi/4|z_j|^2)$ in a fictuous magnetic field of strength Φ_0 per lattice plaquet [57]:

$$\psi^{\mathrm{CSL}}[\boldsymbol{z}] = S[\boldsymbol{z}, \boldsymbol{w}]\, \phi[\boldsymbol{z}]\phi[\boldsymbol{w}]. \tag{2.51}$$

Here $\boldsymbol{w}$ are the $N - M$ lattice sites complementary to the M sites $\boldsymbol{z}$. This is a manifestation of a 'particle-hole'-type of symmetry between up- and down-spin spinons. $S[\boldsymbol{z}, \boldsymbol{w}]$ is an order dependent sign related to $G(z_i)$ which can be expressed using electron destruction operators $c_{z\downarrow}$

$$S[\boldsymbol{z}, \boldsymbol{w}] := \langle 0 | c_{z_1\downarrow} \dots c_{z_M\downarrow} c_{w_1\downarrow} \dots c_{w_{N-M}\downarrow} | \underbrace{\downarrow\downarrow \dots \downarrow}_{\text{all } N \text{ spins } \downarrow} \rangle\,. \tag{2.52}$$

This formulation of the CSL is of high practical relevance to us, as our numerical procedure to write out explicit $S = 1/2$ CSL wave functions makes direct use it.

The for $M = N/2$ the state $|\psi^{\mathrm{CSL}}\rangle$ can also be expressed as the Gutzwiller-projection of a

Slater-determinant of single particle states

$$|\psi_+^{\mathrm{CSL}}\rangle = P_{\mathrm{GW}}\,|\psi_{\mathrm{SD}}^N\rangle \tag{2.53}$$

where

$$P_{\mathrm{GW}} = \prod_j (1 - c_{i\uparrow}^\dagger c_{i\uparrow} c_{i\downarrow}^\dagger c_{i\downarrow}) \tag{2.54}$$

eliminates configurations with doubly occupied sites and

$$|\psi_{\mathrm{SD}}^N\rangle = \sum_{\{z_1,\ldots,z_N\}} \prod_{i<j} (z_i - z_j) \prod_j \mathrm{e}^{-\frac{\pi}{2}|z_j|^2}\; c_{z_1\uparrow}^\dagger \ldots c_{z_M\uparrow}^\dagger c_{z_{M+1}\downarrow}^\dagger c_{z_N\downarrow}^\dagger\,|0\rangle \tag{2.55}$$

This is clearly a singlet, and since Gutzwiller-projection does not affect the spin on each site, *i.e.*,

$$[P_{\mathrm{GW}}, \boldsymbol{S}_j] = 0$$

so is $|\psi^{\mathrm{CSL}}\rangle$.

The Gutzwiller construction is especially useful when we want to describe states with spinon or holon excitations. For instance

$$|\psi_{+\,\eta_1\downarrow\ldots\eta_L\downarrow}^{\mathrm{CSL}}\rangle = P_{\mathrm{GW}} c_{\eta_1\uparrow}\ldots c_{\eta_L\uparrow}\,|\psi_{\mathrm{SD}}^{N+L}\rangle \tag{2.56}$$

is a state with N spins and L down-spin spinons obtained from the Slater- determinant state for $N+L$ spins on N sites by removing up-spins on sites η_1 to η_L. A state with $L = 2K$ holons can be written as

$$|\psi_{+\,\eta_1\ldots\eta_L}^{\mathrm{CSL}}\rangle = P_{\mathrm{GW}} c_{\eta_1\uparrow}\ldots c_{\eta_K\uparrow} c_{\eta_{K+1}\downarrow}\ldots c_{\eta_L\downarrow}\,|\psi_{\mathrm{SD}}^N\rangle\,. \tag{2.57}$$

The spinon excitations of the CSL have half-Fermi statistics if $M = N/2$. Once again, this can be worked out from the complete analogy to the fractional QHE [12]: We have 2 flux quanta per degree of freedom z_i which corresponds to fictuous filling factor of $\nu' = 1/2$ and therefore statistical parameter $\theta = \pi/2$. When constructing these excitations explicitly we again add factors $\prod_j(\xi - z_i)$, each representing a hole at position ξ, which need not be a lattice site! This might be somewhat counter-intuitive, but there is no mathematical or other reason to demand that restriction.

From the statistics we can deduce the topological degeneracy of the Laughlin CSL to be 2. This confirms the result one obtains when adapting the CSL explicitly to (quasi-)periodic boundary conditions.

3 Fractional spin liquid hierarchy

In this chapter we present one of the main results of this work, a hierarchy of spin S liquids built by Schwinger projection from $2S$ copies of Laughlin's chiral spin liquid.

These liquids are characterized by the numbers of constituent CSLs with chiralities '+' and '-' and support excitations with non-Abelian statistics as soon as a chirality appears more than once, *i.e.*, for all $S \geq 3/2$. We investigated the topological degeneracy (TD) of all liquids up to $S = 2$ by numerically writing out their wave function on up to $N = 16$ site clusters with periodic boundary conditions and varying the center-of-mass-zero parameters and found it to be given by

$$\mu_{\mathrm{TD}}(k_+, k_-) = (k_+ + 1)(k_- + 1) \tag{3.1}$$

where k_+ and k_- are the number of chirality '+' and '-' CSLs respectively, *i.e.*, $2S = k_+ + k_-$.

A particularly interesting example is the $S = 2$ liquid obtained from merging 2 CSLs of each chirality (S2CL). It exhibits a topological degeneracy of 9, not $2^4 = 16$ as a straighforward extrapolation of the CSL degeneracy would imply. There must therefore be some kind of blocking mechanism at work, like the one described in the previous chapter, and this is indicative of non-Abelian statistics. Moreover, its wave function is real, it therefore preserves parity (P) and time reversal (T) unlike the original $S = 1/2$ CSL. The S2CL might make a good candidate trial state for disordered quantum antiferromagnets, since their hamiltonian generally also conserves P and T and should exhibit sponeneous symmetry breaking only in peculiar cases. We want to note, that since the CSL is well defined on any lattice, so are all our liquids derived from it (see appendix A.3).

In the following, we first show how Schwinger-boson projection can be used to merge $S = 1/2$ CSLs into liquids with higher spin per site, then we review the first two members of the hierarchy, the $S = 1$ chiral spin liquid (NACSL) obtained from two ($S = 1/2$) CSLs of *equal* chirality and the $S = 1$ 'chirality liquid' (CL) built from two CSLs of *opposite* chirality. Each was individually described in [58] and [57] respectively, however they were not understood as part of a general scheme of constructing non-Abelian liquids presented here nor were the topological properties confirmed in 'ab initio' numerical studies.

3.1 Setting up the hierarchy

The main idea behind the construction is to replace SU(2) spin S operators $\hat{\boldsymbol{S}}$ by products of $2S$ boson operators $a^\dagger, b^\dagger$ (Schwinger bosons) in the expression for the state $|\psi^{\mathrm{CSL}}\rangle$. This allows merging them into liquids with higher spin per site by simple multiplication.

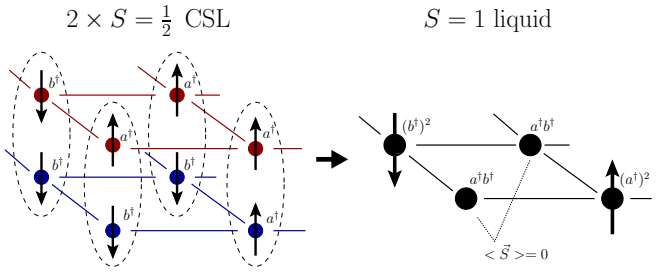

Figure 3.1: Using Schwinger bosons, merging $S = 1/2$ liquids, here 2 of them, is done by simple multiplication of liquid creation operators

3.1.1 Rewriting the CSL

In section 2.4.3 we showed that ψ^{CSL} is expressible as the product of two lowest-Landau-level wave functions ϕ. This property we now use to write down a creation operator for the $S = 1/2$ chiral spin liquid on a cluster of N sites.

To recall the CSL wave function, it is given by (see (2.51))

$$\psi_+^{\mathrm{CSL}}[\boldsymbol{z}] = S[\boldsymbol{z}, \boldsymbol{w}]\, \phi[\boldsymbol{z}]\phi[\boldsymbol{w}]$$

with the many-particle fermionic sign $S[\boldsymbol{z}, \boldsymbol{w}]$ ensuring the proper sign associated with a configuration $(z_1, \ldots, z_M)$, which is basically the sign of the permutation needed to bring $(z_1, \ldots, z_M)$ into (some) standard order.We should point out again, that the set of sites $\{w_1, \ldots, w_{N-M}\}$ can be thought of as the complementary set to $(z_1, \ldots, z_M)$ and is therefore determined up to reordering, which will in all sums below only yield a prefactor that can be absorbed into normalisation.

The idea is now to replace spin operators by Schwinger bosons $a^\dagger, b^\dagger$ in the expression for $|\psi^{\mathrm{CSL}}\rangle$. These operators obey the usual bosonic commutation relations. The connection between the spin state $|S, S^{\mathrm{z}}\rangle$ and a state with $2S$ Schwinger bosons is given by

$$|S, S^z\rangle = \frac{(a^\dagger)^{S+S^{\mathrm{z}}}(b^\dagger)^{S-S^{\mathrm{z}}}}{\sqrt{(S+S^{\mathrm{z}})!(S-S^{\mathrm{z}})!}}\,|0\rangle\,. \tag{3.2}$$

The key advantage this formulation offers, is the ease with which we can project two individual spins S_1, S_2 onto their symmetric total spin state $|S = S_1 + S_2, S^{\mathrm{z}}_{\mathrm{tot}}\rangle$ for all values of $S^{\mathrm{z}}_{\mathrm{tot}}$. What in SU(2) language requires a sum over all states $S^{\mathrm{z}}_1 + S^{\mathrm{z}}_2 = S^{\mathrm{z}}_{\mathrm{tot}}$, with Schwinger bosons reduces to a simple product of creation operators (see also appendix B.1 for more details).

Spin $S = 1/2$ is represented in this new language by states with only a single Schwinger boson. The two possible states are therefore $a^\dagger|0\rangle \mathrel{\hat{=}} |1/2, 1/2\rangle$ and $b^\dagger|0\rangle \mathrel{\hat{=}} |1/2, -1/2\rangle$ and these are mapped onto each other by the operators $a^\dagger b$ and $ab^\dagger$ respectively. This motivates the definition of a CSL creation operator

$$\hat{\Psi}_+^{\mathrm{CSL}}[a^\dagger, b^\dagger] := \sum_{\{z_i\},\{w_j\}} \psi_+^{\mathrm{CSL}}[\boldsymbol{z}] a^\dagger_{z_1} \ldots a^\dagger_{z_M} b^\dagger_{w_1} \ldots b^\dagger_{w_{N-M}}. \tag{3.3}$$

Here, as in section 2.4.3, the sum is over all ways of choosing sites $z_1, \ldots, z_M$ and $w_1, \ldots, w_{N-M}$ from the lattice where $\boldsymbol{z}$ and $\boldsymbol{w}$ are disjoint. Note, that we do not have to require single occupancy for either set of sites, because configurations with double occupancies are eliminated by the wave function anyway.

From our observation about products of Schwinger operators in the previous paragraph it is clear, that applying $\hat{\Psi}_+^{\mathrm{CSL}}$ to the vacuum k times will give a state with k Schwinger boson operators $a^\dagger$, $b^\dagger$ per site corresponding to a total spin $S = k/2$ per site. This remains true, if we mix in CSLs with opposite chirality, $\hat{\Psi}_-^{\mathrm{CSL}}$, and the order in which we apply the different chiralities does not matter, since the operators are all bosons. Thus, we use (3.3) to construct states

$$|\psi^{S,k_+}\rangle = \left(\hat{\Psi}_-^{\mathrm{CSL}}\right)^{2S-k_+} \left(\hat{\Psi}_+^{\mathrm{CSL}}\right)^{k_+} |0\rangle \tag{3.4}$$

characterised by their total spin S and the number of CSLs with positive chirality k_+. This is the hierarchy of spin liquids we announced at the start of this chapter. We will now elaborate the methods we used for analysing their topological degeneracy, the results obtained and what we can infer about the physics of their fundamental excitations (statistics, gap, edges). In particular we will have a close look at the $S = 2$ state made from two chirality '+' and '-' CSLs each, because it is the first example of a state which unites non-Abelian statistics with parity and time-reversal symmetry.

3.2 Numerical determination of Topological degeneracy

We now turn to our numerical implementation of the Schwinger boson scheme and how within it we can determine topological degeneracy of the $S = 1/2$ chiral spin liquid and any higher-spin liquid we might construct from the CSL.

There are various ways to determine the topological degeneracy. One would be obtaining the entanglement entropy of a topologically nontrivial region as will be described in more detail in the next chapter about entanglement spectra. With the computational resources available to us, this is however very challenging to do for higher spins on clusters of meaningful size: the simplest nontrivial region on a square lattice is a holed-out 3×3 sector, *i.e.*, ring of 8 sites enclosing one single site and therefore we need at least $4 \times 4 = 16$ sites to make this ring well defined (separated) in all directions (on a triangular lattice the required minimal region is the same while on a hexagonal lattice it is much bigger). In this case even the $S^{\mathrm{z}} = 0$ subspace of the $(S = 2)^{\otimes 16}$ product space has dimension $\approx 10^{10}$.

And even on a 16-site lattice, finite size effects would probably mask topological effects, since in deriving the scale invariant entropy Kitaev *et al.* [6] assumed the region studied to be large enough, that the boundaries can be considered smooth on the scale of the lattice constant.

We therefore opted for the more viable approach of exploiting the analytical form (3.3) of the $S = 1/2$ CSL. The basic idea is to write down two lowest Landau-level wave functions ϕ_{Z_0} adapted to the torus on the Hilbert space spanned by all $S^{\mathrm{z}}_{\mathrm{tot}} = 0$ product states of an N site lattice cluster. We then combine the LLL wave functions into a CSL as described in 2.4.3. The LLL wave functions depend on one center of mass coordinate Z_0 each, but in fact only their difference is of relevance (cp. appendix A), so that ψ^{CSL} also has only one effective

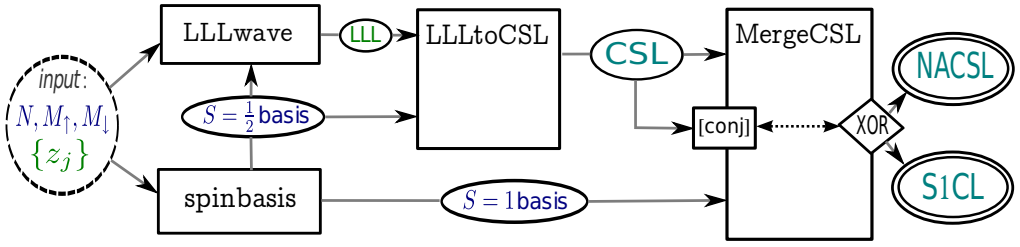

Figure 3.2: Flowchart of the numerics involved in determining the topological degeneracy for $S = 1$.

center-of-mass parameter Z_0. After having constructed the basic building block, we proceed in different ways, depending on the spin per site of the liquid we wish to obtain in the end: For $S = 1$, we create a copy of ψ^{CSL}, apply complex conjugation if necessary, compute a list with all $S^{\mathrm{z}}_{\mathrm{tot}} = 0$ product states for $S = 1$ per site and feed these three inputs to a program implementing the Schwinger boson procedure. The output is a list of $S = 1$ product states together with their amplitudes. The liquid we obtain will be a $S = 1$ analog if we use two CSLs of equal chirality (no complex conjugation), which we call the non-Abelian chiral spin liquid (NACSL), or a real-valued, P and T conserving liquid, the $S = 1$ chirality liquid (CL), if we use one complex conjugated CSL (see Fig. 3.2).

If $S = 3/2$, there are also basically only two different cases to distinguish: either all 3 CSLs have the same chirality ($k_+ = 3$ or $k_+ = 0$) or only two have ($k_+ = 1, 2$). The numerical work is again nearly the same in both cases: we call a merging procedure with 3 copies of a CSL wave function, one possibly conjugated, and a basis list of $S^{\mathrm{z}}_{\mathrm{tot}} = 0$ product states.

The $S = 2$ liquids were however not obtained by merging 4 CSLs, but rather from two $S = 1$ liquids. The three cases one must distinguish are 2×NACSL, NACSL× CL or 2× CL. The last can equally well be expressed (and computed) from two NACSLs with opposite chirality and as it will become clear below, this is in fact the appropriate way to describe it, because only this picture describes the correct topological degeneracy.

In all cases above, the final output is a wave function $\psi^S_{Z_0}$ for some spin S per site and a center-of-mass-zero parameter Z_0. Two such wave functions for different Z_0 will i.g. not be collinear. Rather, as Z_0 varies over the principal region, the wave functions $\psi^S_{Z_0}$ will span a manifold of a dimension equal to the topological degeneracy. We can only sample this manifold at finitely many points, so repeat the above procedure several times, each time with a different, randomly chosen center-of-mass-zero $Z_{0,j}$. The random selection minimizes the risk that, by accident, we are stuck in a subspace of the full wave function space. We then determine the dimension of the space spanned by all these states. This can be done simply by computing the rank of the mutual scalar-product matrix

$$\left(\langle \psi^S_{Z_{0,i}} | \psi^S_{Z_{0,j}} \rangle\right) \tag{3.5}$$

In addition to selecting points randomly, we also used as many as were computationally feasible in order to be reasonably certain to really visit all dimensions in the ground state manifold.

spin	*liquid*	O(dim$\mathscr{H}$)	# *samples*	*top. degeneracy*
1/2	CSL	10^2	15	2
1	$\mathrm{CSL}_+\mathrm{CSL}_+$	$5 \cdot 10^4$	20	3
	$\mathrm{CSL}_+\mathrm{CSL}_-$		20	4
3/2	$(\mathrm{CSL}_+)^3$	$4 \cdot 10^6$	9	4
	$(\mathrm{CSL}_+)^2\mathrm{CSL}_-$		9	6
2	$(\mathrm{CSL}_+)^4$	$2 \cdot 10^3$	50	5
	$(\mathrm{CSL}_+)^3\mathrm{CSL}_-$		50	8
	$(\mathrm{CSL}_+)^2(\mathrm{CSL}_-)^2$		50	9
$k/2$	$(\mathrm{CSL}_+)^k$			$k+1$
k	$(\mathrm{CSL}_+)^k(\mathrm{CSL}_-)^k$			$(k+1)^2$

Table 3.1: Topological degeneracies a selected hierarchy liquids. Liquids with $S \leq 2$ have been investigated numerically on up to 16 site square lattice clusters by varying the center-of-mass-zero(s).

A priori, there are $2S$ center-of-mass parameters, one from each CSL. But we found empirically, that they need not be varied separately: using two independent parameters in the $S = 1$ and $S = 2$ liquids as well as 3 independent ones for $S = 3/2$, we obtained the same topological degeneracy as when we used the same Z_0 for all constituent CSLs.

Table 3.1 gives the results we obtained on square lattice clusters of size 16 in the case of $S \leq 3/2$ and 8 for $S = 2$. The last two rows give the values we would expect to obtain for higher spins per site, based on the the equivalence of the spin liquids of power k in our hierarchy with the Read-Rezayi level-k series of liquids from the fractional quantum Hall effect [26].

3.3 Special hierarchy states

We will now take a closer look at some of the liquids in our hierarchy: the two $S = 1$ liquids already known [57, 58] and series of liquids obtained by merging k CSL copies of the same chirality.

3.3.1 $S = 1$ liquids

The possible combinations of two $S = 1/2$ CSLs are the $S = 1$ chiral spin liquid (NACSL) and the $(S = 1)$ *chirality liquid* (S1CL). They are obtained by merging CSLs of equal or opposite chiralities respectively.

Non-Abelian chiral spin liquid. —Let us first consider the NACSL. In Schwinger language,

it is

$$|\psi_+^{\mathrm{NACSL}}\rangle = \hat{\Psi}_+[a^\dagger, b^\dagger]\hat{\Psi}_+[a^\dagger, b^\dagger]\,|0\rangle \tag{3.6}$$

As was shown in [58] it is a spin singlet and supports non-Abelian statistics. The last statement can be understood from its wave function, which is a bosonic Pfaffian FQH state

$$\psi_+^{\mathrm{NACSL}}[\boldsymbol{z}] = \mathrm{Pf}\left[\frac{1}{z_i - z_j}\right]\prod_{i<j}^{N}(z_i - z_j)\prod_j G(z_j)\mathrm{e}^{-\pi/2|z_j|^2} \tag{3.7}$$

where $\mathrm{Pf}\,[z_i - z_j]$ is shorthand for the Pfaffian polynomial obtained by anti-symmetrising over all differences $(z_{2j-1} - z_{2j})$:

$$\mathrm{Pf}\,[z_i - z_j] = \mathscr{A}\left\{(z_1 - z_2)(z_3 - z_4)\dots(z_{N-1} - z_N)\right\} \tag{3.8}$$

The Pfaffian can also be obtained as the square root of the determinant of the anti-symmetric Jastrow-matrix $J_{ij} = (z_i - z_j)$, $i, j = 1 \dots N$:

$$\mathrm{Pf}^2\,[z_i - z_j] = \det\left[(z_i - z_j)\right] \tag{3.9}$$

which implies that it vanishes for odd number of variables, *i.e.*, in all wave functions N must always be even.

This wave function describes 'pairing' of electrons in the following sense: consider the first summand of the Pfaffian, which is just $1/(z_1 - z_2)(z_3 - z_4)\dots(z_{N-1} - z_N)$. This will cancel the respective factors of the Jastrow polynomial $\prod_{i<j}(z_i - z_j)$. Therefore in the product monomial (of degree $N - 2$ in each z_j and $N^2/2 - N$ in total) close approaches of the 'partners' (z_1, z_2), (z_3, z_4) and so on are not suppressed any more, *i.e.*, . they can be considered as 'bound' more closely.

As in the bosonic representation of the $S = 1/2$ CSL this wave function can be combined with spin flip operators, but here these have to be renormalised to account for the different normalisation of the Schwinger bosons (cp. (B.6)).

The non-Abelian chiral spin liquid state with spin-operators is then

$$|\psi^{\mathrm{NACSL}}\rangle = \sum_{\{z_1,\dots,z_N\}} \psi_+^{\mathrm{NACSL}}[\boldsymbol{z}]\,\tilde{S}^+_{z_1}\dots\tilde{S}^+_{z_N}\,|-1\rangle_N\ . \tag{3.10}$$

The summation is over N positions z_j on the lattice where at most double occupancy is allowed, $|-1\rangle_N = |-1, \dots, -1\rangle$ is the fully spin-down polarized state and the renormalised spin flips are defined as $\tilde{S}^+ = \frac{1 \pm S^z}{2} S^\pm$.

How the Pfaffian can be derived starting from (3.6) is demonstrated in appendix B.2. The wave function is complex, *i.e.*, chiral and thus breaks both P and T symmetry. It is equivalent to a bosonic FQH Pfaffian state at filling $\nu = 1$ and exhibits non-Abelian spinon excitation of Ising-type SU(2) level 2 (see appendix B.4). A state with four excitations at the positions $\eta_1, \dots, \eta_4$ (which need not be lattice sites!) can be written:

$$\mathrm{Pf}\left[\frac{1}{z_i - z_j}\right] \to \mathrm{Pf}\left[\frac{(\eta_1 - z_i)(\eta_2 - z_j)(\eta_3 - z_i)(\eta_4 - z_j) - (i \leftrightarrow j)}{z_i - z_j}\right] \tag{3.11}$$

i.e., even index excitations are connected to even index sites and vice versa.

The topological degeneracy follows from the quantum Hall equivalence and is 3, a value we can confirm numerically. The fact that the topological degeneracy is reduced from the product of the two constituent CSLs' is another confirmation of non-Abelian statistics, as there must be some blocking mechanism at work.

$S = 1$ *chirality liquid.* —The other wave function in the $S = 1$ case, the S1CL obtained from 2 CSLs of opposite chirality, is

$$|\psi^{\mathrm{CL}}\rangle = \hat{\Psi}_+[a^\dagger, b^\dagger]\hat{\Psi}_-[a^\dagger, b^\dagger]\,|0\rangle \tag{3.12}$$

It is equally a spin singlet but, as we prove in appendix B.3, also has a real valued wave function and is thus invariant under the action of P and T. Numerically, we obtain a topological degeneracy of 4. The absence of blocking suggests that spinons keep the statistical properties they have in the constituent $S = 1/2$ CSL, but now carry a chirality quantum number. Due to the P and T invariance, this spin liquid appears to be an intersting trial state for $S = 1$ antiferromagnets. We will encounter it again in the next chapter, where we compare its entanglement spectrum to that of an $S = 1$ frustrated J_1-J_2 antiferromagnet on a 4×4 square lattice cluster.

3.3.2 Read-Rezayi series

The hierarchy liquids

$$|\psi_\pm^{k-\mathrm{CSL}}\rangle = \left(\Psi_\pm^{\mathrm{CSL}}[a^\dagger, b^\dagger]\right)^k |0\rangle \tag{3.13}$$

constructed from only one type of chirality, *i.e.*, $k_+ = 2S$ or (equivalently) $k_+ = 0$ in (3.4), have the functional form of bosonic Read-Rezayi [26] quantum Hall states at Landau-level filling fractions $\nu = S$.

In the quantum Hall context, these states describe quasi-particles made from clusters of $k = 2S$ electrons, each carrying a spin $S = 1/2$. Coulomb-repulsion seperates these electrons and can be expected to cause the k-cluster to have an antisymmetric orbital wave function, therefore total spin of the cluster is the completely symmetric spin $S = k/2$ state. The $\psi^{k-\mathrm{CSL}}$ spin liquids reflect this by allowing up to k-fold multiple occupation of the same site by particles in one cluster while otherwise suppressing close approaches of particles from different clusters like $(z_i - z_j)$.

A general Read-Rezayi k-cluster wave function can be written as

$$\psi_{k,M=1}^{\mathrm{RR}} = \sum_{P\in S_N} \prod_{0\le r<s<N/k} \chi(z_{P(kr+1)} \dots z_{P(kr+k)}; z_{P(ks+1)} \dots z_{P(ks+k)}) \tag{3.14}$$

where the polynomial

$$\begin{aligned}\chi(z_1 \dots z_k; z_{k+1} \dots z_{2k}) = {} & (z_1 - z_{k+1})(z_1 - z_{k+2})(z_2 - z_{k+2})(z_2 - z_{k+3}) \\ & \times (z_3 - z_{k+3}) \dots (z_k - z_{2k})(z_k - z_{k+1})\end{aligned} \tag{3.15}$$

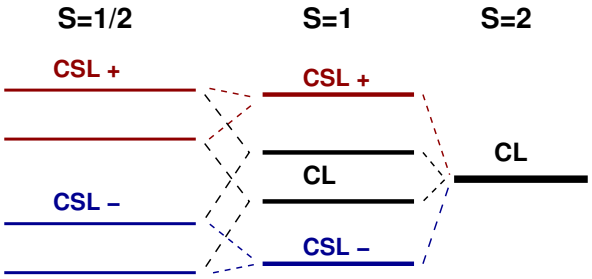

Figure 3.3: The $S = 2$ chirality liquid can be obtained in 2 ways from 2 $S = 1$ liquids. We find a topological degeneracy of 9, indicating that '+' and '-' chirality sectors form independent (at low energies) non-Abelian liquids

connects two k-clusters such that each z_i is linked to exactly two sites from the other cluster. If $k = 1$ this gives $\prod_{i<j}(z_i - z_j)^2$ which is a bosonic Laughlin-state at $\nu = 1/2$. For $k = 2$ the summand for, *e.g.* , the identity permutation is

$$\begin{aligned}\prod_{0\le r<s<N/k} \chi(z_{2r+1}\dots z_{2(r+1)}; z_{2s+1}\dots z_{2(s+1)}) &= \prod_{j=3}^{N}(z_1 - z_j)(z_2 - z_j)\prod_{j=5}^{N}(z_3 - z_j)(z_4 - z_j)\dots \\ &= \prod_{k=1}^{N/2}\prod_{j>2k}(z_{2k-1} - z_j)(z_{2k} - z_j) \\ &= \prod_k \frac{1}{z_{2k-1} - z_{2k}}\prod_{i<j}(z_i - z_j) \\ &\xrightarrow{\Sigma_{P\in S_N}} \mathrm{Pf}\left[\frac{1}{z_i - z_j}\right]\prod_{i<j}(z_i - z_j)\end{aligned}$$

i.e., this reproduces the Pfaffian. The parameter M is the exponent of the Laughlin-Jastrow factor $\prod_{i<j}(z_i - z_j)^M$, *i.e.*, wave functions with stronger repulsion and different statistics can be obtained by multiplying (3.14) with an $M-1$-Laughlin-Jastrow polynomial $\prod_{i<j}(z_i - z_j)^{M-1}$.

The equivalence to the $\psi^{k-\mathrm{CSL}}$ states of our hierarchy can be understood by looking at the expansion of $(\hat{\Psi}^{\mathrm{CSL}})^k$: we have k sets of M sites $\{z_j^\alpha\}$ and z_i^α, z_j^β are not connected by a factor $z_i^\alpha - z_j^\beta$ unless $\alpha = \beta$, *i.e.*, they form a k-cluster. In the appendix B.2 we show explicitly for the $S = 1$ NACSL, which is the first non-trivial member of the Read-Rezayi series, how symmetrization (induced by the sum over all subsets of M lattice sites) yields the exact Pfaffian.

3.4 The $S = 2$ chirality liquid

A particularly interesting spin liquid trial state constructed from 4 $S = 1/2$ CSLs is the $S = 2$ chirality liquid (S2CL). Taking two CSLs of each chirality before projection, we obtain a liquid

with real valued wave function, *i.e.*, P and T invariance are restored.

Interestingly, we arrive at the same state when merging either two S1CLs, or two NACSLs with opposite chirality

$$\begin{aligned} |\psi^{\mathrm{S2CL}}\rangle &= \left(\hat{\Psi}^{\mathrm{S1CL}}[a^\dagger, b^\dagger]\right)^2 |0\rangle \\ &= \hat{\Psi}_+^{\mathrm{NACSL}}[a^\dagger, b^\dagger]\, \hat{\Psi}_-^{\mathrm{NACSL}}[a^\dagger, b^\dagger]\, |0\rangle\,. \end{aligned} \tag{3.16}$$

The topological degeneracy of the final state is 9-fold (see Tab. 3.1), not $4 \times 4 = 16$-fold as one might be lead to believe by the first line in (3.16) above. It is hence the first instance of a blocking mechanism for a non-chiral hierarchy state, which reduces the topological degeneracy from 16 for the constituent S1CLs to 9. The construction as well as the TD suggests that (3.16) exhibits (Ising-type) non-Abelian spinon statistics for both chiralities.

This is apparent in the explicit wave function, which we obtain by expanding the CSL creation operators. It is

$$\begin{aligned} \psi^{\mathrm{S2CL}}(z_1, \ldots, z_N; w_1, \ldots, w_N) = \mathrm{Pf}\left[\frac{1}{z_i - z_j}\right] \mathrm{Pf}\left[\frac{1}{\bar{w}_k - \bar{w}_l}\right] \prod_{i<j}(z_i - z_j) \\ \times \prod_{k<l}(\bar{w}_k - \bar{w}_l) \prod_{i,k} G(z_i) G(\bar{w}_k)\, \mathrm{e}^{-\frac{\pi}{2}(|z_i|^2 + |w_k|^2)} \end{aligned} \tag{3.17}$$

here, $\{z_i\}$ and $\{w_j\}$ are independent sets of sites on the lattice where at most double occupancy is allowed within each set.

In the spirit of the NACSL above, we can also substitute renormalised spin-flip operators $\tilde{S}^+$ for the $a^\dagger$s in the expression for the state:

$$|\psi^{\mathrm{S2CL}}\rangle = \sum_{\{z_i\},\{w_j\}} \psi^{\mathrm{S2CL}}(z_1, \ldots, z_N; w_1, \ldots, w_N) \tilde{S}^+_{z_1} \ldots \tilde{S}^+_{z_N} \tilde{S}^+_{w_1} \ldots \tilde{S}^+_{w_N} |-2\rangle_N \tag{3.18}$$

where

$$\tilde{S}^+_\eta = \sqrt{\frac{2 + S^{\mathrm{z}}}{3 - S^z_\eta}} S^+_\eta \tag{3.19}$$

and $|-2\rangle_N$ is again the fully spin down polarized state of all N $S = 2$ spins.

The $S = 2$ chirality liquid state (3.16) is a promising candidate to capture a universality class of disordered $S = 2$ antiferromagnets, where the spin liquids may be stabilized through itinerant holes of appropriate kinetic energies, as the holon excitations in the hierarchical spin liquids presumably share the very high mobility of the holons of the individual constituent CSLs. The characteristic features of this universality class are, first, a $(S + 1)^2$-fold TD for the P and T invariant spin S hierarchy liquid on the torus, and second, that the spinons and holons obey non-Abelian SU(2) level $k = S$ statistics. The properties of the spinons would manifest itself not only in the spin liquid state, but in the response to all probes which measure energy scales beyond the ordering temperature, such as *e.g.* Raman scattering.

3.4.1 State counting and effective field theory.

There are important subtleties associated with the Schwinger boson projection scheme we employ here to obtain the hierarchy of spin liquids. The Hilbert space of an N-site spin $S = 1/2$ lattice contains 2^N states and is matched by the number of states in the configuration space of the spinon excitations one can create in the CSL. For higher spin, however, the Schwinger boson projection maps a 2^{Nk} dimensional product space to a $(k+1)^N$ dimensional space, in which the resulting spin liquid is defined. This poses the fundamental problem of how this reduction manifests itself for the spinons in the hierarchy liquids. For example, while the $S = 1$ chirality liquid (3.12) suggests a picture of free spinons of different chiralities, this picture can only be true at the lowest energies, since the state counting does not match.

It will be interesting to investigate this issue further from a field theoretical perspective. Starting with an effective Chern-Simons theory for a single chiral spin liquid [33], and the appropriate generalizations for the higher spin CSLs (3.13), we are led to conjecture that doubled Chern–Simons theories with the appropriate k may describe the low energy physics for the non-Abelian higher spin chirality liquids.

The (bulk) effective field theory for a bosonic $\nu = 1$ Pfaffian state is [59]

$$\mathscr{L} = \frac{2}{4\pi}\epsilon^{\mu\nu\sigma}\left(a^a_\mu \partial_\nu a^a_\sigma + \frac{2}{3} f_{abc} a^a_\mu a^b_\nu a^c_\sigma\right) \tag{3.20}$$

where we have 3 (2+1)-component statistical gauge fields a^a_μ and f_{abc} is a fully symmetric rank-3 tensor and the k parameter in front equals 2 (similar to Laughlin $1/m$ states, where it is m). The action is the (2+1)dimensional space time integral of the Lagrangian- density

$$S = \int \mathrm{d}^3x\, \mathscr{L}. \tag{3.21}$$

Given our observation, that the two chiraltity sectors '+' and '-' are independent at the low energies for which effective field theories are useful, we conjecture the full effective field theory for $S = 2$ chirality liquid to be given by a doubled non-Abelian Chern-Simons action

$$\mathscr{L}_{\mathrm{S2CL}} = \frac{2}{4\pi}\epsilon^{\mu\nu\sigma}\left(a^i_\mu \partial_\nu a^i_\sigma + b^i_\mu \partial_\nu b^a_\sigma + \frac{2}{3} f_{ijk}(a^i_\mu a^i_\nu a^i_\sigma + b^i_\mu b^i_\nu b^i_\sigma)\right) + j^\mu_a a^i_\mu + j^\mu_b b^i_\mu \tag{3.22}$$

with two sets of 3-component gauge fields a^i_μ and b^i_μ. The conserved currents j^μ_a and j^μ_b describe the flow of chirality '+' and '-' quasi-particles of statistical charge 1/2. Each sector has a degeneracy of 3, bringing the total to $3 \times 3 = 9$, since the degeneracy of two independent fields on a manifold of genus $g = 1$ and is equivalent to one field on genus $g = 2$.

It is possible, however, that this theory has to be constrained further, even though the number of consistent choices appears to be limited [60].

4 Entanglement spectrum analysis

In recent years, there has been considerable interest in entanglement as an indicator of topological properities of a quantum many body system. One investigation tool enjoying increased popularity is the entanglement spectrum (ES) [7]. It is essentially the set of eigenvalues of the reduced ground state density matrix of one part of a bipartite system. While it is difficult to interpret the structure of such a spectrum by itself, comparing its 'low energy' part to that of other states with known properties is thought to unveil information about global entanglement and can indicate the presence of topological order. However in some cases, like Laughlin $1/m$ FQH liquid on a torus, one can make a direct assignment of levels in the entanglement spectrum to the chiral edge states expected from conformal field theory [18]. This gives a credence to the interpretation of the generic reduced density matrix in terms of a 'thermodynamic' Hamiltonian describing edge states localized at the boundary between the two subsystems.

In this chapter we present the results of an investigation comparing the entanglement spectra of 2 members of our chiral spin liquid hierarchy with the ground states of a frustrated antiferromagnetic model with next nearest neighbour Heisenberg-type spin-spin interaction on square lattice clusters with varying boundary conditions. This work is one of the first ES studies of a 2D system. It involved writing software to compute conserved-quantum-number-resolved entanglement spectra (in our case those are S^z and momentum m along the subsystem boundary, but our program can in principle handle other symmetries as well) from arbitrary wavefunctions on a spin lattice. This software, we think, constitutes a notable achievement in itself. Our implementation is applicable to any system that can be described by product states of single particle orbitals. Further details are given in section 4.2.

The liquids we looked at are the original $S = 1/2$ chiral spin liquid (CSL) with periodic- and the $S = 1$ chirality liquid (CL) with cylindrical boundary conditions. It is true that of highest interest would be the $S = 2$ chirality liquid, as it manages to reconcile non-Abelian topological order with the symmetries of the Heisenberg hamiltonian. But since the Hilbert space of even a few $S = 2$ spins is already very large, the computational effort involved in diagonalizing any hamiltonian on even relatively small clusters is prohibitive. With the $S = 1$ chirality liquid however we do have a hierarchy member which has the full symmetry of the hamiltonian and, inherited from the CSL, also shows short range antiferromagnetic fluctuations. This is why we thought it might be interesting to compare its entanglement spectrum with that of a quantum antiferromagnet. The practical benefit of the $S = 1/2$ CSL is a managable Hilbert-space size up to 24 sites. In an effort to avoid interference effects of the two system edges on the spectrum we mapped the chirality liquid onto a cylinder, because only on this geometry can we cut a system into parts A and B creating only a single edge. The details of this process, which entails rewriting the fundamental $S = 1/2$ CSL for cylindrical boundary conditions, is described below in section 4.3.1.

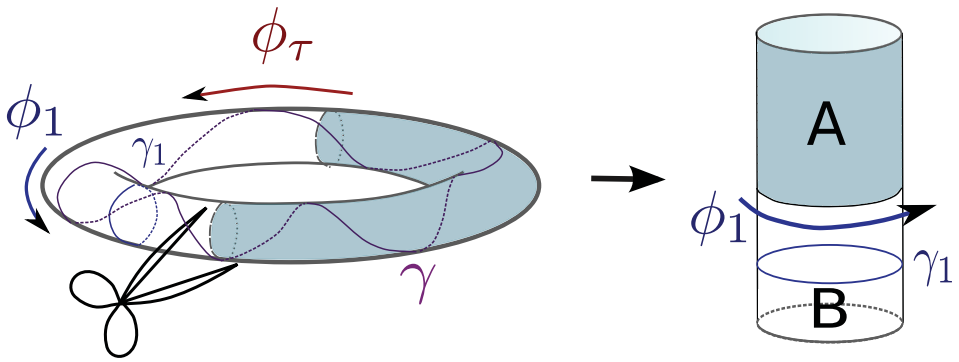

Figure 4.1: We monitor the entanglement spectrum of the CSL and a nnn Heisenberg antiferromagnet as we change boundary conditions from periodic to cylindrical. In the case of the CSL we must cross a topological phase transition, as we know that it has a different TD in both cases.

We find that while both states, the $S = 1$ CL and the Heisenberg ground state, share a common order of low levels in the $S^z = 0, m > 0$ sector, the CL does not show the substantial $S^z = 0, m = 0$ singlet contribution of the antiferromagnet.

A different idea lies behind the comparison of the $S = 1/2$ CSL and the antiferromagnet. We know that with periodic boundary conditions the former possesses topological order with the accompanying fractional statistics and topological degeneracy, while this is not the case on a cylinder: as we shall see, the center-of-mass-zero parameters necessary to ensure quasi-periodicity of the CSL on the torus do not appear for cylindrical boundary conditions. Thus, if we send one dimension of the torus, say L_τ, to infinity, we end up in a different phase without topological order, crossing a phase transition in between. To see whether a frustrated $S = 1/2$ Heisenberg antiferromagnet might behave similarly, we compare the evolution of its entanglement spectrum to the CSL's. The lattice cluster we worked on had $4 \times 6 = 24$ sites. This is far from the in some circumstances numerically feasible maximum of 36 sites for reasons we will explain in section 4.3.3.

We observe that in both systems the lowest level in the ES, lying in the $S^z = 0, m = 0$ sector and thus suggestive of a singlet state on the subsystem A, shows a sharp increase at certain values L_τ respectively $\tilde{L}$ of the effective lengths. In case of the J_1-J_2 Heisenberg antiferromagnet, this increase takes the form of a sharp peak (at $\tilde{L} = 1.15$), while, whithin the resolution of our numerics, it is more like plateau between $L_\tau \approx 1.5 - 2.0$ for the CSL. At the same time the gap between lowest and second lowest level (LL gap) shows the inverse behaviour: a sharp dip for the antiferromagnet and a wide depression for the CSL. In the antiferromagnet this is accompanied by an increased susceptibility to a chiral perturbation, albeit at a slightly different effective length. We take this as preliminary evidence a quantum antiferromagnet at critical frustration exhibits topological order akin to the one in the chiral spin liquid.

We will now go on to introduce entanglement spectra in general, review where they were studied before and what information they are thought to contain. Then we describe our

implementation of an ES analysis program for arbitrary discrete or discretized systems. We introduce the systems we studied, including the model Hamiltonian and the mapping of the CSL wavefunction onto a cylinder. Finally we show the entanglement spectra we obtain and attempt an interpretion.

4.1 Entanglement spectrum

4.1.1 Defintion

The state of a many-body system is completely described by its density matrix ρ. We are interested in zero temperature physics, therefore we will be considering pure state density matrices of the form $\rho(\boldsymbol{Z}) = |\psi(\boldsymbol{Z})\rangle\langle\psi(\boldsymbol{Z})|$, where $\boldsymbol{Z}$ is a set of parameters (*e.g.* the center-of-mass-zeros of the chiral spin liquid). For any partition of the system into parts A and B we can obtain the reduced density matrix of subsystem A by tracing out the degrees of freedom in B

$$\rho_A = \mathrm{Tr}_B\, \rho = \sum_{|\phi^{\mathrm{B}}\rangle \in \mathscr{B}^{\mathrm{B}}} \langle \phi^{\mathrm{B}}| \rho\, |\phi^{\mathrm{B}}\rangle \tag{4.1}$$

where $\mathscr{B}_{\mathrm{A}}$ and $\mathscr{B}_{\mathrm{B}}$ are bases of the subsystems. We can diagonalise ρ_A

$$\rho_{\mathrm{A}} = \sum_i \mathrm{e}^{-\xi_i/2}\ |\phi_i^{\mathrm{A}}\rangle\langle\phi_i^{\mathrm{A}}| \tag{4.2}$$

where normalisation of $|\psi(x)\rangle$ implies unital trace (see C.1)

$$\sum_i \mathrm{e}^{-\xi_i/2} = 1 \tag{4.3}$$

If system and subsystems share some symmetries with associated conserved quantum numbers $\boldsymbol{n} = \boldsymbol{n}_{\mathrm{A}} + \boldsymbol{n}_{\mathrm{B}}$ the density matrix decomposes in to sectors $\boldsymbol{n}_{\mathrm{A}}$ and $\boldsymbol{n}_{\mathrm{B}}$ and we get a reduced density matrix for each label $\boldsymbol{n}_{\mathrm{A}}$

$$\rho_{\mathrm{A}}^{\boldsymbol{n}_{\mathrm{A}}} = \mathrm{Tr}_{\mathrm{B}}^{\boldsymbol{n}-\boldsymbol{n}_{\mathrm{A}}} \rho \tag{4.4}$$

If $\psi(\boldsymbol{x})$ is normalised on the full Hilbert space $\mathscr{H}^{\boldsymbol{n}}$ the $\rho_{\mathrm{A}}^{\boldsymbol{n}_{\mathrm{A}}}$ will not have unital trace anymore.

4.1.2 What it reveals

One of the entanglement measures studied in recent years is the entanglement entropy of a quantum many body system [5, 61]. It is the von-Neumann entropy of subsystem A and can be computed from the reduced density matrix introduced above

$$S_{\mathrm{A}} = \frac{1}{2} \sum_i \xi_i \mathrm{e}^{-\xi/2}. \tag{4.5}$$

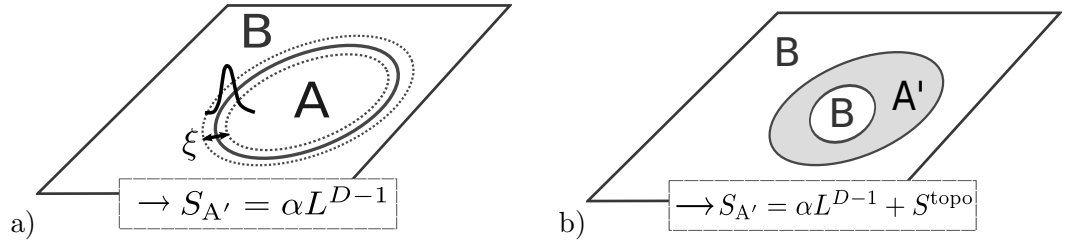

Figure 4.2: a) for a highly entangled spin liquid state devided into regions A and B the topological entropy of A is proportional to its boundary because the main contributions come from edge excitations b) if A is non simply connected, a size independent contribution appears

Using field-theoretical arguments, it has been shown in general that the entanglement entropy of a not simply connected region A′ of a D dimensional topologically ordered system, where is not extensive, but rather proportional to the surface of A [6]

$$S_{\mathrm{A}'} = \alpha L^{D-1} + S^{\mathrm{topo}} + \dots \tag{4.6}$$

where the region size L is assumed large compared to the coherence length ξ of the system and the dots stand for sub-leading order terms. Thus, it appears only states within distance ξ from the ($D-1$ dimensional) boundary $\partial\mathrm{A}'$ contribute to $S_{\mathrm{A}'}$. The even more interesting term however is the intensive contribution S^{topo}: it is directly connected to the ground state degeneracy inherent in a topologically ordered system. In the $1/m$ Laughlin state on a torus for instance, the topological degeneracy is m and $S^{\mathrm{topo}} = \log(m)$.

These considerations were arrived at independently in studies of string-net models of spins on a honeycomb lattice [28], where the authors obtain essentially the same general form (4.6) for $S_{\mathrm{A}'}$.

When we compute the entanglement entropy, most information contained in the full spectrum of the reduced density matrix is lost. One might say knowledge of $S_{\mathrm{A}'}(L)$ is sufficient as it already enables one to recognize topological order in a system, via the size independent contribution S^{topo}. In practice however computing entanglement entropy for many and large enough system sizes L, in order to be able to separate size-dependent and independent parts of $S_{\mathrm{A}'}$, is a numerically challenging task. In a paper from 2008, Li and Haldane [7] argue that looking at the full, conserved-quantum-number-resolved spectrum of the reduced density matrix instead of just the entanglement entropy allows to recognize topological order directly from the low lying part of the spectrum, at least in the case of FQH states on a spherical geometry. A key is the interpretation of the entanglement spectrum as the eigenspectrum of a Hamiltonian describing edge states. Even if the full system is in a pure state $|\psi\rangle$, the reduced matrix ρ_{A} will in general not correspond to a pure state on subsystem A (in fact it only does so if $|\psi\rangle$ is a product state). But we can always write ρ_{A} as a thermal distribution

$$\rho_{\mathrm{A}} = \mathrm{e}^{-H_{\mathrm{A}}} \tag{4.7}$$

for some a hermitian operator H_A with fictious temperature $\beta = 1$.. Thus, the entanglement entropy is equivalent to a thermodynamic entropy and the low 'energy' levels of H_A correspond to the edge excitations at the boundary ∂A.

In the limit of a product state there will only be a single level $\xi_1 = 0$. Accordingly, we can expect for the case of weak, non-zero entanglement to find a 'ground state' of high weight $\xi_1 \ll 1$ separated by a large gap from the remainder of the spectrum $\xi_j \gg \xi_1$, $j > 2$.

With our knowledge about the scaling of the entanglement entropy with system size, we can expect the eigenstates $|\phi'_j\rangle$ of ρ_A with the highest weights $\mathrm{e}^{-\xi/2}$, to be localized near the boundary between A and B: the scaling with the boundary size can only be explained if states in the bulk do not contribute significantly.

When we classify levels in ρ_A by quantum number, *i.e.*, compute the density matrices $\rho_\mathrm{A}^{\boldsymbol{n}_\mathrm{A}}$, we obtain information about the quantum numbers of these edge excitations. For spherical geometry, there the algebra discribing edge excitations has long been known [18, 46] and was just this spectrum which was observed by Li and Haldane [7]. But also in the case of the $1/m$ Laughlin state on a torus it is possible make, at least in the thin torus limit, a direct analytic connection between edge excitations as obtained from conformal field theory and the levels of the entanglement spectrum [50].

4.2 Our implementation

In this section, we want to describe the computational problem involved in obtaining the entanglement spectrum of a many-body spin state and explain how we implemented it.

The systems we studied were lattice clusters of N spins S ($S = 1/2, 1$). We considered states ψ of the whole system with vanishing z-component of the total spin $S^\mathrm{z}_\mathrm{tot} = 0$. The partition is between sets of sites A and B on which one can then obtain product bases $B^{S^\mathrm{z}}_{\mathrm{A—B}}$.

The input to our program are

- the wavefunction ψ, which implicitly includes a $S^\mathrm{z}_\mathrm{tot} = 0$ basis of the complete system
- the bases for the subsystems A and B
- the specifications of the lattice cluster

Of course, in principle it would suffice to know ψ and the lattice specifications (including the number of sites an spins) and have the program generate the subsystem basis internally. But going the route of decreased automation makes it easier to generalize the program to other geometries, filling fractions or encodings of the orbitals.

The lattice specifications must include the dimension of the cluster (width×height), its symmetries in the form of permutations of sites, the list of sites belonging to subsystem A as well as the symmetries of A (also given as permutations). Common symmetries of the region A and the entire system will provide quantum numbers labelling the reduced density matrices. In our problem we considered systems and subsystems with cylinder symmetry where the associated quantum number is the momentum along the boundary between A and B.

The basis used to write down the total system state $|\psi\rangle$ and the subsystem bases for A and B must be product bases satisfying the following compatibility criteria

- the numbers of both sites and particles must add up $N_\mathrm{A} + N_\mathrm{B} = N$ and $N_\mathrm{A}^\mathrm{p} + N_\mathrm{B}^\mathrm{p} = N^\mathrm{p}$
- the z-components of total spin must add up $S_\mathrm{A}^\mathrm{z} + S_\mathrm{B}^\mathrm{z} = S_\mathrm{tot}^\mathrm{z}$
- in the total system basis, the orbitals belonging to A must come before those of B, *i.e.*, a configuration must look like $|\sigma_1^\mathrm{A}, \ldots, \sigma_{N_\mathrm{A}}^\mathrm{A}; \sigma_1^\mathrm{B}, \ldots, \sigma_{N_\mathrm{B}}^\mathrm{B}\rangle$ where σ_j encodes the state/particle encountered on site j (for instance, the codes we use are $S + 1 - S^\mathrm{z}$ if there is a spin on site j and either 0 or $2(S+1)$ if there is a hole)
- the total system basis may be in symmetry reduced form to save memory (*i.e.*, of all different configurations $\{|\sigma_1, \sigma_2, \ldots, \sigma_N\rangle, |\sigma'_1, \sigma'_2, \ldots, \sigma'_N\rangle \ldots\}$ connected by a symmetry only one representative is kept)
- subsystem bases must not be symmetry reduced

the last condition could be relaxed if we included the symmetry specifications for subsystem B, since then we could restore the full, unreduced subsystem-bases internally. As the subsystem Hilbert-spaces are usually negligibly small as compared to that of the full system ($N_\mathrm{A} \approx N/2$ and $\dim\mathscr{H}$ grows exponentially), this restriction hardly affects performance.

The details of how the computation proceeds given these input data can be found in appendix C.2. We only want to mention some important practical issues. The first concerns a performance bottleneck of our program. Currently, diagonalisation of the reduced density matrix is performed with a straighforward implementation of Gauss' algorithm. We are therefore restricted to sizes of about 5000×5000. So far, this has not been a problem for the quantum number resolved density matrices we were analyzing. The largest subsystems we considered were $N_\mathrm{A} = 16$ spins $S = 1/2$, with an unreduced $S_\mathrm{A}^\mathrm{z} = 0$ Hilbert space of 11440. Region A was a 4×4 square cluster, which means we had the 4 momentum numbers $m = 0, 1, 2, 3$ along its boundary with region B (of the same shape). The largest ρ_A^m were therefore on the order of 3000×3000, still within the capabilities of the internal diagonalisation procedure. Yet only two more spins, $N_\mathrm{A} = 18$, already take us beyond the limit.

The next is the question when and how the eigenvalues $\lambda_i = \mathrm{e}^{-\xi_i/2}$ of ρ_A should be resolved into separate levels. We allow specification of a threshold above which the eigenvalues are to be treated as separate levels while below they are counted as one degenerate level. The question is now whether one should apply this 'binning' or 'coarse graining' to the eigenvalues λ_i themselves or their logarithms ξ_i. One might argue in favour of the ξ_i, but we feel binning the λ_i is more useful as it gives a better 'resolution' in the interesting lower part of the spectrum $\lambda_i \lesssim 1$, which is where we want maximum information. Of course this means that many levels $\lambda_i \ll 1$ will not be resolved, but since they do not carry much weight anyway, this does in fact help to 'tidy up' the spectrum.

Lastly, there is an issue concerning the comparability of levels from different S^z sectors. We renormalize the matrix $\rho_A^{S^\mathrm{z}}$ in order to make them indiviually plottable. This means if we want

to compare two levels from different sectors, say $\xi_{S_1^z}$ and $\xi_{S_2^z}$ we need to add a correction

$$\Delta\xi^{\text{true}} = \xi_{S_1^z} - \xi_{S_2^z} + 2\ln\frac{\dim\mathscr{H}_{S_2^z}}{\dim\mathscr{H}_{S_1^z}} \tag{4.8}$$

4.3 The systems

This section takes a close look at the states/systems of which we want to compare the entanglement spectra. One class, the chiral spin liquid on the torus is already known from chapter 2, but here we rewrite it for cylindrical boundary conditions and show how it loses its topological degeneracy in the process. Then we introduce the antiferromagnetic Heisenberg model with next-nearest-neighbour interaction whose ground state spectrum we will be comparing with that of our spin liquids. We have chosen this model, because the nature of the phase around the critical coupling strength $J_1 = 2J_2$ is still an open question, and it just might be described by a spin liquid. We close the section with a brief look at the system sizes we can tackle numerically.

4.3.1 $S = 1$ chirality liquid on a cylinder

So far we have seen the chiral spin liquid wavefunction in two incarnations: with open and with quasi-periodic boundary conditions. Now we are looking for a form suited to a cylinder geometry. In the following, we choose complex coordinates z such that the periodic dimension is in direction $\mathrm{Re}[z] = x$.

Just as the Jacobi-theta functions are the means to make an open-boundary CSL wavefunction quasi-periodic and so adapt it to the torus, we are looking for an anti-symmetric function with periodicity in one direction to satisfy the cylindrical boundary conditions. The straightforward choice is the sin-function. Replacing factors $(z_i - z_j)$ in the open-boundary CSL by $\sin(\pi(z_i - z_j))$ we obtain

$$\psi_{\text{cyl}}^{\text{CSL}}[\boldsymbol{z}] = \mathrm{e}^{iKZ}\prod_{ij}\sin^2(\pi(z_i - z_j))\prod_j G(z_j)\,\mathrm{e}^{-\frac{\pi}{2}\mathrm{Im}[z_j]^2} \tag{4.9}$$

for the wavefunction of an $S = 1/2$ chiral spin liquid on a cylinder. The M lattice positions $\{z_j\}$ are again coupled to either spin flips or Schwinger boson operators.

Since the Gaussian depends only on the non-periodic coordinate '$y = \mathrm{Im}[z]$', it is evidently invariant under the operation of transporting one particle around the cylinder in x-direction. By demanding the wavefunction to be quasi-periodic with boundary phase ϕ_1 we get the condition

$$\mathrm{e}^{iK}(-1)^{M-1} \stackrel{!}{=} \mathrm{e}^{i\phi_1}. \tag{4.10}$$

One should note, that any additional center-of-mass parameters are conspicuously absent. Apparently, relinquishing one periodicity as compared to the torus makes them unnecessary. This also means there is no function space of CSLs and therefore no topological degeneracy: the wavefunction (4.9) still describes a spin liquid with broken P and T, but it is no longer

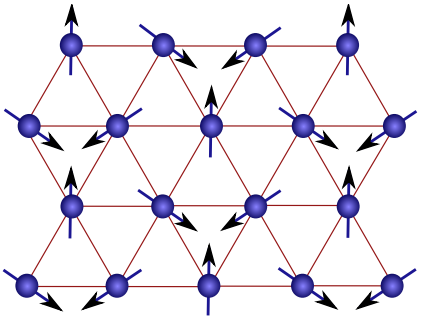

Figure 4.3: chiral antiferromagnetic phase on a triangular lattice. the order parameter depends on 2 directions instead of just 1 as in a Néel AF

topologically degenerate! This does not mean excitations lose there half-fermionic statistics, but since there is only one Wilson-loop and one flux insertion operator the link between statistics and topological degeneracy is broken. With the circumference of the torus in 1-direction our lengthscale, τ is a parameter we can use to control the boundary conditions. Sending $\tau \to i\infty$ and using the limit behaviour of $\vartheta(z|\tau) \to \sin(\pi z)$ derived in appendix A.1 we can motivate (4.9) starting from the quasi-periodic form (2.50) (appendix C.3).

Expressing $\hat{\Psi}^{\mathrm{CSL}}$ with Schwinger boson operators allows us to set up our spin liquid hierarchy 3.4 on a cylinder just as with other boundary conditions. The hierarchy state we will be comparing to the antiferromagnet described in the next subsection is the $S = 1$ chirality liquid obtained by projecting one CSL of each chirality. We chose it as a good candidate because, as explained in the previous chapter, it is the first element in the hierarchy which is P and T invariant and thus shares all symmetries with the frustrated Heisenberg hamiltonian.

4.3.2 Frustrated Antiferromagnet ground state

In the context of spin systems one commonly considers the Heisenberg model

$$H_{\mathrm{Heisenberg}} = \sum_{ij} J_{ij} \hat{\boldsymbol{S}}_i \hat{\boldsymbol{S}}_j \tag{4.11}$$

In strongly correlated systems on a lattice, it arises in the large U limit from the Hubbard-model at half filling (which does not have an explicit spin-spin coupling) if we include second-order hopping processes.

The possible phases of this *quantum magnet* model are very rich: there is ferromagnetism if $J_{ij} = J < 0$, Néel antiferromagnetism if $J > 0$, but also spin glass phases for randomly distributed J_{ij}. Especially interesting and theoretically challenging phases are encountered in frustrated systems. A nearest-neighbour Heisenberg model on a triangular lattice for instance exhibits spiral antiferromagnetic order with coplanar spin polarization [38], and the phase of spins on a Kagomé-lattice is still the subject of ongoing debate (see [30] and citations therein), with most approaches favouring some kind of liquid state.

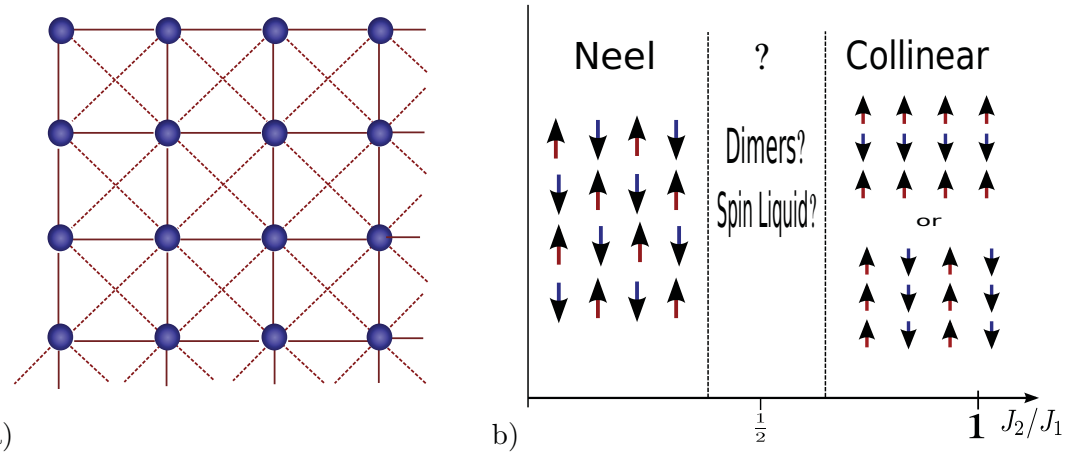

Figure 4.4: a) Graphical depiction of a 4×4 lattice cluster with nnn interaction and PBC b) $T = 0$ phase diagram of a J_1-J_2 Heisenberg model for $S = 1/2$ spins. The nature of the phase between the Néel- and the Collinear orders is not known

Triangular and Kagomé lattice are examples of geometric frustration, but some materials, most notably the cuprates and iron pnictides showing high temperature superconductivity, are thought to be described by a model of spins $S = 1/2$ on a square lattice where frustration comes from the presence of a next-nearest neighbour coupling:

$$H_{J_1 J_2} = J_1 \sum_{\text{nn}} \hat{\boldsymbol{S}}_i \hat{\boldsymbol{S}}_j + J_2 \sum_{\text{nnn}} \hat{\boldsymbol{S}}_i \hat{\boldsymbol{S}}_j \tag{4.12}$$

The parameter controlling the phase is the ratio $g = J_2/J_1$. Classical spins ($S \to \infty$) are Neel-ordered below $g = 1/2$ and show collinear order above. The transition at the critical value $g = 1/2$ has been found to be of first order. For finite spin, quantum fluctuations change the picture however. For instance spin $S = 1/2$ particles show a non-magnetic phase in the region $0.4 \lesssim g \lesssim 0.65$. This phase has variably been conjectured to be a valence bond solid, a chiral spin liquid or a chiral plaquet ordered phase. A thorough treatment of this model is given in [30].

The idea we pursue is to monitor the entanglement spectrum of both the ground state of $H_{J_1 J_2}$ at critical coupling strength $J_1 = 2J_2$ and a $S = 1/2$ chiral spin liquid as we transition from periodic to cylindrical boundary conditions. Somewhere during the process, the chiral spin liquid undergoes a quantum phase transition from a topologically ordered phase to one without such order which should be visible in its symmetry resolved entanglement spectrum. The hope is to find similar features in the entanglement spectra of the J_1-J_2 ground states.

A practical issue is the length parameter used: in the CSL wavefunction we have the parameter τ, defining the circumference of the torus in that direction, which we can send to infinity. In $H_{J_1 J_2}$ we achieve the change in boundary conditions by slowly reducing both couplings between two rows of the lattice creating an edge in the system (see figure 4.5 a)). We define

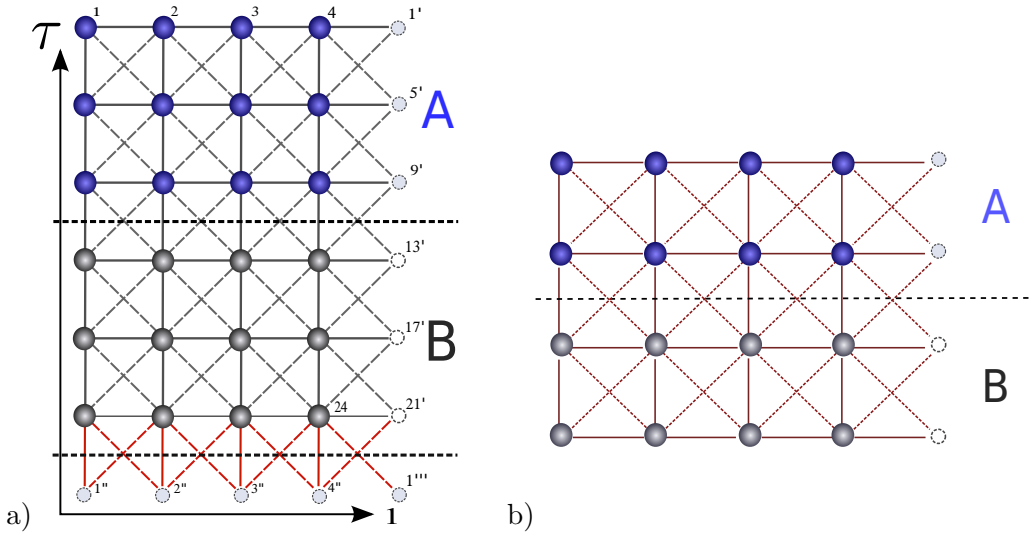

Figure 4.5: We compute entanglement spectra of a J_1-J_2 Heisenberg antiferromagnet and compare them with spectra of our spin liquids on a) a 4×6 square lattice of $S = 1/2$ spins as boundary conditions change from periodic to cylindrical. The transition is achieved by slowly decreasing the couplings between two rows $J_{\text{edge}} \to 0$ (links shown in red). b) a 4×4 lattice of $S = 1$ spins

the dimensionless length

$$\tilde{L} := J_{\text{bulk}}/J_{\text{edge}} \tag{4.13}$$

The subsystems A and B where chosen of equal size and such, that each had one edge in common with the total system.

As mentioned in the previous section, the other geometry we diagonalise $H_{J_1 J_2}$ on is a 4×4 square lattice cluster of $S = 1$ spins (figure 4.5 b)). We compare the ES of the ground state to that of the chirality liquid, in the hope of finding similar edge structures or other features, corroborating that the latter captures the essence of the former.

4.3.3 Cluster sizes

Three things determine the possible cluster sizes: hardware, lattice symmetries and intrinsic properties of our building block, the $S = 1/2$ CSL. The first is the most obvious limitation. To give some numbers: For lattice clusters of $S = 1/2$ spins with full translational and reflexion symmetry diagonalizing a Heisenberg Hamiltonian on a 6×6 lattice is just barely possible with the hardware we have. The reduced Hilbert space of this system has a dimension of $9 \times 10^9/250 \approx 32 \times 10^6$.

But we cannot reach this if we may not use all symmetries. And on a cylinder translation symmetry in one direction is broken. Other factors decreasing our available choice of cluster size are that we want the two subsystems A and B be as equal as possible and also as close to a square-shape as possible (better bulk to edge ratio). All this means, that there are actually

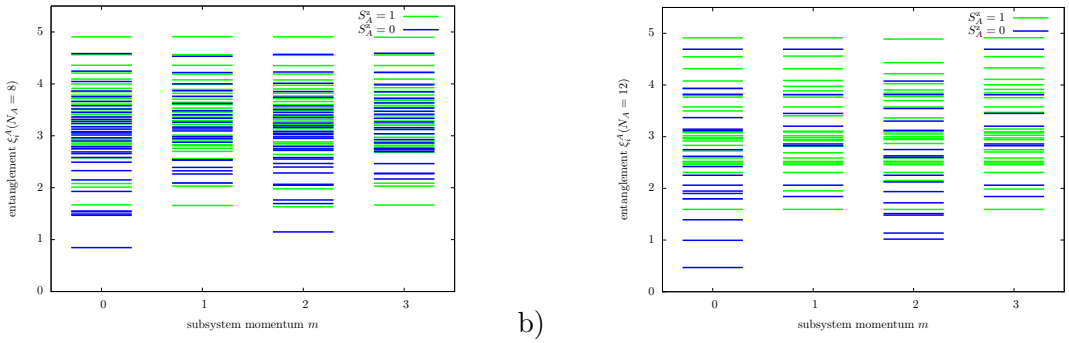

Figure 4.6: Entanglement spectra of the $S = 1/2$ CSL on a 4×6 cluster for a) $L = 1$ and b) $L = 3$. The lowest level is singlet contribution $S^z = 0, m = 0$ and decreases markedly between $L = 2 \ldots 2.5$ and the same hold for the lowest-level gap. Both the lowest and second lowest level have for all length the same quantum numbers of $S^z = 0, m = 0$ and $S^z = 0, m = 2$ respectively.

very few suitable cluster sizes and shapes available and they are significantly below the 'upper bound' of 36.

The best choice would be $N = 32 = 4 \times 4 + 4 \times 4$, the combination of two 16 site square lattices. But the Hilbert space of this cluster is still 40×10^6 and therefore slightly too large for us to handle (at one point we did generate the J_1, J_2-Heisenberg hamiltonian and it has a size of ≈ 25 Gigabytes).

Both subsystems should have even numbers of sites, because we want to avoid generating bulk excitations in the CSL as we cut the system, therefore the total system size must be a multiple of 4. 28 cannot be arranged in a shape with any bulkyness, leaving 24 as the largest feasible and useful size.

In the case of the spin $S = 1$ chirality liquid and $S = 1$ Heisenberg model, the largest feasible geometry satisfying (most of) the conditions is a $4 \times 4 = 16$ site square cluster, which we again cut in half. The results found in such a small system are hard to extrapolate to the thermodynamic limit and the computations would have to be repeated with larger clusters as soon as it computationally feasible.

4.4 Results

Here we present the results of our numerical investigation of the systems described above. The focus lies on the comparison of $S = 1/2$ CSL and critical J_1-J_2-Heisenberg model on the 4×6 lattice cluster since due to its somewhat larger size, this system should be less affected by finite-size effects than the 4×4 spin $S = 1$ lattice.

4.4.1 $N = 24, S = 1/2$ lattice cluster

On the 4×6 cluster of $S = 1/2$ spins we computed the entanglement spectra of both a Laughlin CSL wavefunction and a the ground state of a J_1-J_2 frustrated Heisenberg model as we vary boundary conditions from fully periodic to cylindrical. In the case of the CSL this is done by sending the parameter τ to infinity, while keeping the flux $\Phi = N_\Phi \Phi_0$ finite. The result of this limiting process is the CSL spin liquid decribed by equation (4.9). Its form can be understood in terms of periodicity arguments, but a derivation is shown in C.3. For the CSL we therefore define our control parameter

$$L := \tau/2\tau_{\text{initial}} \tag{4.14}$$

The starting value τ_{initial} is 1.5, as that is the extent in Im[z]-direction of a 4×6 cluster if the size in Re[z]-direction is set to 1. The additional factor of 2 in the denominator makes common plots of values for the CSL and the J_1-J_2 model simpler. As described above, the length scale for the J_1-J_2 model is defined via the ratio of the coupling stengths in the bulk to those across the edges we create in the system (4.13)

$$\tilde{L} := J_{\text{bulk}}/J_{\text{edge}}$$

We will keep there ratio $J_2/J_1 = 1/2$ everywhere, *i.e.*, also at the edge.

As an additional probe we implemented a chiral perturbation of the pure J_1-J_2 model $H_{J_1J_2}$. It is basically a lattice-sum of chirality operators $\chi_{ijk} := \boldsymbol{S}_i \cdot (\boldsymbol{S}_j \times \boldsymbol{S}_k)$ as defined in (2.43):

$$H_{\text{chi}} = \chi \sum_{ijk} \hat{\boldsymbol{S}}_i \cdot (\hat{\boldsymbol{S}}_j \times \hat{\boldsymbol{S}}_k) \tag{4.15}$$

where the sum runs over all neighbouring triples of sites (ijk) with $((\boldsymbol{R}_j - \boldsymbol{R}_i) \times (\boldsymbol{R}_k - \boldsymbol{R}_i))_z > 0$. We varied χ between 0 and $\approx J_1/5$ and observed the response in the ground state energy as well as the entanglement spectrum.

A selection of the spectra we obtained is shown in figures 4.6, 4.7 and 4.8. In all of them, we used a cutoff of $\xi_i < 4.5$ and a level resolution of $\exp(-\xi_i/2) - \exp(-\xi_{i-1}/2) = \pm 10^{-4}$. We plot only the first two S^z sectors, since only they are relevant to find the gap between lowest and second lowest level (LL gap).

The main feature exhibited by both the CSL and the frustrated AF is a peak in the lowest level with an accompanying dip in the LL gap. In the limit of large $L, \tilde{L}$, the lowest level (gaps) settle down at a lower (higher) value than in the initial state. This is means that for both systems subsystem entanglement is much weaker in cylindrical geometry. However, This might in fact simply be a consequence of the reduction in the common boundary between A and B.

Furthermore we find that the chiral perturbation H_{chi} causes a linear response in the chirality

$$\chi_{GS}(L) = \langle \psi_{GS}(L,\chi) | \sum_{ijk} \chi_{ijk} | \psi_{GS}(L,\chi) \rangle = -a(L)\chi \tag{4.16}$$

where $a(L)$ is a length dependent 'chiral susceptibility'. There is a the peak in the chiral susceptibility at around $\tilde{L} = 1.5$. Interestingly this does not quite coincide with the position of the dip in the LL gap.

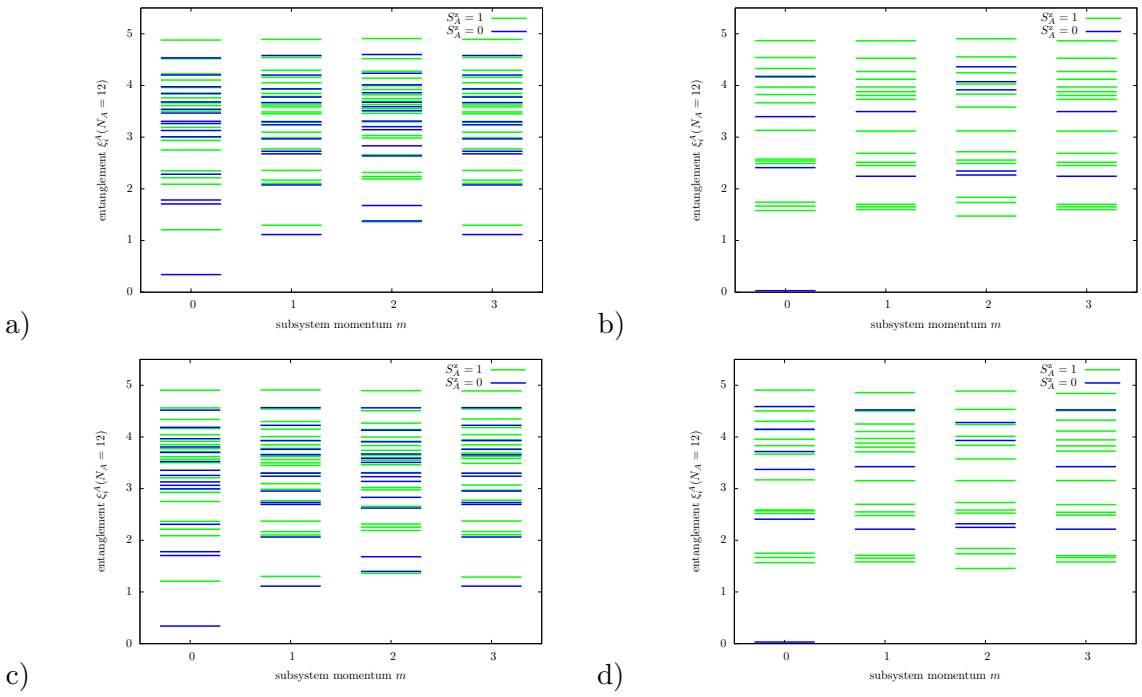

Figure 4.7: Entanglement spectra of the nnn-Heisenberg ground state a),b) without and c),d) with chiral perturbation ($\chi = J_1/10$) on a 4×6 cluster below and above the transition for lengths a),c) $\tilde{L}_\tau = 1$ and b),d) $\tilde{L}_\tau = 2$. The main singlet contribution $S^z = 0, m = 0$ decreases exponentially and the minimal gap increases linearly $L = 2 \ldots 2.5$. The sector of the second lowest level changes from $S^z = 1, m = 0$ to $S^z = 1, m = 2$.

In conclusion, while both the $S = 1/2$ CSL and a frustrated AF show a reduction of lowest-level gap in the entanglment spectrum followed by a relatively fast approach to the limit value as the effective lengths are increased. The positions where these occur cannot really be compared as the scales of the effective lengths we use are unrelated.

The peak in the chiral susceptibility $a(\tilde{L})$ occurs at $\tilde{L} = 1.5$, which is significantly different from the position of the dip in the LL gap (at $\tilde{L} = 1.15$). Currently we do not have a convincing explanation for this, but we believe that it is nonetheless an effect of the same transition responsible for the features seen in the lowest level and LL gap.

Unfortunately, the LL gap might not be the right quantity to look at. Whether the dip in the LL gap as well as the other features observed for the AF indicate a transition between topologically different phases can only be decided by going to larger systems where a finer momentum resolution might make it possible to observe the full set of low lying 'topological' states in the CSL and, if such a set indeed exists there, in the AF, which [29] identified as the fingerprint of topological order in FQH-like spin liquids.

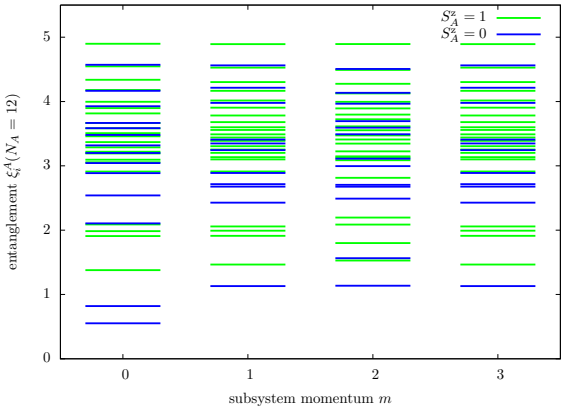

a)

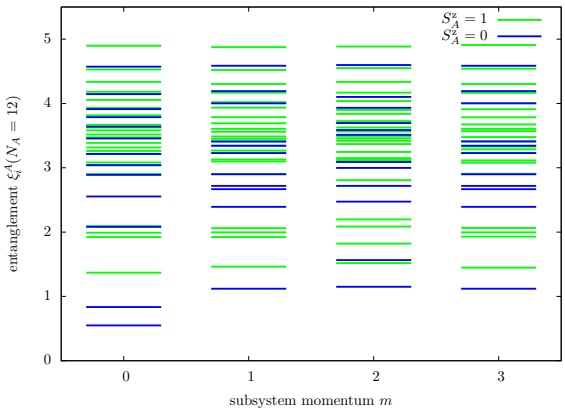

b)

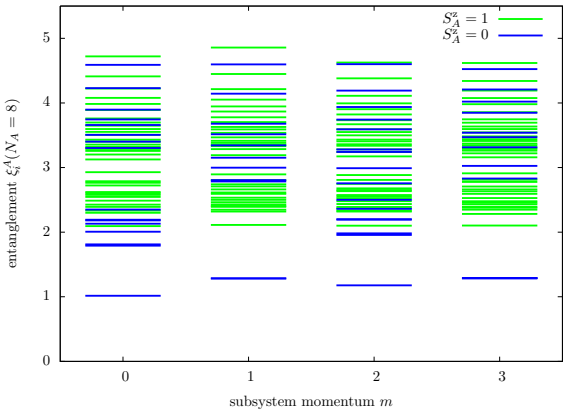

c)

Figure 4.8: Entanglement spectra at the minimal LL gap lengths: nnn-Heisenberg ground state at $\tilde{L} = 1.15$ a) without and b) with chiral perturbation. c) CSL at $L = 1.5$ Note that for both the gap is between levels with quantum numbrs $S^z = 0, m = 0$ and $S^z = 0, m = 2$. For the CSL this is the case for all lengths, while the AF shows this feature only around the critical length $\tilde{L} = 1.15$. One can also see, that the levels structure is not visibly changed by the chiral perturbation, in contrast to the region $\tilde{L} \approx 1.5$. where the lowest levels are shifted up with increasing χ, leaving the LL gap almost unchanged.

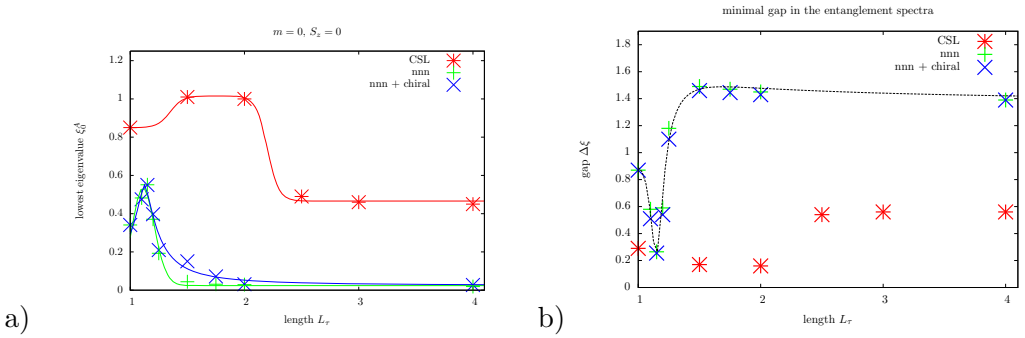

a) b)

Figure 4.9: a) The lowest level (=main contribution) in all entanglement spectra and b) the minimal gap between the lowest level and the next higher one. The lowest level is always in the $S^z = 0, m = 0$ sector and therefore most likely a singlet. For both the CSL and the AF we observe an increase in the lowest level with an according decrease of the gap. The peak positions (rather a plateau for the CSL) are not comparable as the scale of the two 'effective' lengths used are unrelated. Note also, that while both lowest and second lowest level of the CSL are in the $S^z = 0, m = 2$ sector for all values of L, it is not so in case of the AF ground state. There we observe a switch from $S^z = 1, m = 0$ for $\tilde{L} = 1$ via $S^z = 0, m = 0$ around the transition length $\tilde{L} \approx 1.15$ to $S^z = 1, m = 2$ for large $\tilde{L}$. The chiral term seems to delay the 'rearrangement' of the of the system as the changes in both lowest level and minimal gap size are significantly weaker in b).

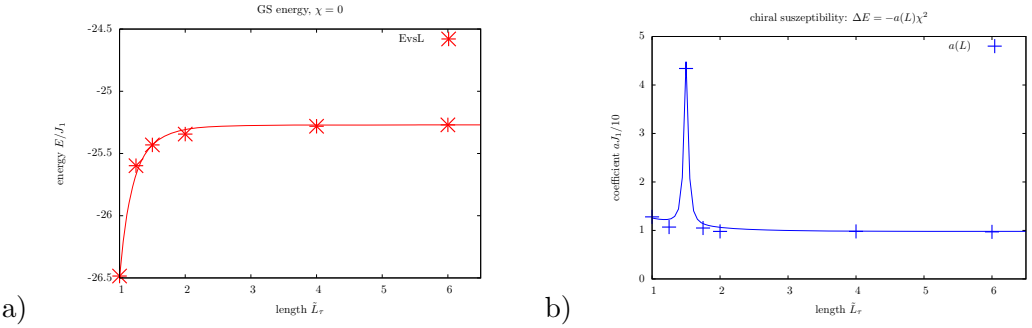

a) b)

Figure 4.10: a) The ground state energy is well described by a hyperbola $E = E_\infty - a/L^b$ with $E_\infty = -25.27$, $a = 1.225$ and $b = 5.07$ where energy is in units of (bulk) coupling strength J_1. b) When we add a chiral perturbation $H_{\text{chi}} = \chi \sum_{ijk} \boldsymbol{\chi}_{ijk}$ to the Heisenberg hamiltonian we observe a change in the ground-state energy almost exactly like $\Delta E = -a(L)\chi^2$ indicating a linear response of the chirality. The 'susceptibility' $a(\tilde{L})$ has a sharp peak at $\tilde{L} = 1.5$ which coincides with the point where the chiral perturbation causes the biggest deviations in the entanglement spectrum (cp. Fig. 4.9)

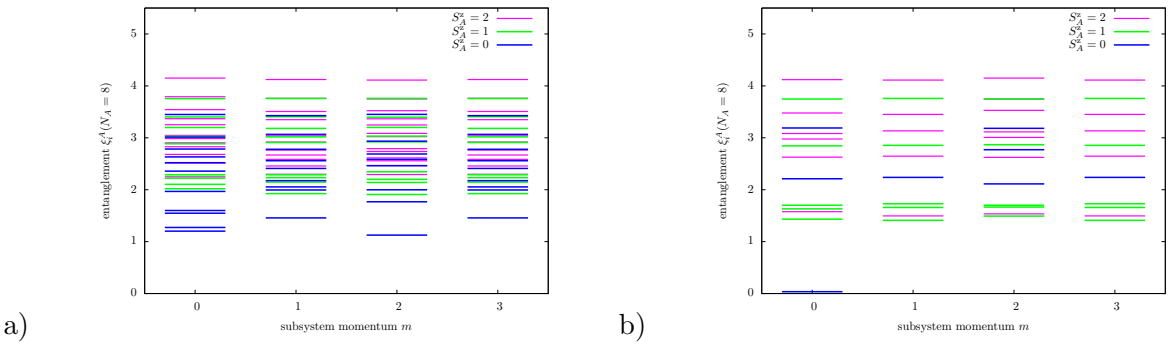

Figure 4.11: The spectra of a) the chirality liquid and b) a $J_1 = 2J_2$-Heisenberg ground state. The scarcity of levels for the AF is due to the overwhelming singlet contribution $S^z = 0, m = 0$: most levels where eliminated by the enforced cut-off of 4.

4.4.2 $N = 16, S = 1$ cluster

We now come to the comparison of the spin $S = 1$ chirality liquid with the ground state of a antiferromagnetic next-nearest-neighbour J_1-J_2 Heisenberg model at critical coupling strength $J_1 = 2J_2$ on a 4×4 spin $S = 1$ square lattice cluster with cylindrical boundary conditions. As was already indicated, the chirality liquid has a real valued wavefunction and thus preserves P and T symmetries, just like the Heisenberg Hamiltonian $H_{J_1 J_2}$. So it would be interesting to check whether one can find any indication, that the CL is a suitable description for the non-magnetic $T = 0$ phase of the antiferromagnet in the $J_2/J_1 \approx 1/2$ regime.

Figure 4.11 shows the entanglement spectra of the CL and the frustrated antiferromagnet ground state. As can be seen, both have a significant singlet contribution ($S_z = 0$, $m = 0$) but in the AF it is far stronger than in the CL. Both this and the large LL gap causes are a clear indication, that in the AF the subsystems A and B are not as strongly entangled as the chirality liquid. A way to explain this is that even for critcal coupling strength, the is close to a state with 'classical' antiferromagnetic ordering, which in mathematical terms are product-states. On the other hand the structure of the other $S^z = 0$ levels does indeed show a similarity: in the $m = 1, 2, 3$ sector we have the same succession of levels $m = 2$, $m = 1, 3$, $m = 2$ and $m = 2$ degenerate with $m = 1, 3$

As a second check, we also computed the overlaps between both states and the expectation value $\langle \psi^{\mathrm{S1CL}} | H_{J_1 J_2} | \psi^{\mathrm{S1CL}} \rangle$ for different ratios of the coupling strength. The results are given in table 4.1.

Both overlap and energy show the best agreement for $J_2/J_1 = 0.5$. An overlap of 0.92 and 88% energy saturation ($\langle \psi^{\mathrm{S1CL}} | H_{J_1 J_2} | \psi^{\mathrm{S1CL}} \rangle \approx E_{\mathrm{GS}} + 5J_1$, *i.e.*, an average of 5 links is not satisfied) is decent, but not impressive. We should note however, that there was no fitting involved here, as the chirality liquid is parameter-free on the cylinder. There is a slight tilt towards lower ratios of J_1/J_2, which might be an effect of the edge the system has in cylindrical boundary conditions: when one reduces boundary conditions from periodic to cylindrical, one cuts twice as many nnn-links as nn-links, so that Néel order will become

g	$\lvert\langle\psi^{\mathrm{CL}}\lvert\psi_{\mathrm{GS}}\rangle\rvert$	$\langle\psi^{\mathrm{CL}}\lvert H_{J_1,J_2}\rvert\psi^{\mathrm{CL}}\rangle$	$\langle\psi^{\mathrm{GS}}\lvert H_{J_1,J_2}\rvert\psi^{\mathrm{GS}}\rangle$
0.00	0.6151	-65.50	-72.0
0.25	0.7657	-50.48	-56.0
0.49	0.9031	-36.78	-41.45
0.50	0.9152	-35.44	-40.0
0.51	0.8907	-34.84	-42.15
0.60	0.3504	-29.44	-45.0
1.25	0.0092	03.85	-51.0

Table 4.1: the table contains overlaps and energy expectation values of a $\psi^{\mathrm{CL}}(Z_0)$ with the exact ground state of a J_1, J_2-Heisenberg Hamiltonian for a N=16 square lattice

slightly more favourable as compared to collinear order.

This strikes upon the ratio of edge-to-bulk as the major weakness of this investigation: The system as a whole in general and the subsystems A, B in particular are admittedly rather small, so that extrapolating these results to the infinite lattice is difficult.

While the entanglement spectra do show common features, the chirality liquid is obviously much more strongly entangled than the AF ground state and as the overlap and energy saturation are also not outstanding we must conlude that, for such small systems at least, the chirality liquid is of only limited value as an ansatz for the non-magnetic phase in the critical nnn-Heisenberg antiferromagnet. However, a final verdict of how well for instance correlations in chirality or higher order operators agree in both systems or whether the AF develops the same (Abelian) edge structure must await computations on clusters with significantly larger size.

5 Extended Young tableaux

In this chapter we present the method of extended Young tableaux, originally devised to find the spinon-excitation content of eigenstates of a Haldane-Shastry spin chain composed of *fundamental* SU(n) spins. We show how it can be generalized to higher, *symmetric* representations of SU(n). We also use it to compute the eigenvalues of the cyclic permutation (the translation of a chain by one lattice site) faster than traditional methods based on group characters or diagonlisation of total weight representations.

5.1 Motivation

The study of spin lattice models in low dimensions is an important and vibrant field of contemporary condensed matter physics and has produced many interesting insights into novel states of matter and manifestations of order. Many currently studied systems, for instance frustrated quantum antiferromagnets, have deceptively simple looking Hamiltonians, which are nonetheless hard to investigate with analytical methods. In this case numerical methods, like density matrix renormalisation group (DMRG), Coupled Cluster, Quantum Monte Carlo variational methods, functional renormalisation group (FRG) based schemes or exact diagonalisation (ED) can be used to probe for the presence of order. This order can exist as spontaneous symmetry breaking or as topological order and numerical methods help in obtaining the phase diagram. Even fully tractable, integrable models can benefit from numerics in general and ED in particular, when perturbation corrections to the analytically given eigenstates are to be calculated. Among these methods exact diagonalisation (ED) stands out as the only one being applicable regardless of the specifics of the physical model and its geometry.

A spin model consists of a cluster of N spins arranged on some lattice tile, with periodic, or possibly other, boundary conditions, and a Hamiltonian describing the interaction of the spins with each other or with external fields. The spins transform like some irreducible representation σ of SU(n), usually SU(2) but higher n have also enjoyed attention [62–67]. For any n, the Hamitonian acts on a tensor product space whose dimension grows exponentially in N. This unfortunately makes ED computationally much more demanding than the other numerical methods, which deal with this problem either by restricting themselves to a subset of suitably chosen states containing most of the information that is physically relevant (DMRG) [68], by starting from some ansatz for the wave function which is then refined variationally (Monte-Carlo) [69] or by taking interactions into account only up to some finite order (Coupled Cluster) [70] or, in a recently developed approach, using auxillary particles to bring the power of diagrammatic methods to bear on the problem (FRG [30]).

The most commonly considered interaction is of the Heisenberg form $J_{ij}\hat{\boldsymbol{S}}_i\hat{\boldsymbol{S}}_j$ between spins on sites i and j with a coupling constant J_{ij}. Such a Hamiltonian is inherently invariant under

global SU(2) (SU(n)) rotations and conserves both S^{tot} and S_z^{tot} and (or, for general SU(n), total weight $\boldsymbol{w}$ and highest total weight $\boldsymbol{w}^{\mathrm{tot}}$) respectively. In many models the J_{ij} are such that the Hamiltonian also has the full symmetry of the lattice, which implies the existence of additinal conserved quantum numbers. While the currently most common approach to ED in does exploit the S_z^{tot} and lattice symmetry conservation, a viable scheme to utilize S_{tot} has, to our knowledge, not been implemented yet, even though it does promise significant performance gains.

5.1.1 Total spin bases

For spin independent Hamiltonians, the problem is in principle solved by Gelfand and Tsetlin's construction of an inherently orthonormal basis for irreducible representations of U(n) (complete with a prescription how to obtain the matrices of the infinitesimal generators of U(n), in fact it works for the general linear group GL(n) too) [71, 72]. It has been used extensively in numerical quantum chemistry and molecular physics after it was made practical by the invention of many ingenious schemes of obtaining the involved matrices efficiently (see e.g. [73–78]). For the spin-dependent Hamiltonians of spin-lattice systems this method is not applicable unfortunately. If however the system is composed of spins transforming like the *fundamental* representation of SU(n), one can use the Dirac identity relating $\hat{\boldsymbol{S}}_i\hat{\boldsymbol{S}}_j$ to the transposition P_{ij} [79], and Yamanouchi's construction of the representation matrices of irreducible representations λ of the symmetric group S_N (with respect to a basis given by all standard Young tableaux on λ) [80, 81] to write down the hamiltonian in a total spin (total highest weight) basis. For higher spins, this is not possible anymore, because there is no equivalence to the Dirac identity to express $\hat{\boldsymbol{S}}_i\hat{\boldsymbol{S}}_j$ in terms of transpositions/permutations (all one can do is write P_{ij} as a sum of powers of $\hat{\boldsymbol{S}}_i\hat{\boldsymbol{S}}_j$ as first described by Schrödinger [82], but not the other way around).

5.1.2 The labelling problem

An interesting problem encountered in this context is to determine the quantum numbers labelling states in a total hightest weight basis in addition to weight $\boldsymbol{w}^{\mathrm{z}}$ and highest weight $\boldsymbol{w}$, the generalisation of S^{z} and S of SU(2). They must be eigenvalues of operations from the point symmetry group $\mathscr{S}$ of the lattice. Since for any lattice $\mathscr{S}$ is just subgroup of S_N, the full permutation group on N objects, these labels are the eigenvalues of a commuting subset $\mathscr{L}$ of the lattice symmetries plus the eigenvalues of as many further commuting permutations $q \in \mathscr{L}' \subset S_N \backslash \mathscr{S}$ as are needed to provide a unique labelling. The theoretical benefit of such a basis is clear: since the Hamiltonian H is invariant under the lattice symmetries, its matrix will be (block-) diagonal in the quantum numbers coming from $\mathscr{L}$ (and $\mathscr{L}'$).

How can we determine these eigenvalues? There are two traditional ways: Say $V_\sigma^{\otimes N}$, the N-fold product of an irreducible SU(n) representation V_σ contains the SU(n) IR $V_{\boldsymbol{w}}$ exactly a_w times and we want to know the eigenvalues of our commuting lattice symmetries on the subspace $V_{\boldsymbol{w}}^{\oplus a_{\boldsymbol{w}}}$ Then one way is to use character theory to decompose $V_w^{\oplus a_w}$ into irreducible representations of S_N. The eigenvalues of the permutations $\mathscr{L} \cup \mathscr{L}'$ are then obtained by

diagonalising the representation matrices in these S_N IRs (which is possible for all of $\mathscr{L}$ simultaneously since it is assumed to be commuting). Alternatively, we could write down all product states $\phi_{\boldsymbol{w}^z} \in V_\sigma^{\otimes N}$, which have the total weight $\boldsymbol{w}^z$, obtain the representation matrices of all labelling operations ($\mathscr{L} \cup \mathscr{L}'$) and again diagonalise all of them simultaneously. In both cases, we need to repeat the process for (some of) those higher weight multiplets, that are contained in the subspace of the total weight $\boldsymbol{w}$. In the case of SU(2) for instance, where the total weight is just the z-component S^z_{tot} of S_{tot}, it is sufficient to consider the next higher total spin, *i.e.*, $S^z_{\text{tot}} + 1$, and discount all sets of eigenvalues which appear for both S^z_{tot} and $S^z_{\text{tot}} + 1$.

The decomposition of $V_\sigma^{\otimes N}$ into irreducible representations of SU(n) can be done elegantly using the method of Young tableaux. It allows us to determine the a_λ in

$$V_\sigma^{\otimes N} = \bigoplus_\lambda V_\lambda^{\oplus a_\lambda} \tag{5.1}$$

Here (σ) and (λ) are integer partition of N corresponding to some highest weight $\boldsymbol{s}$ and $\boldsymbol{w}$ respectively of SU(n). As we will describe in more detail below, an integer partition can be visualized in the form of a diagram of left-aligned rows of boxes called a Young diagram or shape. The existence of the correspondance between irreducible representations and integer partitions makes it possible to use the terms 'weight' and 'shape' interchangeably in the context of SU(n).

In a recent paper, [8] the method of extended Young tableaux was introduced which allows the spinon content of an eigenstate of the Haldane-Shastry-Model for a chain of N fundamental SU(n) spins to be read off directly from slightly modified Young Tableaux. An interesting consequence is that this also solves the labelling problem we described above for the case $\mathscr{L} = \{C_N\}$, C_N being the generator of the cyclic subgroup $\mathscr{C}_N$ of S_N. The eigenvalues of C_N are usually identified with the momentum along the chain. To our knowledge it is the only such method working directly with Young tableaux.

As one of the results of this thesis we show how the extended Young tableaux method generalizes to higher symmetric representations of SU(n). We were not able to find a rigorous mathematical proof of their correctness, but we present numerical evidence that it indeed gives the correct results for the eigenvalues of C_N, as long as the representations V_σ which are coupled are *symmetric*, *i.e.*, correspond to Young tableaux with a single row. We also find, that while it does give the correct distribution of momenta on the subspace $V_\lambda^{\oplus a_\lambda}$ of all multiplets λ, it does not assign these momenta to the individual YT in a way which would help in finding the irreducible representations of S_N contained in $V_\lambda^{\oplus a_\lambda}$. Lastly we show how exploiting the advantage of working directly with the Young tableaux can significantly speed up the computational solution of the labelling problem for C_N over the traditional methods.

This chapter is organized as follows: In section 2 we review the method of Young tableaux for S_N and how it relates to the irreducible representations of SU(n), we then in section 3 restate the extension procedure for fundamental representations and give some examples. In section 4 we turn to our main result of applying the procedure to higher representations: we reformulate the extension rule in a way that allows its application to YT built from higher symmetric representations, present some evidence, that it does indeed give the correct results as

far as the multiplet space as a whole is concerned and assess the suitability of extended Young tableaux to obtain the decomposition into IRs of S_N. In section 5 we analyse the computational effort of traditional methods of obtaining the eigenvalues of the cyclic permutation C_N and show that an extended Young tableaux based scheme can yield a significant speed up.

5.2 Young Tableaux and SU(n)

We want to give a short summary of Young tableaux and their traditional uses in the context of the symmetric and the (special) unitary groups.

The symmetric group S_N is the group of permutations of N distinguishable things and is of finite order $|S_N| = N!$. It can serve as a role model for all finite groups, since every finite group G is isomorphic to a subgroup of $S_{|G|}$ (Sydney's theorem). Both for this and its application in physics, where many-body wave functions in three spatial dimensions have been found to always transform like trivial (bosons) or the alternating representation (fermions), the representations of the symmetric group have been the focus of intense study over the years. In principal, the mathematical problem of finding the representations and characters of S_N was essentially solved by Alfred Young [83] in an influential series of papers based on Frobenius' earlier work for general finite groups and published at the beginning of the 20th century.

There are different ways to write a permutation suited to different situations. The most compact and as we find illustrative is the *cycle notation*: the elements which are mapped one onto the next are written within parentheses with the lowest index in the cylce appearing first by default. E.g. (142) is a cycle of length 3 and maps 1 onto 4, 4 onto 2 and 2 back onto 1. (214) would denote the same permutation in non-standard order. One-cylces, e.g. (3), also called a *fixed points*, are usually omitted from the cyclic notation. That means, in the context of S_5, (142) corresponds to the full permutation (142)(3)(5). A permutation consisting of a single 2-cycle is called a *transposition*. The set of transpositions $G_N = \{(i, i{+}1),\, i = 1, \ldots, N-1\}$ acts as the canonical set of generators for S_N, *i.e.*, every permutation can be written as products of elements in G_N. While these products are not unique, their parities are, and thus we can uniquely associate every $P \in S_N$ with a sign $\sigma_P = (-1)^{|P|}$, where $|P|$ is the number of transpositions needed to generate P.

In the theory of representations of the symmetric group S_N, both the conjugacy classes and the irreducible representations are intimately related to partitions of N into sums of k integers

$$\begin{aligned} &(\lambda) = (\lambda_1, \lambda_2, \ldots, \lambda_k),\ \lambda_1 \geq \lambda_2 \geq \cdots \geq \lambda_k > 0 \\ &|\lambda| := \sum_j \lambda_j = N \end{aligned} \tag{5.2}$$

In the case of the conjucacy classes $[c] = (S_N)^{-1} c (S_N)$ the connection is quite direct: a conjugacy class contains all permutations of the same cycle structure. For instance, the class of (12)(345) in S_5 is formed by all $P \in S_5$ made up of a transposition and a 3-cycle. For the irreducible representations the connection is via the Young tableaux which we will now review briefly.

5.2.1 Young tableaux and Young symmetrizers

We can depict an integer partition $(\lambda_1, \ldots, \lambda_k)$ graphically by a so called *Young diagram* or *shape* , which consists of k left aligned rows of boxes where row j has length λ_j (cp 5.1). A *Young tableaux* on the shape (λ) is a Young diagram of shape (λ) where the boxes are filled with integers $b_{ij} \in \{1, 2, \ldots, N\}$. The two most important classes of YT are the semi-standard and standard tableaux. A semi-standard tableaux T of *type* μ on the *shape* λ is a filling of λ with μ_1 1's, μ_2 2's and so on such that the entries are non-decreasing in each row and strictly increasing in each column (clearly this requires $|\mu| = |\lambda|$). The standard tableaux on λ are defined as all semi-standard tableaux of type $(1, 1, \ldots, 1)$, *i.e.*, each number $1, \ldots, N$ appears exactly once.

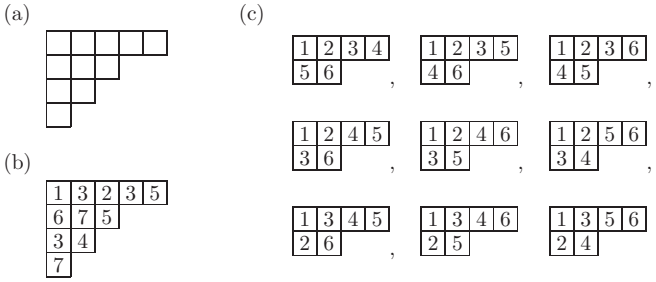

Figure 5.1: (a) the Young diagram or shape to the partition $(5, 3, 2, 1)$, (b) the same diagram as Young tableaux filled with indices $i \in 1, \ldots, 7$ and (c) all standard Young tableaux on the shape $(4, 2)$

The connection to the irreducible representations of S_N is now the following: Given any tableaux T of type $(1, 1, \ldots, 1)$ (not only standard ones, *i.e.*, the indices could be out of order too), one can interpret it as a symmetrization a_T over all indices in the same row followed by anti-symmetrization b_T over indices in the same column. The resulting operation $c_T = a_T b_T \in \mathbb{C}S_N$ is an element of the group ring of $A = \mathbb{C}S_N$ and generates a minimal left-ideal Ac_T, *i.e.*, an irreducible representation (cp. appendix D.3) Moreover, the ideals Ac_T generated as T varies over all standard YT sum directly and the space they span is the subspace of all equivalent irreducible representations associated with the diagram $\lambda(T)$. Therefore, since the irreducible representation V of a finite group G appears $\dim V$ times in the group ring $\mathbb{C}G$, the number N_λ of all standard YT on λ must equal the dimension of the irreducible representation associated with λ.

5.2.2 Hook length and branching

N_λ can be computed by the famous hook-length formula

$$N_\lambda = \frac{N!}{\prod_{i,j \in \lambda} h_{ij}} \tag{5.3}$$

where i, j are the coordinates of the box in row i and column j and h_{ij} is the length of the 'hook' associated with box i, j, which is the number of boxes below and to the right plus the

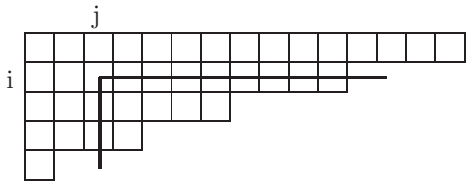

$$h_{ij} = \lambda_i - j + \lambda'_j - i + 1$$

Figure 5.2: The hook length formula allows to compute N_λ, the number of standard YT on a shape λ

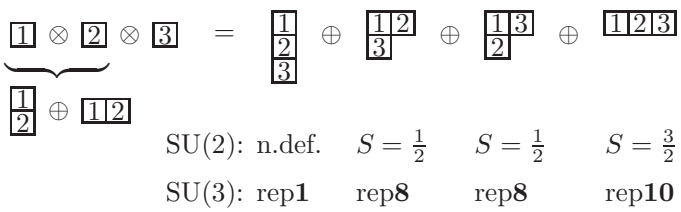

Figure 5.3: The first few examples how one can use the branching rule to built up all Young tableaux to a shape λ. In this way it is possible to decompose tensor products of SU(n) representations, where the tableaux in the decomposition must have $\leq n$ rows. Also, taking tensor products is an evidently distributive operation.

box itself. Thus, $h_{ij} = \lambda_i - j + \lambda'_j - i + 1$, where the conjugate diagram λ' is obtained from λ by interchange of rows and columns.

We can built up all standard YT on λ, $|\lambda| = N$ in the following step-by-step manner: Start with a single box. Then write down all ways in which one can add a second box such that the resulting tableaux is a standard YT of which there are two: one can put the '2' to the right or below the '1'. To both of the two tableaux thus obtained we can add a '3' in two ways, resulting in four different tableaux (see Fig. 5.3). If we continue in this fashion, making sure that all intermediate shapes ν are contained in λ, we will arrive at all standard YT on λ. This leads to the following recursive formula for N_λ (branching relation):

$$N_\lambda = \sum_\mu N_\mu \tag{5.4}$$

where the sum extends over all $\mu \subset \lambda$ which can be obtained from λ by removing one box.

5.2.3 SU(n)

The Young operators c_λ can also be applied to product states of SU(n) representations. If we define the action of a permutation in the natural way for $P \in S_N, |v\rangle = |v_1, v_2, \ldots, v_N\rangle \in V^{\otimes N}$:

$$p\,|v\rangle \to |v_{p(1)}, v_{p(2)}, \ldots, v_{p(N)}\rangle$$

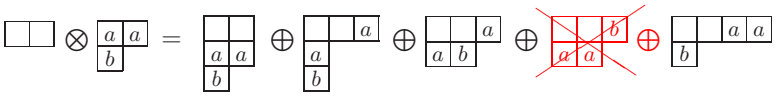

Figure 5.4: The Littlewood-Richardson rule allows us to decompose tensor spaces of non-fundamental representations. The crossed-out tableaux is the one of the 'naive' expansion which is forbidden by the LR rule

it commutes with the operations of the unitary group $SU(n)$ (in fact with all linear automorphisms in $\mathrm{GL}(V)$). If $V_{(1)} = \mathbb{C}^n$ is the fundamental representation of $\mathrm{SU}(n)$, this leads to the conclusion that the subspace of all equivalent irreducible $\mathrm{SU}(n)$ representations forms an IR of S_N and therefore we may use the standard YT to label the IRs of $\mathrm{SU}(n)$. This is the well known Schur-Weyl duality [84, 85]. There is also a more intuitive way of seeing this: we may built up total highest weight states by adding the spins one after the other, deciding each time with which spins to symmetrize and anti-symmetrize. But this is exactly the branching-rule way of constructing the standard YT given above (cp Fig. 5.3). Since we cannot anti-symmetrize on more elements than the dimension of the elementary representation $V_{(1)}$, we know that the YT involved can only have $\dim(V_{(1)})$ rows.

Thus we arrive at the prescription for decomposing the product space of fundamental representations

$$V_{(1)}^{\otimes N} = \bigoplus_{\lambda} V_{\lambda}^{\oplus N_\lambda} \tag{5.5}$$

Thus, the multiplicity with which each IR of $\mathrm{SU}(n)$ appears is given by N_λ and each subspace $V_\lambda^{\oplus N_\lambda}$ also forms *the irreducible* representation of S_N associated with that shape λ.

5.2.4 Non fundamental

Even if the elementary representations V_σ coupled together are not fundamental, which is equivalent to $|\sigma| > 1$, we can still use Young tableaux to obtain the decomposition: in this case the multiplicities $a_\lambda(\sigma, N)$ in the product space are the number of semi-standard Young tableaux on the shape λ, $|\lambda| = |\sigma|N$ of type $(\sigma_1, \sigma_2, \ldots, \sigma_k, \sigma_1, \ldots, \sigma_k, \ldots, \ldots, \sigma_1 \ldots, \sigma_k)$ which satisfy the *Littlewood-Richardson rule*. This means, if we fill a diagram of $|\sigma|N$ boxes with σ_1 '1's, σ_2 '2's, ..., σ_k 'k's, again σ_1 '$(k+1)$'s and so on until at last we enter σ_k 'kN's, such that for each constituent σ the Littlewood-Richardson rule is satisfied: Reading the rows from right to left and top to bottom and counting the frequencies c_l how often we encounter each number $l = k(j-1)+1$, $k(j-1)+2$,...,kj coming from the jth elementary shape σ we must at all times during this process have: $c_{k(j-1)+1} \geq c_{k(j-1)+2} \geq \cdots \geq c_{kj}$ for all $j = 1, \ldots, N$. An example is given in 5.4. If the Young shape σ associated with the IR V_σ of $\mathrm{SU}(n)$ consists of only one row, *i.e.*, $(\sigma) = (\sigma_1)$, it is called a symmetric representation. The name comes from the fact that we can be built it as the complete symmetrization of σ_1 fundamental representations). When coupling these single-row representations, the Littlewood-Richardson rule is trivially satisfied, *i.e.*, all semi-standard YT (of type $(\sigma_1, \sigma_1, \ldots, \sigma_1)$) are permissible.

5.2.5 Relation to S_N

Unfortunately however, for product spaces of higher SU(n) representations the decomposition into IRs of SU(n) does not automatically give the decomposition into IRs of the symmetric group S_N anymore. Each multiplet subspace $V_\lambda^{\oplus a_\lambda}$ certainly does still form a representation of S_N, but *i.g.* not an irreducible one. To our knowledge, it is not possible to determine which IRs of the symmetric group are contained in $V_\lambda^{\oplus a_\lambda}$ by straightforward analysis of the Young tableaux. Rather one has to employ character theory to find the answer and we will now briefly sketch one way in which this can be done. As mentioned before, the shape (or diagram) labelling an IR of SU(n) stands in one-to-one correspondance to the highest weight (state) contained in it. In case of SU(2) for instance, the highest possible value S^z_{tot} can attain in a total multiplet is simply the total spin S_{tot} itself. In terms of shapes it corresponds to a single-row diagram of $2S_{\text{tot}}$ boxes.

Say we want to decompose $V_\lambda^{\oplus a_\lambda}$. We take one representative permutation P from each conjugacy class in S_N and check how many states it leaves invariant in a basis $\mathscr{B}_{\boldsymbol{w}^z}$ of the subspace spanned by product states with a certain total weight $\boldsymbol{w}^z = \boldsymbol{w}(\lambda)$. This yields a vector of non-negative integers $\boldsymbol{\chi}_{\boldsymbol{w}}$ (with dimension equal to the number of classes in S_N) which is a compound character of S_N and can be analysed using the characters $\boldsymbol{\chi}_\nu$ of the irreducible representations:

$$\tilde{b}^\nu_{\boldsymbol{w}} = \frac{1}{N!} \sum_{p \in S_N} \chi_\nu(p) \chi_{\boldsymbol{w}}(p).$$

The numbers $\tilde{b}^\nu_{\boldsymbol{w}}$ are not yet the desired multiplicities however. Because a total weight subspace $\mathscr{B}_{\boldsymbol{w}^z}$ always also contains some multiplets of higher highest weight $\boldsymbol{w}' > \boldsymbol{w}$, each a certain number $c^{\boldsymbol{w}'}_{\boldsymbol{w}} \geq 0$ times. The $c^{\boldsymbol{w}'}_{\boldsymbol{w}}$ are non-negative integers and can be determined from the weight structure of the SU(n) IRs and is trivially equal to 1 for SU(2) but quickly becomes messy to compute as n increases. Already SU(3) is too complex to be shown here (the formula is given in appendix D.4). Therefore we must repeat the procedure for a number $h_{\boldsymbol{w}}$ of higher weights $\boldsymbol{w}' > \boldsymbol{w}$ and subtract a suitable linear combination:

$$b^\nu_{\boldsymbol{w}} = \tilde{b}^\nu_{\boldsymbol{w}} + \sum_{\boldsymbol{w}' > \boldsymbol{w}} d_{\boldsymbol{w}'} \tilde{b}^\nu_{\boldsymbol{w}'}$$

The $d_{\boldsymbol{w}'}$ are coefficients determined from the $c^{\boldsymbol{w}'}_{\boldsymbol{w}}$ in such way, that

$$\sum_{\boldsymbol{w}' \geq \boldsymbol{w}} d_{\boldsymbol{w}'} \tilde{\boldsymbol{w}}' = \sum_{\boldsymbol{w}\text{“} \geq \boldsymbol{w}' \geq \boldsymbol{w}} d_{\boldsymbol{w}'} c^{\boldsymbol{w}''}_{\boldsymbol{w}'} \boldsymbol{w}\text{“} \propto \boldsymbol{w} \,. \tag{5.6}$$

with $\tilde{\boldsymbol{w}}' = \sum_{w''} c^{\boldsymbol{w}''}_{\boldsymbol{w}'} \boldsymbol{w}''$ ($\boldsymbol{w}'$ is a $n-1$ dimensional vector). Lets give an example of what we mean. Say we have 3 weights $\boldsymbol{w}_1 < \boldsymbol{w}_2 < \boldsymbol{w}_3$. The $c^{\boldsymbol{w}_j}_{\boldsymbol{w}_i}$ describing how often the IR $\boldsymbol{w}_j$ appears in the total weight representation $\boldsymbol{w}_i$ can be arranged in form of a matrix, which will always be an upper or lower triangular one depending on whether the weights are in increasing or decreasing order respectively. We use increasing order and thus an example of a matrix might

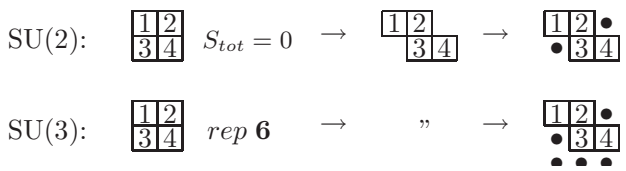

Figure 5.5: A simple example for the extension procedure: the lower row slides to the right, s.t. '2' is above '3'. How many empty spaces are counted depends on the Lie group under consideration.

be

$$\left(c_{\boldsymbol{w}_i}^{\boldsymbol{w}_j}\right) = \begin{pmatrix} 1 & 1 & 2 \\ 0 & 1 & 1 \\ 0 & 0 & 1 \end{pmatrix} \tag{5.7}$$

Say we want to extract the information about $\boldsymbol{w}_1$. This means we have to form linear combinations of the rows of the matrix, such that the entries in all columns except the first vanish. The coefficients $d_i = d_{\boldsymbol{w}_i}$ we need for this are easily seen to be $d_1 = 1$ and $d_2 = d_3 = -1$.

Once the S_N-IR content of a multiplet space is known, all eigenvalues of permutations are known as well. Thinking again of the problem of finding a total highest weight basis, one in general has to do this character analysis to obtain the quantum numbers of lattice symmetries. However, at least for the special case of the cyclic permutation C_N on N objects, there is a procedure to find its eigenvalues directly from the Young tableaux involved in the decomposition of $V_\sigma^{\otimes N}$. This is what we are going to turn to now.

5.3 Fundamental extended Young tableaux

In this section, we review how the method of extended Young tableaux, originally devised as method to obtain the spinon content of eigenstates of the Haldane-Shastry spin-chain, can be used to determine eigenvalues of the cyclic permutation $C_N \in S_N$. We first restate the rule for the case of fundamental SU(n) representations (*i.e.*, $(\sigma) = (1)$) as it was introduced in [8] and then lay the ground for its generalization to tableaux of higher representations in the next section by reformulating the construction as a stepwise process.

All eigenvalues of C_N on $V_\lambda^{\oplus N_\lambda}$ are of the form e^{ip_T}, where we use the Young tableaux T on λ to index the momenta p_T. We obtain these p_T in the following way:

Rule, old version— Let T be a standard YT of size N. By sliding them to the right where necessary, arrange all boxes of T such that in each column of the resulting *extended* tableau the numbers in the boxes are in sequence (*i.e.*, i above i+1 above i+2 etc.). This will often require leaving empty rows between boxes (cp. Fig 5.5). Mark each empty space by a dot. To each dot i we assign a number a_i in such a way that the average of all a_i within one column equals the average of the numbers in all boxes in that column and the a_i have integer or half-integer values with a spacing of 1 between the numbers from one column.

As we mentioned, the origin of this procedure lies in the physical problem of the Haldane-Shastry model (HSM), which consists of N spins on the complex unit circle with a Heisenberg-

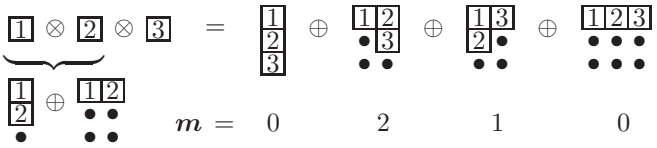

Figure 5.6: Building extended tableaux box-by-box. Three rows are marked with dots, so here we consider SU($n = 3$). However, the momenta assigned do not depend on n

type $J_{ij}\hat{\boldsymbol{S}}_i\hat{\boldsymbol{S}}_j$ interaction where the coupling $J_{ij} = |\eta_i - \eta_j|^{-2}$ decreases quadratically in the chord distance. This model has a singlet groundstate and the excitations are spinons, which can be thought of as delocalised domain walls ('half a spin flip') in a background liquid with strong antiferromagnetic short range correlations [86, 87].

By interpreting each dot in the extended Young tableaux as a spinon, they allow determining the spinon content of the eigenstates (which conserve total spin and total momentum) and moreover assigning each spinon a momenum number p_i connected to the a_i from above via $p_i = 2\pi(a_i - 1/2)/N$. The total momentum of a state is obtained by summing over all individual momenta while the energy is essentially the sum of the squares of the momenta [8]. In both quantities we need to include the constant offset p_0 and p_0^2 respectively given by

$$p_0 = \pi\frac{n-1}{n}N \tag{5.8}$$

If one intends using extended YT to obtain eigenvalues of C_N, both a more readily implementable formulation of the extention rule and more streamlined formulae for the total momentum computation will prove valuable.

Rule, new version: We start with a standard YT T, and an incomplete extended tableaux $E_1(T)$ containing only one column with the box 'N' in the same row as in T (say r). Now take the box $N-1$, which in T appears in, say, row s. If $s > r$ we put an $N-1$-box into the row s of N's column in $E_1(T)$, if $s \leq r$ we open a new column to the left of N's and place $N-1$ into the sth row there. The new, still incomplete, extended tableaux we call $E_2(T)$. We continue in this fashion with the boxes $N-2, \ldots, k, \ldots 1$ until the last box ('1') is placed and $E(T) = E_N(T)$ is completed by adding dots until all n rows are filled.

This procedure is more efficient and unlike the old formulation it is directly implementable and above all it is important in generalising the procedure to products of higher (symmetric) representations. To compute the total momentum p_T, we combine the spinon momentum numbers a_i in each column c of the extended tableau $E(T)$ into one *column number* b_c

$$b_c = \sum_{i\in c} a_i \tag{5.9}$$

Written directly in terms of the average of the box-labels $\langle i\rangle_c$ and the number of boxes k_c in the column, b_c becomes:

$$b_c = (n - k_c)\left(\langle i\rangle_c - 1/2\right) \tag{5.10}$$

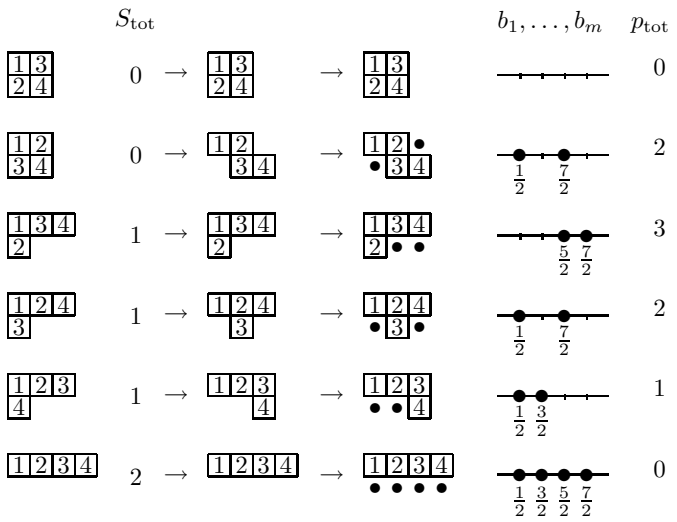

Figure 5.7: All extended Young tableaux for $N = 4 \times S = 1/2$ spins of SU(2)

the momentum p_T associated with T is then simply the sum of all column momentum numbers

$$p_T = \frac{2\pi}{N}\frac{1}{n}\left(b_0 + \sum_{c \in E(T)} b_c\right) \tag{5.11}$$

The offset momentum number $b_0 := -(n-1)N^2/2$ is necessary to ensure a linear scaling of the sum (5.11) with n. Thus, no matter as pertaining to which SU(n) we interpret a tableau T, it is always assigned the same momentum p_T (see appendix E.3).

In figure 5.7 we show as an example the extension procedure for all total spin multiplets of the tensor product space $\left(\frac{1}{2}\right)^{\otimes 4}$ of four $S = 1/2$. Since this is the tensor product of a fundamental representation we can use the Schur-Weyl duality to easily check, that the extension procedure gives the correct values: The lone quintuplett $S^{\text{tot}} = 2$ must be fully symmetric and has therefore momentum 0, the three tripletts $S^{\text{tot}} = 1$ form the standard representation V_4 of S_4 (of dimension 3 and associated with the partition $(3,1)$) while the two singlets are the self-conjugate IR W_4 (2 dimensional, associated with $(2,2)$) which stems from the standard representation $V_3 \hat{=} (2,1)$ of S_3 and therefore must have momenta 0 and 2 (in units $2\pi/N$).

The spin degrees of freedom $\boldsymbol{S}_i$ in the Haldane-Shastry model can be taken to transform like any fundamental representation of SU(n) and the mechanism of constructing excitations remains the same. Therefore this connection of extended YT and HSM eigenstates exists not only for SU(2) but higher unitary groups as well and it provides the strongest argument in favour of the correctness of our procedure. A rigorous mathematical proof, e.g. in the form of an equivalence to the results obtained from character theory would be desirable however.

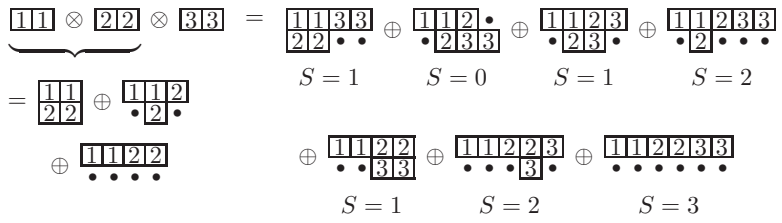

Figure 5.8: Higher representation extended YT can be built box-wise as well. Ambiguity above which of two identical k-boxes to place a $(k-1)$-box does not affect the resulting momentum

5.4 Higher Representations

While the spins in the Haldane-Shastry model can be from any fundmantal SU(n) representations, not just SU(2), a straightforward generalisation to higher representations runs into difficulty. One can nonetheless hope, that the *mathematical* statement remains valid for a suitable generalisation of the rule, which is what we investigated. It turns out, that for products of symmetric SU(n) representations V_σ, *i.e.*, those which are represented by single row YT with $|\sigma|$ boxes in them, the box-by-box approach to building extendend tableaux generalises almost directly (cp. Fig 5.8), which is one of the main results of this work.

We have to introduce only one additional condition coming from an ambiguity in where to put a box 'k' if there are several eligible open columns with boxes 'k+1'in the incomplete extended tableau $E_{N-k}(T)$. Given a tableau T representing a multiplet in $V_\sigma^{\otimes N}$ (*i.e.*, each number appears $|\sigma|$ times) we demand the resulting extended tableau $E(T)$ be *minimal*, *i.e.*, it should have as few dots/empty spaces as possible. The way to achieve it is, for each k, to consider the boxes with number 'k' *in decreasing order of their row index in* T, *i.e.*, place lowest boxes first.

Consider the fourth YT from the top in Fig. 5.9. Assume we have already placed all '3's, giving us an (incomplete) extended tableaux with two columns, one containing '3' in the second, the other in the third row. If we now were to place the '2' from the first row first, then we would have a choice to which of the two columns to add it. Depending on our decision, we would end up with two different extended tableaux, one with momentum $p = 0$ the other with $p = 1$. Placing the lower '2' (the one from the second row) first, there is no ambiguity, and we identify the extended YT with $p = 1$ as the correct minimal one.

The only further change required is a shift of the momentum offset b_0:

$$b_0(\sigma) = -\frac{n-1}{2} N\sigma \tag{5.12}$$

The origin of the $|\sigma|$ dependence is explained in App. E.3.

In the absence of a rigorous mathematical understanding why it works, we verified the method numerically and find that it does give the right answers in all cases we checked, which were for SU(n) up to $n = 4$ and N up to $N = 16$ (cp. Table 5.1).

Figures 5.9 and 5.10 show examples of the extension for coupling two-box tableaux, Fig. 5.9

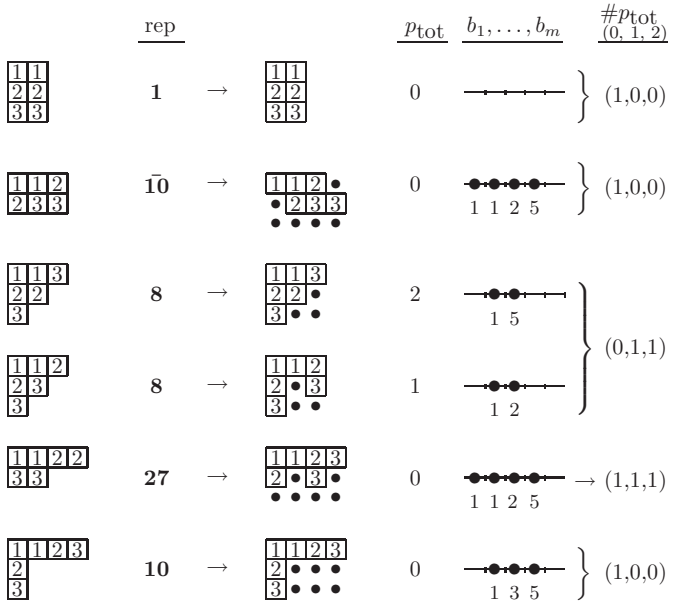

Figure 5.9: Some of the extended YT we find when coupling $N = 3$ rep **6** ($\hat{=}(2,0)$) of SU(3). As offset momentum we have from (5.12): $b_0 = -18$. The last column gives the tally of all total momenta in the subspace of multiplets of that shape where curly braces indicate that the YT shown are all there are for that shape.

group	representation	shape σ	$N_{\max}$	$\dim(V^{\otimes N})$
SU(2)	$S=1/2\,\hat{=}(1)$	$\square$	16	65536
	$S=1\,\hat{=}(2)$	$\square\square$	14	4782969
SU(3)	$\underline{3}\,\hat{=}(1,0)$	$\square$	12	531441
	$\underline{6}\,\hat{=}(2,0)$	$\square\square$	9	10077696
	$\underline{10}_3\,\hat{=}(3,0)$	$\square\square\square$	7	10000000
SU(4)	$\underline{4}\,\hat{=}(1,0,0)$	$\square$	10	1048576
	$\underline{10}_4\,\hat{=}(2,0,0)$	$\square\square$	7	10000000

Table 5.1: Unitary groups SU(n) and maximal tensor powers N for which we verified the correctness of extendend Young tableaux method

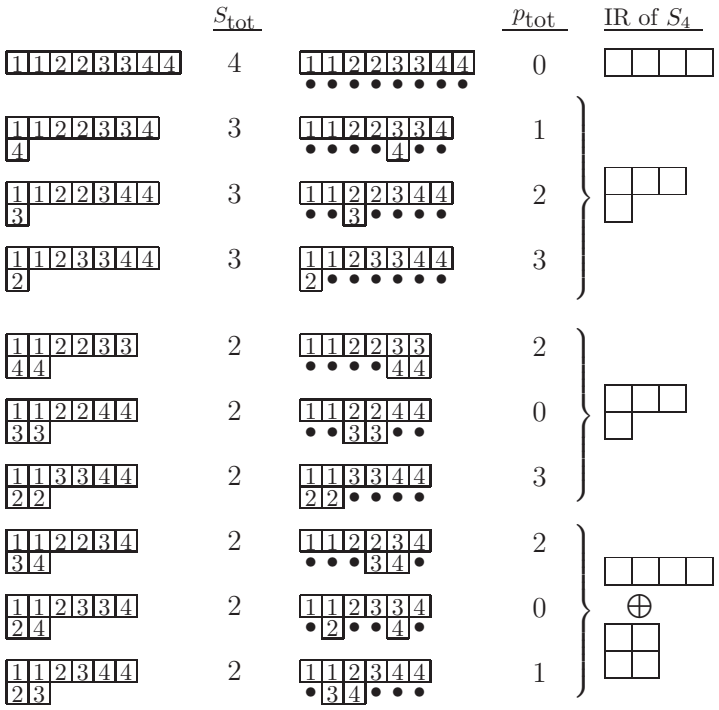

Figure 5.10: The complete decomposition of $V_{S=1}^{\otimes 4}$ together with momenta assigned by our method. In the right column we depict the identification of YT with the IRs of S_4 contained in the multiplet subspaces as far as we can do this unambiguously. Clearly, the extended Young tableaux procedure does not agree with this identification.

three SU(3) representation **6**s and Fig. 5.10 four spin $S = 1$ of SU(2) respectively.

The latter also serves to illustrate one of the limitions of our method: decomposing multiplet subspaces $V_{\boldsymbol{\lambda}}^{\oplus a_{\boldsymbol{\lambda}}}$ (e.g. the subspace of all quintetts in $(S = 1)^{\otimes 4}$ would be $V_{S=2}^{\oplus a_{S=2}}$ and $a_{S=2} = 6$) into IRs of S_N and then assigning each tableaux to the IR it should belong to according to its internal structure (rightmost column of Fig. 5.10) one can see that our extension procedure is not compatible with this decomposition. Let us elaborate on this in the following.

The method for assigning YT to IRs of S_N we employed here was a very intuitive one: we look at which shape remains when we remove the boxes first with indices Ns then $N-1$s, and so on and how the relationships between different YT we get in this way relate to the ones of *standard* YT for the same N. This method and 'works' only for small N, and even there it is ambiguous in some cases. Consider the subspace $V_{S^{\text{tot}}=2}^{\oplus 6}$ of the product space $V_{S=1}^{\otimes 4}$ which consists of 6 total spin quintuplets. Of the 6 tableaux representing these multiplets, three are basically the same as the ones of the S_N IR $(3, 1)$, the only difference being that each number

is doubled:

$$\begin{array}{|c|c|c|c|c|c|}\hline 1&1&2&2&3&3\\\hline 4&4\\\cline{1-2}\end{array}\quad,\quad\begin{array}{|c|c|c|c|c|c|}\hline 1&1&2&2&4&4\\\hline 3&3\\\cline{1-2}\end{array}\quad,\quad\begin{array}{|c|c|c|c|c|c|}\hline 1&1&3&3&4&4\\\hline 2&2\\\cline{1-2}\end{array}\tag{5.13}$$

Thus it seems straightforward to identify these three tableaux with the single representation $(3,1)$ which we know from other methods does indeed appear in $V_{S^{\mathrm{tot}}=2}^{\oplus 6}$. The other three tableaux remaining would have to be assigned to the two S_4 representations U_4 and W_4 (the trivial representation and the two dimensional IR induced from the standard representation of S_3) and it is this assignment which we cannot make unambiguously. However, it is not really necessary to resolve this ambiguity, since even with the identifications we can make the limitation we mentioned is appareant: the tableaux (5.13) belonging to $(3,1)$ are assigned momenta 2,3 and 0, while from a representation V_4 one would expect 1,2 and 3.

Thus, while extended YT do produce the correct frequencies of momenta for each subspace $V_{\boldsymbol{\lambda}}^{\oplus a_{\boldsymbol{\lambda}}}$ *as a whole*, the way momenta are assigned to the individual tableaux violates the decompostion into IRs of S_N even in cases where the identification YT→IR of S_N would be fairly clear.

5.5 Fast extension procedure

In this section we want to propose a computational scheme for obtaining the eigenvalues of the cyclic permutation C_N which translates the extended YT procedure's inherent advantage of working directly with Young tableaux into a notable speedup over traditional methods. Let us begin by describing these methods and analysing their asymptotic complexity.

At the beginning of this chapter, we already briefly described the two classes of traditional computational methods for obtaining the eigenvalues of C_N. They are character theory to find the IR content of representation (from which the eigenvalues of C_N follow directly) and diagonalisation of the matrix of C_N on total weight representations. Both start by writing down a product-state basis $\mathscr{B}_{\boldsymbol{w}}$ of a total weight subspace. If for instance we want to know, which representations of S_4 are contained in the subspace $V_{S_{\mathrm{tot}}=2}^{\oplus 6}$ of all six total spin quintuplets in $V_{S=1}^{\otimes 4}$, we write down all product states having a weight $S_{\mathrm{tot}}^{\mathrm{z}}$ of $S_{\mathrm{tot}}^{\mathrm{z}}=2$. These are the ten states

$$C_4^i\left|1,1,1,-1\right\rangle, C_4^j\left|1,1,0,0\right\rangle, C_4^k\left|1,0,1,0\right\rangle\tag{5.14}$$

where $i,j=0..3$, $k=1,2$ and the cyclic permutation C_4 is applied to a state in the natural way. Clearly, these states form the basis of a representation of S_4.

5.5.1 Character theory

The character method now goes on to obtain the character $\boldsymbol{\chi}$ of this total weight representation and from this the multiplicities of irreducible S_N representations, which yields the eigenvalues of C_N, since each IR λ comes with a fixed set of eigenvalues for each permutation.

To continue our example we simply take a representative from each of the 5 classes in S_4 and check how many states it leaves invariant. The classes are (labelled by a representative

permutation in cycle-notation) [id], [(12)], [(123)], [(1234)], [(12)(34)] with sizes $1, 6, 8, 6, 3$ respectively, the character is $\boldsymbol{\chi} = (10, 4, 1, 0, 2)$. Multiplying this with e.g. $\chi_{U_4} = (1, 1, 1, 1, 1)$, the character of the trivial representation, gives

$$\langle \chi_{U_4} | \chi \rangle = \frac{1}{4!}(10 + 24 + 8 + 0 + 6) = 2$$

Therefore, two trivial IRs are contained in the our total weight representation. We can do the same for all other characters and thus arrive at the complete decomposition

$$V_{S^{\mathrm{z}}_{\mathrm{tot}}=1} = 2 \times U_4 \oplus 2 \times V_4 \oplus W_4$$

Of these, one U_4 and one V_4 belong to higher total spin multiplets ($S^{\mathrm{tot}} = 4$ and $S^{\mathrm{tot}} = 3$ respectively) and therefore need to be excluded. This brings the final tally to

$$V^{\oplus 6}_{S^{\mathrm{z}}_{\mathrm{tot}}=2} = V_4 \oplus W_4 \oplus U_4$$

V_4 is three-, W_4 two- and U_4 one dimensional, so all 6 quintuplets are accounted for (this decomposition is the one shown in 5.10). In section 5.2.5 we already described the problem of distinguishing between S_N IRs which belong to a highest weight $\boldsymbol{w}$ and those which come from higher highest weights $\boldsymbol{w}' > \boldsymbol{w}$. The upshot is that we have to repeat the above steps for all those higher weights $\boldsymbol{w}'$, where the coefficients $d_{\boldsymbol{w}'}$ introduced there are non-zero. Let $h_{\boldsymbol{w}}$ be the number of such $d_{\boldsymbol{w}'} \neq 0$. In the case of SU(2), $h_S = 1$ for all S, because we only have to look at next higher the total S^{z} representation, *i.e.*, the one with $S^{\mathrm{z}}_{\mathrm{tot}} = S + 1$. The computational complexity of this method is determined by the size of the total weight state basis, $n_{\boldsymbol{w}} = |\mathscr{B}_{\boldsymbol{w}^{\mathrm{z}}}|$, the number of classes in S_N, which is $p(N)$ (number of integer partitions of N) and also $h_{\boldsymbol{w}}$:

$$\mathrm{C}_{\mathrm{char},S_N} = \mathrm{O}\left(p(N)\, h_{\boldsymbol{w}}\, n_{\boldsymbol{w}}\right) \tag{5.15}$$

There is however another way in which we can employ characters to get what we want: The product basis $\mathscr{B}_{\boldsymbol{w}^{\mathrm{z}}}$ is also a representation of the cyclic group $\mathscr{C}_N$. Therefore the multiplicity f_p of a momentum p can be computed via

$$f_p = \frac{1}{N} \sum_{k=1}^{N} \mathrm{e}^{i2\pi pk/N} \mathrm{Tr}\, C_N^k \tag{5.16}$$

where $p = 0, \ldots, N-1$ labels the irreducible representations and $k = 1, \ldots, N$ the classes of $\mathscr{C}_N$ and $\mathrm{Tr}\, C_N^k$ is the trace of the $(n_{\boldsymbol{w}} \times n_{\boldsymbol{w}})$ representation matrix of the kth power of C_N. Already intuitively this appears to be faster than the full character decomposition and it is definitely simpler, for instance no knowledge of all the simple S_N characters is required (above we just assumed them to be given from somewhere, which in practice means we would have to compute them first). We do however have to generate all the powers C_N^k of C_N, which takes $\mathrm{O}\left(N\, n_{\boldsymbol{w}}\right)$ steps. Thus, total complexity is

$$\mathrm{C}_{\mathrm{char},C_N} = \mathrm{O}\left(N\, h_{\boldsymbol{w}}\, n_{\boldsymbol{w}}\right) \tag{5.17}$$

where we have also taken into account the $h_{\boldsymbol{w}}$-fold repetition required here just as in all the methods based on total weight representations. This is significantly better than (5.15), but still not as good as the straightforward diagonalisation described next.

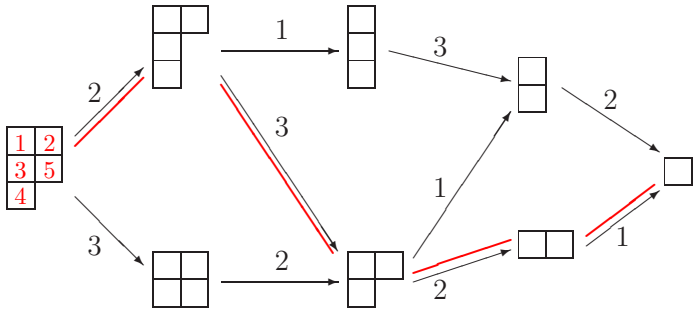

Figure 5.11: The standard YT branching graph for the shape $\lambda = (2, 2, 1)$. For all depth j the arrow-labels denote into which line the index $N-j+1$ goes. Thus, the paths through the BG correspond 1-1 to all standard YT. An example of such a path and the YT it corresponds to is shown in red.

5.5.2 Diagonalisation

The diagonalisation method really writes out the representation matrix of C_N in the basis $\mathscr{B}_{\boldsymbol{w}}$ and diagonalises it. In general, diagonalisation is of (time) complexity $O(n^3)$ in the matrix size n, but since we are dealing with a permutation matrix (in each row and column all entries are zero except for exactly one '1') we only need $O(n)$ steps. Like with the previous character method, we will also obtain C_N eigenvalues belonging to higher IRs (of SU(n)) which we can get rid of in the usual way, incurring the usual $h_{\boldsymbol{w}}$ factor. In the end therefore, diagonalisation is even faster than using $\mathscr{C}_N$ characters if we assume that the representation matrix of C_N can be written down in $O(n_{\boldsymbol{w}})$ time:

$$\mathrm{C}_{\mathrm{diag}} = \mathrm{O}\left(h_{\boldsymbol{w}}\, n_{\boldsymbol{w}}\right) \tag{5.18}$$

5.5.3 Young tableaux scheme

The extension procedure on the other hand works by writing down the N_λ Young tableaux on a shape λ and assigning each a momentum number $m(T) = 0, \ldots, N-1$. The key here is that it is possible to do both things efficiently by merging it into one process. How can we do this? It might be a good idea to exploit the neat branching property, but a naive ansatz building up tableaux by adding box after box while starting from scratch for each tableaux will require $\mathrm{O}\left(N\, N_\lambda\right)$, which will not be much better than diagonalisation in the interesting cases (low highest weight states) and due to the more intricate nature of the algorithms involved probably turn out to be worse in some less interesting ones (highest weight states close to the fully symmetric one).

We really can achieve $\mathrm{O}\left(N_\lambda\right)$ however, if we store the branching information in a suitable way: the branching graph (BG). It encodes the relations between a shape λ and all $\mu \subset \lambda$ derivable from it by removing the elementary shapes σ in the form of a directed graph. The node of th graph are the shapes $\mu \subseteq \lambda$ (with λ the root) and a directed, labeled edge $(\mu \to \nu; \mathrm{label}l)$ connects shape μ and ν if and only if the latter can be obtained from the former by a regular

removal of one elementary shape σ. A regular removal is the inverse of a regular addition, which is defined as the addition of $|\sigma|$ boxes filled with σ_1 'a's, σ_2 'b's and so on such that (i) the resulting shape is valid (ii) the resulting tableaux obeys the Littlewood- Richardson rule (cp. 5.2.4). The label l will be a list of length $|\sigma|$, recording into which rows we put the 'a's, 'b's, etc. An example of a branching graph for standard YT on the shape $(2, 2, 1)$ is depicted in Fig. (5.11). In this case, $|\sigma| = 1$ and the label is a single row-index. As long as σ is a single-row tableaux (*i.e.*, stands for a symmetric representation), there will be at most one edge between nodes. If σ has multiple rows however, it can happen that there is more than one edge (the edges differ in their labels however). Irrespective of the basic tableaux σ, each node in a BG can be assigned a depth, *i.e.*, a unique distance from the root, and it also holds that all BGs have a unique lowest element (leaf) given simply by the elementary shape σ itself.

Computing the branching graph of a compound shape λ with k rows for some elementary shape σ (where obviously $|\lambda| = N|\sigma|$) can be done very fast: it requires only $\mathrm{O}\left(\begin{pmatrix} k+|\sigma| \\ k \end{pmatrix} D_\lambda\right)$ steps, where D_λ^σ is the number of shapes μ obtainable from λ by regular removal of σ. It can easily be bounded from above by (cp. appendix E.2)

$$D_\lambda^\sigma \leq \sum_{\lambda_1 \geq j_1 \geq \cdots \geq j_k \geq 0} 1 = \begin{pmatrix} \lambda_1 + k \\ \lambda_1 \end{pmatrix} \tag{5.19}$$

The leading contribution is $D_\lambda^\sigma = \mathrm{O}\left(N^k\right)$ and thus we find that BG generation requires only polynomial time:

$$\mathrm{C_{BG}} = \mathrm{O}\left(k^{|\sigma|}\, N^k\right) \tag{5.20}$$

One can now use the efficient graph iteration described in appendix E.1 to extract all paths through the BG along with the extended YT they correspond to in $\mathrm{O}\left(N_\lambda\right)$ time. It is necessary to compute this all at once, because a modularised approach of extracting the paths first and then translating them one by one into YT incurs an additional $\mathrm{O}\left(N\right)$ time factor coming from the fact that each path is of length $N - 1$.

The total time complexity achievable is therefore indeed determined purely by the number of YT on λ

$$\mathrm{C}^{\mathrm{time}}_{\text{extended YT}} = \mathrm{O}\left(N_\lambda\right). \tag{5.21}$$

The memory requirement depends on whether we store the full extended tableaux or only its momentum. In the former case we incur an additional factor $\mathrm{O}\left(N\right)$.

5.5.4 SU(2) example

Why is this superior to diagonalisation? In practice we are mostly interested in low-weight $\mathrm{SU}(n)$ representations (in particular singlets), and for these, the number of all multiplets N_λ grows significantly slower than n_λ, the size of the corresponding total weight space.

Take for instance N spin $S = 1/2$ (N even): there are $\begin{pmatrix} N \\ N/2 \end{pmatrix}$ $S_z^{\mathrm{tot}} = 0$ states but only

$$\begin{pmatrix} N \\ N/2 \end{pmatrix} - \begin{pmatrix} N \\ N/2 - 1 \end{pmatrix} = \frac{2}{N+2} \begin{pmatrix} N \\ N/2 \end{pmatrix}$$

$S^{\text{tot}} = 0$ singlets.

In addition, the other methods incur the factor $h_\lambda(\boldsymbol{w})$ because they also need to look at higher total weights in order to clearly distinguish which momenta belong to the representation with highest weight λ and which do not. This factor, while trivial for SU(2), does indeed become increasingly important as n increases, growing like $\mathrm{o}(k)$, where k is the number of rows in λ.

6 Conclusion

We investigated topological properties of the $S = 1/2$ chiral spin liquid (CSL), the model system in which the notion of topological order was first developed, in comparison with other states, either derived from it or thought to be described by it.

Spin liquid hierarchy. —Our primary result is a hierarchy of fractional spin

$$S = k_+/2 + k_-/2$$

liquids where each element is obtained by forming products of k_+ CSLs of positive chirality and k_- CSLs of negative chirality in Schwinger boson representation. With the analytical form of these liquids known, we wrote out numerically the explicit wavefunctions on spin lattice clusters with periodic boundary conditions (PBC) and spins up to $S = 2$. We obtained the topological degeneracy (TD) by sampling the center-of-mass-parameter manifold at randomly selected points, computing the wave function for each point and then determining the rank of the overlap matrix between all these wave functions. We find that all these liquids obey

$$\mathrm{TD}(k_+, k_-) = (k_+ + 1)(k_- + 1).$$

Since there is an analytical correspondence of our hierarchy states obtained from CSLs of only one chirality ($k_- = 0$ or $k_+ = 0$) to the series of Read-Rezayi k-cluster states of the fractional quantum Hall effect, we conjecture that this result generalizes to $S > 2$. It is a clear indication that the elementary (spinon) excitations in these liquids obey non-Abelian statistics for $S > 1$. Since positive and negative chirality CSLs are related via parity (P) or time reversal (T) operations, the hierarchy states which are the result of merging $k_+ = k_- = S$ CSLs of each chirality ('chirality liquids' CL) are real valued and thus P and T invariant [57]. This makes these liquids the first states where non-Abelian statistics and P, T invariance are reconciled. In particular, we propose the spin S chirality liquids for $S \geq 2$ as promising candidates to capture a universality class of $S \geq 2$ antiferromagnets, where, away from half filling, spin liquids may be stabilized through itinerant holes of appropriate kinetic energy, as the holon excitations in the hierarchical spin liquids presumably share the high mobility of holons in the underlying CSLs. The characteristic features of this universality class are, first, the mentioned $(S + 1)^2$-fold TD on a torus and second, that spinons (and holons) obey non-Abelian SU(2) level $k = S$ statistics. In future numerical studies, we would like to test this conjecture at least for the most numerically accessible of the non-Abelian CLs, the $S = 2$ chirality liquid. Unfortunately, even for spin $S = 2$, the Hilbert space of lattice clusters is too large to allow studies of meaningful cluster sizes with current computing facilities.

Entanglement spectrum. —In one of the first entanglement spectrum studies of two dimensional spin systems we compared the spectra of two liquids from our hierarchy, the CSL itself

and the $S = 1$ chirality liquid, with the spectra of next-nearest-neighbour J_1-J_2 Heisenberg antiferromagnets (AF) at critical frustration $J_1 = 2J_2$. The geometries we looked at were a 4×6 (square) lattice cluster in case of the $S = 1/2$ spins and a cluster of dimension 4×4 with $S = 1$. In both cases, the retained subsystem A and the traced-over subsystem B, were geometrically congruent regions, and the conserved quantum numbers were the z-component of the total spin S^z_A and momentum along the A-B boundary $m_A = 0, 1, 2, 3$ (in units $2\pi/4$).

By changing boundary conditions for the CSL and the AF on the 4×6 (square) lattice cluster of $S = 1/2$ spins from periodic to cylindrical by varying effective length parameters between 1 and ∞, we investigated, whether the entanglement spectrum of the AF shows the same features as the CSL's, which we know must undergo a topologicial phase transition in the process.

In the AF, at a critical effective length $\tilde{L} = 1.15$ we find indeed a sharp dip in the gap between lowest and second lowest level in its ES and a feature of equal magnitude appears in the spectrum of the CSL, albeit, whithin the accuracy of our numerics, in the form of a plateau between lengths $L \approx 1.5 - 2.0$. Furthermore, the lowest level of both states, at all effective lengths in the $S^z = 0, m = 0$ sector, settles at a lower value for the cylindrical boundary conditions as compared to periodic ones, while the inverse is true of the gap. Another salient feature is a peak in the chiral susceptibility of the AF as a function of the effective length, signalling an increased sensitiviy to chiral perturbations. The position of this peak is somewhat separated from that of the dip in the gap, but we nevertheless think the two come from the same physical transition, as opposed to two separate transitions. We take our observations as indications, that the AF undergoes a similar transformation as the chiral spin liquid. However, due to the small circumference of our system and consequent coarse momentum resolution it is not clear, whether this gap carries topological information as do the low lying levels seen in entanglement spectrum studies of fractional quantum Hall states on a spherical geometry. So the main focus of future work would have to lie on increasing the circumference to 6 or 8 while keeping a reasonable height. Of the resulting system sizes, 48 or even 64 sites will be far beyond the possible for many years, even as algorithms improve and hardware capability continues to grow. A 36 site cluster, on the other hand, would be realisable already today, if we could use all symmetries of the 6×6 cluster. Unfortunately the cylindrical geometry implies we have only translation and reflexion in one direction.

On the 4×4 spin $S = 1$ cluster, we imposed cylindrical boundary conditons on both the CL and the AF groundstate. The entanglement spectra show marked differences: whereas the CL has hardly any gap, *i.e.*, is still highly entangled even on the cylinder, the antiferromagnet behaves very similar to the $S = 1/2$ case featuring a very large gap due to the extremely strong $S^z = 0, m = 0$ 'singlet' contribution. While the sequence of levels in the $S^z = 0, m > 0$ sectors is similar, and the overlap and energy expectation are still 0.92 and 88% (corresponding to $\approx 5J_1$ above the ground state) respectively, judging from the entanglement gap it appears that the CL is of limited value as a description of the frustrated AF. To conclusively rule out the CL as a, at least partially useful, description of antiferromagnetic states will require numerical investigation of larger systems.

In a tangential line of work inspired by our hope to speed up numerical spin lattice computations, we were able to generalize the method of extended Young tableaux invented in the

context of the Haldane-Shastry model for fundamental representations of SU(n), to arbitary higher symmetric representations. Based on this method we were also able to find an algorithm which speeds up the computation of eigenvalues of the cyclic permutation, essentially eigenvalues of the total momentum along the chain, in total (SU(n))-spin representations at least linearly. To our knowledge this is the first method which is able to achieve this for any element of the permutation group by working directly with Young tableaux.

A Notes on Topological order

A.1 Jacobi theta functions

The four Jacobi theta functions are defined as

$$\vartheta_{a.b}(z|\tau) \equiv \sum_{n=-\infty}^{\infty} \mathrm{e}^{i\pi\tau(n+a)^2}\, \mathrm{e}^{2\pi i(n+a)(z+b)} \tag{A.1}$$

where $a, b = 0, \frac{1}{2}$ and $\mathrm{Im}(\tau)¿0$.

It is easily verified that there is exactly on *odd* function among the four

$$\vartheta_{a,b}(-z|\tau) = \begin{cases} -\vartheta_{a,b}(z|\tau) & \text{if } a, b = \frac{1}{2} \\ \vartheta_{a,b}(z|\tau) & \text{otw.} \end{cases} \tag{A.2}$$

Everywhere in this thesis, ϑ with the parameters a, b omitted stands for $\vartheta_{\frac{1}{2},\frac{1}{2}}$.

The main property of these functions is their double-(quasi-)periodicity on the principal region $\mathscr{P} = \{z = a + b\tau | a, b \in [0, 1)\}$

$$\vartheta_{a,b}(z+1|\tau) = \mathrm{e}^{2\pi i a}\vartheta_{a,b}(z|\tau) \tag{A.3}$$

$$\vartheta_{a,b}(z+\tau|\tau) = \mathrm{e}^{-i\pi\tau}\mathrm{e}^{-2\pi i(z+b)}\vartheta_{a,b}(z|\tau) \tag{A.4}$$

Each has exactly one zero in $\mathscr{P}$ as is shown in figure A.1.

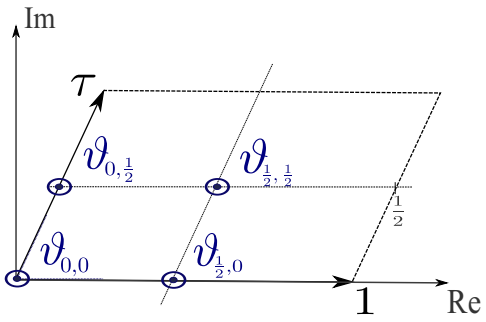

Figure A.1: Each theta function has exactly one zero in the principal region.

The defining relation for $\vartheta_{a,b}$ can be rewritten

$$\begin{aligned}\vartheta_{a,b}(z|\tau) &= \mathrm{e}^{i\pi(2ab+\tau a^2)}\mathrm{e}^{2\pi iza}\sum_{n=-\infty}^{\infty}\mathrm{e}^{i\pi\tau\, n(n+a)}\mathrm{e}^{2\pi i(z+b)n} \\ &= \mathrm{e}^{i\pi(2ab+\tau a^2)}\mathrm{e}^{2\pi iza}\left(1+\sum_{n=1}^{\infty}\cos\left(2\pi n(z+b+(n+a)\tau/2)\right)\right) \end{aligned} \tag{A.5}$$

Starting with this one can quickly derive the following alternative representations which are often encountered

$$\vartheta_1(z,q) \equiv \vartheta_{\frac{1}{2},\frac{1}{2}} = 2q^{1/4}\sum_{n=0}^{\infty}(-1)^n q^{n(n+1)}\,\sin\left(\pi(2n+1)z\right) \tag{A.6}$$

$$\vartheta_2(z,q) \equiv \vartheta_{\frac{1}{2},0} = 2q^{1/4}\sum_{n=0}^{\infty} q^{n(n+1)}\,\cos\left(\pi(2n+1)z\right) \tag{A.7}$$

$$\vartheta_3(z,q) \equiv \vartheta_{0,0} = 1+2\sum_{n=1}^{\infty} q^{n^2}\cos(2\pi nz) \tag{A.8}$$

$$\vartheta_4(z,q) \equiv \vartheta_{0,\frac{1}{2}} = 1+2\sum_{n=0}^{\infty}(-1)^n q^{n^2}\cos(2\pi nz) \tag{A.9}$$

where we introduced the substitution $q = \mathrm{e}^{i\pi\tau}$. In the literature it is quite common to find theta defined with q instead of τ.

Assume Re[τ]=0. Then $q = \mathrm{e}^{i\pi\tau} = \mathrm{e}^{-\pi\,\mathrm{Im}\tau} < 1$ is purely real. Since it is smaller than 1, the series $\sum_n q^{n^2}$ will converge very fast, even for rather small Re[τ]. Thus, we can usually restrict ourselves to the first order and this approximation is very good for Re[τ] $\gg 1$. In this case, the odd theta function will reduce to a simple sine-function

$$\vartheta(z|\tau) \overset{\mathrm{Im}[\tau]\gg 1}{\longrightarrow} 2\mathrm{e}^{-\pi\mathrm{Im}[\tau]/4}\sin(\pi z) \tag{A.10}$$

A.2 $S = 1/2$ CSL on a torus

A chiral spin liquid state on a torus written in terms of fermionic electron creation operators $c^\dagger_{z,\sigma}$ is given by

$$|\psi^{CSL}_{\mathrm{torus}}(Z_0)\rangle = \sum_{\{z_1,\ldots,z_M,w_1,\ldots,w_M\}} \psi^{CSL}_{\mathrm{torus}}\left[\boldsymbol{z}, Z_0\right]\, c^\dagger_{z_1,\uparrow}\ldots c^\dagger_{z_M,\uparrow}c^\dagger_{w_1,\downarrow}\ldots c^\dagger_{w_M,\downarrow}\,|0\rangle \tag{A.11}$$

where the summation is over all ways to destribute sites z_i and w_j disjointly over the principal region $\mathscr{P} = \{z = a+ib | a,b \in [0,1)\}$ lattice. The wavefunction is given by a product of two lowest-Landau-level (lll) wavefunctions (for up- and down-spins respectively) and contains an additional parameter Z_0 coming from the quasi-periodic boundary conditions, as will be explained in detail further down. Its effect is to fix a further zero of the wavefunction at the

position of the center-of-mass of all up and down spins, $Z = \sum_i z_i$ and $W = \sum_j w_j$ respectively. The wavefunction itself is

$$\begin{aligned}\psi^{\mathrm{CSL}}_{\mathrm{torus}}[\boldsymbol{z}; Z_0] &= \phi_{Z_0}[\boldsymbol{z}]\,\phi_{Z_0}[\boldsymbol{w}] \\ &= \mathrm{e}^{i\,K(Z_0)Z}\,\vartheta(Z-Z_0|\tau)\vartheta(W-Z_0|\tau)\prod_{i<j}\vartheta(z_i-z_j|\tau) \\ &\quad\times\prod_{i<j}\vartheta(w_i-w_j|\tau)\prod_j \mathrm{e}^{-\frac{\pi}{4}(|z_j|^2-z_j^2+|w_j|^2-w_j^2)} \qquad \text{(A.12)} \\ &= \mathrm{e}^{i\,K(Z_0)Z}\,\vartheta(Z-Z_0|\tau)\vartheta(C-Z-Z_0|\tau) \\ &\quad\times\prod_{i<j}\vartheta^2(z_i-z_j|\tau)\prod_j G(z_j)\,\mathrm{e}^{-\frac{\pi}{2}|z_j|^2-z_j^2} \qquad \text{(A.13)}\end{aligned}$$

where we have as usual neglected normalisation constants. $\vartheta(z|\tau)$ stands for the odd Jacobi theta function $\vartheta_{\frac{1}{2}\frac{1}{2}}(z|\tau)$, K is a parameter determined by the boundary conditions (along with the center-of-mass zero Z_0). In the second equation also $G(z_i)$ appears, which is a site dependent sign necessary to ensure the singlet property and is well defined on any lattice (see next section). $C = 1/N\sum_j^N z_j = \frac{1+\tau}{2}$ is the center of the cluster. From now we will choose the origin to coincide with C: $C = 0$.

The $\{w_j\}$ do not appear on the lhs, because the *set* as such is uniquely determined by the $\{z_i\}$ (the two sets are disjoint and thus complementary), and the *order* does not matter: if we reorder the $\{w_j\}$ by a permutation $P \in \mathrm{S}_M$, the signs $(-1)^P$ coming from both the function $\phi_{K,Z_0}[\boldsymbol{w}]$ and the fermionic creation operators $c^\dagger_{w_1,\downarrow}\ldots c^\dagger_{w_M,\downarrow}$ cancel.

The $\phi_{Z_0,K}[\boldsymbol{z}]$ and $\phi_{Z_0,K}[\boldsymbol{w}]$ are lowest Landau level wavefunctions for $M = N/2$ particles, with $1/4l^2$ as for a (fictious) magnetic field of M flux quanta in the principal region, *i.e.*, 1 flux quantum per plaquet of size a. We can see this when using $1/4l^2 = \pi N_\phi/2A$ and $A = N\,a = 2M\,a$:

$$\frac{1}{4l^2} = \frac{\pi}{4\,a} \qquad \text{(A.14)}$$

The boundary conditions we demand are for the wavefunction to be periodic up to phases ϕ_1 and ϕ_τ). It is to accomodate these boundary phases that we need to include the additional parameter Z_0 in a lll wavefunction on a torus. A phasefactor $\mathrm{e}^{i\,KZ}$ can be added as well, where K is then not free, but uniquely determined by our choice of Z_0 and the boundary phases ϕ_1 and ϕ_τ. In the absence of a *real* magnetic field the only physically sensible choice is $\phi_1 = \phi_\tau = 0$ *i.e.*, $\psi^{CSL}_{\mathrm{torus}}$ to thus be single valued under magnetic translation of single particle coordinates. In all, a lll wavefunction must be ($K = K(Z_0)$):

$$\phi_{Z_0,K}[\boldsymbol{z}] = \mathrm{e}^{i\,KZ}\vartheta(Z-Z_0|\tau)\prod_{i<j}\vartheta(z_i-z_j|\tau)\prod_j \mathrm{e}^{-\frac{\pi}{4}(|z_j|^2-z_j^2)} \qquad \text{(A.15)}$$

When we combine two such lll wavefunctions into a CSL, each coms with a center-of-mass-zero. Effectively, there is only one though, because only the difference plays a role in satisfying the boundary conditions.

Boundary conditions investigated

A magnetic translation of particle at z_i (translation in the presence of a magnetic field) is realized by the operator:

$$T_i(\xi_\alpha) = \exp\left[\xi_\alpha \frac{\partial}{\partial \bar{z}_i} + \bar{\xi}_\alpha \frac{\partial}{\partial z_i} + \frac{1}{4l^2}(\xi_\alpha \bar{z}_i - \bar{\xi}_\alpha z_i)\right] \tag{A.16}$$

where ξ_α, $\alpha = 1, 2$ are the principal displacements. The first part is just the usual mathematical translation operator mapping

$$f(\dots z_i \dots) \overset{T_i(\xi_\alpha)}{\longrightarrow} f(\dots z_i + \xi_\alpha \dots)$$

while the latter corresponds to a phase acquired due to the magnetic field (in zero field, $l = \infty$ and the phase vanishes as it should). Applying this operator to the lll wavefunction we require (wlog. it suffices to show it for the first particle):

$$T_1(\xi_\alpha)\phi_{Z_0,K}[\boldsymbol{z}] = \mathrm{e}^{\frac{1}{4l^2}(\xi_\alpha \bar{z}_1 - \bar{\xi}_\alpha z_1)} \phi_{Z_0,K}(z_1 + \xi_\alpha, z_2, \dots) \overset{!}{=} \mathrm{e}^{i\phi_\alpha} \phi_{Z_0,K}[\boldsymbol{z}] \tag{A.17}$$

This means, winding one particle around the torus in either of the principal directions should, as stated before, merely result in a phasefactor to the wavefunction. So the wavefunction can be regarded to obey quasi-periodic boundary conditions. In the absence of a (real) magnetic field we would expect traditional periodic boundary conditions to hold, *i.e.*, the physically reasonable choice for the boundary phases in zero field is $\phi_\alpha = 0$. Expanding and rewriting the condition (A.17) is a somewhat lengthy and subtle business, but nevertheless we want to show it here. Remember that for these lowest Landau level functions we have $1/4l^2 = \pi M/2A = \pi/4a$, the surface area of the torus is $A = \mathrm{Im}[\tau] = Na$. The quasiperiodicity conditions of the Jacobi-theta functions were given in the previous section. For brevity, we will write $\vartheta(z)$ instead of $\vartheta(z|\tau)$ for the rest of the paragraph where ϑ still stands for $\vartheta_{\frac{1}{2}\frac{1}{2}}$.

Translation in direction $\xi_1 = 1$:

$$\begin{aligned}
T_1(1)\phi_{Z_0,K}[\boldsymbol{z}] &= \mathrm{e}^{-\frac{\pi}{4}(\bar{z}_1 - z_1)}\, \mathrm{e}^{iK(Z+1)} \vartheta(Z + 1 - Z_0) \prod_{1<i<j} \vartheta(z_i - z_j) \\
&\quad \times \prod_{j=2}^{M} \vartheta(z_1 + 1 - z_j) \mathrm{e}^{-\frac{\pi}{4}(|z_j|^2 - z_j^2)}\, \mathrm{e}^{-\frac{\pi}{4}(|z_1+1|^2 - (z_1+1))} \\
&= \mathrm{e}^{-\frac{\pi}{4}(\bar{z}_1 - z_1)}\, \mathrm{e}^{iK} \mathrm{e}^{i\pi M} \mathrm{e}^{-\frac{\pi}{4}(\bar{z}_1 + z_1 + 1 - 2z_1 - 1)} \phi_{K,Z_0}[\boldsymbol{z}] \\
&= \mathrm{e}^{iK}(-1)^M \phi_{K,Z_0}[\boldsymbol{z}] \\
&\overset{!}{=} \mathrm{e}^{i\phi_1} \phi_{K,Z_0}[\boldsymbol{z}]
\end{aligned}$$

Translation in direction $\xi_2 = \tau$: Here we use $i\pi\, M = \frac{\pi M}{\mathrm{Im}[\tau]} i\mathrm{Im}[\tau] = \frac{\pi}{2}\frac{\tau-\bar\tau}{2}$

$$\begin{aligned}
T_1(\tau)\phi_{Z_0,K}[\boldsymbol{z}] &= \mathrm{e}^{-\frac{\pi}{4}(\tau\bar z_1 - \bar\tau z_1)}\,\mathrm{e}^{iK(Z+\tau)}\vartheta(Z+\tau-Z_0)\prod_{1<i<j}\vartheta(z_i-z_j)\\
&\quad\times\prod_{j=2}^{M}\vartheta(z_1+\tau-z_j)\mathrm{e}^{-\frac{\pi}{4}(|z_j|^2-z_j^2)}\,\mathrm{e}^{-\frac{\pi}{4}(|z_1+\tau|^2-(z_1+\tau)^2)}\\
&= \mathrm{e}^{iK\tau}(-1)^M\,\mathrm{e}^{-i\pi\tau M}\,\mathrm{e}^{-2\pi i\left(Z-Z_0+M\,z_1-\sum_j z_j\right)}\\
&\quad\times\mathrm{e}^{-\frac{\pi}{4}\left[\tau(2z_1+\tau)-2z_1\tau-\tau^2\right]}\,\phi_{K,Z_0}[\boldsymbol{z}]\\
&= \mathrm{e}^{iK\tau}(-1)^M\mathrm{e}^{2\pi iZ_0}\,\mathrm{e}^{-i\pi M(2z_1+\tau)}\mathrm{e}^{\frac{\pi}{4}(\tau-\bar\tau)(2z_1+\tau)}\,\phi_{K,Z_0}[\boldsymbol{z}]\\
&= \mathrm{e}^{iK\tau}(-1)^M\mathrm{e}^{2\pi iZ_0}\,\phi_{K,Z_0}[\boldsymbol{z}]\\
&\overset{!}{=} \mathrm{e}^{i\phi_\tau}\,\phi_{K,Z_0}[\boldsymbol{z}]
\end{aligned}$$

Altogether, we obtain the following conditions for K and Z_0 in terms of the boundary phases:

$$\mathrm{e}^{iK}(-1)^M \overset{!}{=} \mathrm{e}^{i\phi_1} = 1 \tag{A.18}$$

$$\mathrm{e}^{iK\tau}(-1)^M\,\mathrm{e}^{2\pi iZ_0} \overset{!}{=} \mathrm{e}^{i\phi_\tau} = 1 \tag{A.19}$$

Since the boundary phases are assumed zero for now, both rhss are 1. We have 3 equations for the 3 real parameters $K, \mathrm{Re}[Z_0], \mathrm{Im}[Z_0]$, *i.e.*, all three are fixed by the boundary conditions. A freedom in our choice of Z_0 only reappears when we merge two lll-wavefunctions into a CSL, since there enter a priori two center-of-mass-zeros Z_1 and Z_2, but only their difference $Z_1 - Z_2$ enters in the boundary conditions:

$$\begin{aligned}
T_1(\tau)\psi^{\mathrm{CSL}}_{Z_1,Z_2}[\boldsymbol{z}] &= \mathrm{e}^{\frac{\pi}{2}(\bar z_1\tau - z_1\bar\tau)}\mathrm{e}^{iK(Z+\tau)}\,\vartheta(Z+\tau-Z_1)\vartheta(-Z-\tau-Z_2)\prod_{j=2}^{N}\vartheta^2(z_1+\tau-z_j)\\
&\quad\times\mathrm{e}^{-\frac{\pi}{2}[(z_1\bar\tau+\bar z_1\tau-\tau(2z_1+\tau)]}\prod_{1<i<j}\vartheta^2(z_i-z_j)\prod_{j=1}^{N}G(z_j)\mathrm{e}^{-\frac{\pi}{2}\left(|z_j|^2-z_j^2\right)}\\
&= \mathrm{e}^{iK\tau}(-1)^{2N+1}\left(\mathrm{e}^{-i\pi\tau}\right)^{2N}\mathrm{e}^{-2i\pi\left[2Z-Z_1+Z_2-2\sum_{j=2}^{N}z_j+2(N-1)z_1\right]}\\
&\quad\times\mathrm{e}^{-\frac{\pi}{2}(\bar\tau-\tau)(2z_1+\tau)}\,\psi^{\mathrm{CSL}}_{Z_1,Z_2}[\boldsymbol{z}]\\
&= \mathrm{e}^{iK\tau}(-1)^{2N+1}\mathrm{e}^{2i\pi(Z_1-Z_2)}\,\mathrm{e}^{-2i\pi N(2z_1+\tau)}\mathrm{e}^{\frac{\pi}{2}(\tau-\bar\tau)(2z_1+\tau)}\,\psi^{\mathrm{CSL}}_{Z_1,Z_2}[\boldsymbol{z}]\\
&= \mathrm{e}^{iK\tau}(-1)^{2N+1}\mathrm{e}^{2i\pi(Z_1-Z_2)}\mathrm{e}^{-\frac{\pi}{2}(\tau-\bar\tau)(2z_1+\tau)}\,\psi^{\mathrm{CSL}}_{Z_1,Z_2}[\boldsymbol{z}]
\end{aligned}$$

where we made use of the identity $N/\mathrm{Im}[\tau] = 1$ in the last step. In all:

$$T_1(\tau)\psi^{\mathrm{CSL}}_{Z_1,Z_2}[\boldsymbol{z}] = \mathrm{e}^{iK\tau}(-1)^{2N+1}\mathrm{e}^{2i\pi(Z_1-Z_2)}\mathrm{e}^{-\frac{\pi}{2}(\tau-\bar\tau)(2z_1+\tau)}\,\psi^{\mathrm{CSL}}_{Z_1,Z_2}[\boldsymbol{z}] \tag{A.20}$$

Two things become appearent: First, the boundary conditions depend only on the *difference* $Z_1 - Z_2$, *i.e.*, in effect there is only one free center-of-mass parameter. Second, and more important, is the observation that the site variable does *not drop out*!

A.3 CSL on general lattices

The chiral spin liquid must be a spin singlet to be invariant under global spin rotations. On a square lattice (one atomic basis) the simple gauge sign $G(z_j = x_j + iy_j) = (-1)^{(x_j+1)(y_j+1)}$ ensures this where z_j is measured in units of the lattice constant a. The singlet property does however hold on general lattices too, as we show in the following.

The Perelomov identity [88]— Consider a lattice spanned by $\eta_{n,m} = na + mb$ in the complex plane, with n and m integer and the area of the unit cell Ω spanned by the primitive lattice vectors a and b set to 2π,

$$\Omega = \left|\mathrm{Im}(a\bar{b})\right| = 2\pi \tag{A.21}$$

where Im denotes the imaginary part. Let $G(\eta_{n,m}) = (-1)^{(n+1)(m+1)}$. Then

$$\sum_{n,m} P(\eta_{n,m})G(\eta_{n,m})e^{-\frac{1}{4}|\eta_{n,m}|^2} = 0 \tag{A.22}$$

for any polynomial P of $\eta_{n,m}$.

Proof— It is sufficient to proof the identity for the generating functional

$$\sum_{n,m} e^{\frac{1}{2}\eta_{n,m}\bar{z}}G(\eta_{n,m})e^{-\frac{1}{4}|\eta_{n,m}|^2} = 0. \tag{A.23}$$

Since $G(\eta_{n,m})$ takes the value -1 on a lattice with twice the original lattice constants, which we may rewrite this as

$$\sum_{n,m} e^{\frac{1}{2}\eta_{n,m}\bar{z}}e^{-\frac{1}{4}|\eta_{n,m}|^2} = 2\sum_{n,m} e^{\eta_{n,m}\bar{z}}e^{-|\eta_{n,m}|^2} \tag{A.24}$$

Kalmeyer and Laughlin [89] observed that for the square lattice, the sum on the r.h.s. can be expressed as a sum of the Fourier tranform of the function we sum over on the l.h.s. We demonstrate here that their proof can be extended to arbitrary lattices.

To begin with, since the area of the unit cell of our lattic is taken to be 2π, the reciprocal lattice is given by the original lattice rotated by $\frac{\pi}{4}$ in the plane without any rescaling of the lattice constants. In complex coordinates,

$$\zeta_{n',m'} = i(n'a + m'b), \tag{A.25}$$

as this immediately implies

$$\begin{aligned}
\boldsymbol{R}_{n,m} \cdot \boldsymbol{K}_{n',m'} &= \mathrm{Re}(\eta_{n,m}\bar{\zeta}_{n',m'}) = \\
&= \mathrm{Re}\left((na + mb)(-i)(n'\bar{a} + m'\bar{b})\right) \\
&= nm'\mathrm{Im}(a\bar{b}) + mn'\mathrm{Im}(b\bar{a}) \\
&= 2\pi \cdot \text{integer},
\end{aligned}$$

where Re denotes the real part and we have used (A.21). We define the Fourier transform in complex coordinates

$$\tilde{f}(\zeta) = \int d^2\eta f(\eta) e^{i\mathrm{Re}(\eta\bar{\zeta})}. \tag{A.26}$$

Then

$$\sum_{n',m'} \tilde{f}(\zeta_{n',m'}) = \Omega \sum_{n,m} f(\eta_{n,m}) \tag{A.27}$$

Eq. (A.27) follows directly from

$$\sum_{n',m'} e^{i\mathrm{Re}(\eta\bar{\zeta}_{n',m'})} = \Omega \sum_{n,m} \delta^{(2)}(\eta_{n,m} - \eta), \tag{A.28}$$

which is just the two-dimensional equivalent of the identity

$$\sum_{n'=-\infty}^{\infty} e^{2\pi i n' x} = \sum_{n=-\infty}^{\infty} \delta(x - n) \tag{A.29}$$

The r.h.s. of (A.29) is obviously zero if x is not an integer, and manifestly periodic in x with period 1. To verify the normalization, observe that since for any N odd,

$$\sum_{n'=-\frac{N-1}{2}}^{+\frac{N-1}{2}} e^{2\pi i n' y/N} = \begin{cases} N & \text{for } y = N \cdot \text{integer} \\ 0 & \text{otherwise.} \end{cases}$$

This implies

$$\frac{1}{N} \sum_{y=-\frac{N-1}{2}}^{+\frac{N-1}{2}} \sum_{n'=-\frac{N-1}{2}}^{+\frac{N-1}{2}} e^{2\pi i n' y/N} = 1,$$

which in the limit $N \to \infty$ is equivalent to

$$\int_{-\frac{N}{2}}^{+\frac{N}{2}} \frac{dy}{N} \sum_{n'=-\frac{N-1}{2}}^{+\frac{N-1}{2}} e^{2\pi i n' y/N} = 1$$

Substituting $x = y/N$ yields

$$\int_{-\frac{1}{2}}^{+\frac{1}{2}} dx \sum_{n'=-\infty}^{\infty} e^{2\pi i n' x} = 1,$$

which proves the normalization in (A.29).

We proceed by evaluation of the Fourier transform of $f(\eta) = e^{\frac{1}{2}\eta\bar{z}} e^{-\frac{1}{4}|\eta|^2}$:

$$\begin{aligned} \tilde{f}(\zeta) &= \int d^2\eta\, e^{\frac{1}{2}\eta\bar{z}} e^{-\frac{1}{4}|\eta|^2} e^{i\mathrm{Re}(\eta\bar{\zeta})} \\ &= \int d^2\eta\, e^{\frac{1}{2}\eta\bar{z}} e^{-\frac{1}{4}|\eta|^2} e^{\frac{i}{2}(\eta\bar{\zeta}+\bar{\eta}\zeta)} \\ &= 4\pi e^{-|\zeta|^2 + i\zeta\bar{z}} \end{aligned} \tag{A.30}$$

where we have used the integral

$$\begin{aligned}\int d^2\eta \quad F(\eta) \quad & e^{-\frac{1}{\alpha}(|\eta|^2-\bar{\eta}w)} \\ &= \quad F(\alpha\partial_{\bar{w}})\big|_{\bar{w}=0}\int d^2\eta\, e^{-\frac{1}{\alpha}(|\eta|^2-\bar{\eta}w-\eta\bar{w})} \\ &= \quad F(\alpha\partial_{\bar{w}})\big|_{\bar{w}=0}\int d^2\eta\, e^{-\frac{1}{\alpha}(|\eta-w|^2-w\bar{w})} \\ &= \quad \alpha\pi\, F(\alpha\partial_{\bar{w}})\big|_{\bar{w}=0} e^{\frac{1}{\alpha}w\bar{w}} \;=\; \alpha\pi\, F(w)\end{aligned}$$

with $F(\eta) = e^{\frac{1}{2}\eta\bar{z}+\frac{i}{2}\eta\bar{\zeta}}$, $\alpha = 4$, and $w = 2i\zeta$.

Substituting (A.30) into (A.27) we obtain

$$\sum_{n,m} f(\eta_{n,m}) = 2\sum_{n',m'} e^{-|\zeta_{n',m'}|^2+i\zeta_{n',m'}\bar{z}} \tag{A.31}$$

If we now substtute $n' = -n$, $m' = -m$, $i\zeta_{n',m'} = \eta_{n,m}$ into the l.h.s. of (A.31), we obtain (A.24). This completes the proof.

How does this relate to the CSLs singlet property? A state is a singlet iff it is annihilated by both S^+_{tot} and S^-_{tot}. Since $S^\pm_{\text{tot}} = \sum_j S^\pm_j$, applying either of these will in each term of the overall sum give a factor $\sum_j (z_j - z_k)^2 G(z_j) \mathrm{e}^{-\pi/2|z_j|^2}$. But this is zero according to the identity shown above, therefore $|\psi^{\text{CSL}}\rangle$ is a singlet on any lattice.

A.4 Laughlin $1/m$-liquid manifold as degenerate ground states

The Quantum Hall hamiltonian has the general form

$$H = \frac{1}{2m^*}\sum_j (\hat{\boldsymbol{p}}_i + \frac{e}{c}\hat{\boldsymbol{A}}_j)^2 + \sum_j V_1(|z_j|) + \sum_{i<j} V_2(|z_i - z_j|) \tag{A.32}$$

with $V_2(z)$ a two body interaction potential and $V_1(z)$ the background potential required to compensate divergences for long-range V_2. In the real-life Quantum Hall effect, V_2 is given by the Coulomb-potential.

In their 1985 paper [44], Trugman and Kivelson give a short-range potential V_2 which has the Laughlin $1/m$ trial states as ground states in the limit range $\to 0$. It is given by

$$V_2(|\boldsymbol{r}|) = \sum_{n=0}^{\infty} c_n b^{2n} \nabla^{2n} \delta^2(\boldsymbol{r}) \tag{A.33}$$

where b is a parameter which can be identified with the range of the potential: for infinitesimal b, only $n = 0$ contributes and V_2 is a Dirac-delta, while for finite, increasing b the higher derivatives of the wavefunction (at $\boldsymbol{r} = 0$) become more and more important, effectively increasing the distance from the origin at which the wavefunction is affected by V_2.

Although [44] consider only open boundary conditions, their argument can be generalized to the torus, as we will show now.

We are interested in the expectation value $\langle\psi_m[Z_\nu]|V_2|\psi_m[Z_\nu]\rangle$, where $|\psi_m\rangle$ is the Laughlin wavefunction and we made its dependence on the center-of-mass parameters Z_ν in periodic boundary conditions explicit. Consider one term in the sum $\sum_{i<j} V_2(|z_i - z_j|)$, *e.g.* $z = z_1 - z_2$. The matrix element

$$\langle\psi_m[Z_\nu]|V_2|\psi_m[Z_\nu]\rangle = \sum_n c_n b^{2n} \int \mathrm{d}z \psi_m^*(z, z_2, \ldots, z_N|\{Z_\nu\})(\Delta^n \delta^2(z))\psi_m(z, z_2, \ldots, z_N|\{Z_\nu\}) \tag{A.34}$$

can be computed by integration by parts which moves the Laplacians Δ to the wavefunction giving $\Delta^n|psi_m|^2$. The key observation now is that since m is odd and $psi_m(z, z_2, \ldots, z_N)$ thus and odd function of z, the lowest non-zero contribution comes from $m-1$ applications of Δ to the factor $\vartheta^m(z)$ in ψ_m (see 2.13 for the full wavefunction on the torus):

$$\Delta^n|\vartheta(z)|^{2m} = |\vartheta(z)|^{2m-2n-2}[\ldots]$$

and the Dirac-$\delta(z)$ function in the integral picks $|\vartheta(z=0)|^{2m-2n-2}$ which is zero unless $n = m-1$. Therefore, following the same reasoning as [44] did for open boundary conditions, we can conclude that for vanishing $b \to 0$, ψ_m has energy vanishing like b^{2m-2}. *i.e.*, it is an exact zero energy state state of A.32 with $V_1 \equiv 0$ and V_2 given by A.33 if $b = 0$ or $c_n = 0$ for $n \geq m-1$. Crucially, this is true independent of the Z_ν, which shows that one can really identify the function space spanned by $\psi_m\{Z_\nu\}$ as a degenerate eigenspace of a quantum Hall hamiltonian (since ψ_m is a combination of lowest-Landau-level orbitals the kinetic part of A.32 contibutes just a constant $\frac{1}{2}\hbar\omega_c N$ when applied to a Laughlin state).

B Addenda: Spin liquid hierarchy

B.1 Schwinger bosons

Like the Holstein-Primakov transformation used, *e.g.* , to solve the ferromagnetic Heisenberg model, Schwinger bosons are a technique to express SU(2) representations of, integer or half-integer, spin S in terms of bosonic operators. Here we introduce a pair raising/lowering operators $a_j^\dagger$, a_j and $b_j^\dagger$, b_j for each lattice site j. Commutation relations are the canonical bosonic

$$\begin{aligned}[a_i, a_j^\dagger] &= \delta_{ij} \\ [a_i, a_j] &= [a_i^\dagger, a_j^\dagger] = 0\end{aligned} \tag{B.1}$$

and the same for $b, b^\dagger$ with the additional mixed commutators

$$\left[a_i, b_j^\dagger\right] = \left[a_i^\dagger, b_j^\dagger\right] = [a_i, b_j] = 0 \tag{B.2}$$

for all i, j in the lattice.

These operators act on vacuum states $|0,0\rangle_j$ in the natural way:

$$\begin{aligned}a_j^\dagger |n,m\rangle_j &= \sqrt{n+1}\,|n+1,m\rangle_j \\ a_j |n,m\rangle_j &= \sqrt{n}\,|n-1,m\rangle_j \\ b_j^\dagger |n,m\rangle_j &= \sqrt{m+1}\,|n,m+1\rangle_j \\ b_j |n,m\rangle_j &= \sqrt{m}\,|n,m-1\rangle_j\end{aligned} \tag{B.3}$$

The total vacuum $|0\rangle$ is simply

$$|0\rangle := |0,0\rangle_1 |0,0\rangle_2 \ldots |0,0\rangle_N . \tag{B.4}$$

The connection between these operators and a state $|S, S^{\mathrm{z}}\rangle$ of an SU(2) representation S with z-component S^{z} is given by

$$|S, S^z\rangle = \frac{(a^\dagger)^{S+S^{\mathrm{z}}} (b^\dagger)^{S-S^{\mathrm{z}}}}{\sqrt{(S+S^{\mathrm{z}})!(S-S^{\mathrm{z}})!}} |0\rangle . \tag{B.5}$$

for a generic pair $a^\dagger$, $b^\dagger$.

The spin operators $S^{\pm}, S^{\mathrm{z}}$ therefore correspond to

$$\sqrt{\frac{S+S^{\mathrm{z}}}{1+S-S^{z}}}S^{+} \hat{=} a^{\dagger}b \tag{B.6}$$

$$\sqrt{\frac{S-S^{\mathrm{z}}}{1+S+S^{z}}}S^{-} \hat{=} ab^{\dagger} \tag{B.7}$$

$$S^{\mathrm{z}} \hat{=} \frac{1}{2}\left(a^{\dagger}a - b^{\dagger}b\right) \tag{B.8}$$

since the prefactor generated by, say, S^{+}

$$S^{+}\left|S, S^{\mathrm{z}}\right\rangle = \sqrt{S(S+1) - S^{\mathrm{z}}(S^{\mathrm{z}}+1))}\left|S, S^{\mathrm{z}}+1\right\rangle$$

in Schwinger boson language is just

$$\begin{aligned}\sqrt{S(S+1-S^{\mathrm{z}}(S^{\mathrm{z}}+1))} &= \sqrt{(S+S^{\mathrm{z}}+1)(S-S^{\mathrm{z}})} \\ &= \sqrt{(n_a+1)n_b}\end{aligned}$$

which is what $a^{\dagger}b$ generates as prefactor when acting on $|n_a = S+S^{\mathrm{z}}, n_b = S-S^{\mathrm{z}}\rangle$.

The key advantage Schwinger bosons hold over spin operators is the ease with which we can symmetrise two spins. Consider two spins S_1 and S_2. If we want to write down the total spin state $|S_{\mathrm{tot}}, S_t^{\mathrm{z}}ot\rangle$ for some value of $S_{\mathrm{tot}}^{\mathrm{z}}$ this requires in general a sum over all product states $|S_1, S_1^{\mathrm{z}}\rangle\,|S_2, S_2^{\mathrm{z}}\rangle$ with $S_1^{\mathrm{z}} + S_2^{\mathrm{z}} = S_{\mathrm{tot}}^{\mathrm{z}}$:

$$\left|S_{\mathrm{tot}}, S_t^{\mathrm{z}}ot\right\rangle = \sum_{S_1^{\mathrm{z}}+S_2^{\mathrm{z}}=S_t^{\mathrm{z}}ot} \left|S_1, S_1^{\mathrm{z}}\right\rangle\left|S_2, S_2^{\mathrm{z}}\right\rangle \tag{B.9}$$

Using Schwinger bosons to express individual spin states we see that all summands are in fact the same up to normalisation:

$$\begin{aligned}\left|S_{\mathrm{tot}}, S_{\mathrm{tot}}^{\mathrm{z}}\right\rangle \hat{=} & N(S_{\mathrm{tot}}, S_{\mathrm{tot}}^{\mathrm{z}})\left(a^{\dagger}\right)^{S_{\mathrm{tot}}+S_{\mathrm{tot}}^{\mathrm{z}}}\left(b^{\dagger}\right)^{S_{\mathrm{tot}}+S_{\mathrm{tot}}^{\mathrm{z}}} \\ \propto & \sum_{S_1^{\mathrm{z}}+S_2^{\mathrm{z}}=S_{\mathrm{tot}}^{\mathrm{z}}} N(S_1, S_1^{\mathrm{z}})\left(a^{\dagger}\right)^{S_1+S_1^{\mathrm{z}}}\left(b^{\dagger}\right)^{S_1+S_1^{\mathrm{z}}}\; N(S_2, S_2^{\mathrm{z}})\left(a^{\dagger}\right)^{S_2+S_2^{\mathrm{z}}}\left(b^{\dagger}\right)^{S_2+S_2^{\mathrm{z}}}\end{aligned}$$

where we defined $N(n,m) = 1/\sqrt{(n+m)!(n-m)!}$ and used that $a^{\dagger}$, $b^{\dagger}$ commute. Unfortunately there is no equality, because normalisation does not check out:

$$\begin{aligned}1 \neq & \sum_{S_1^{\mathrm{z}}+S_2^{\mathrm{z}}=S_t^{\mathrm{z}}ot} \frac{\sqrt{(S_{\mathrm{tot}}+S_{\mathrm{tot}}^{\mathrm{z}})!(S_{\mathrm{tot}}-S_{\mathrm{tot}}^{\mathrm{z}})!}}{\sqrt{(S_1+S_1^{\mathrm{z}})!(S_1-S_1^{\mathrm{z}})!}\sqrt{(S_2+S_2^{\mathrm{z}})!(S_2-S_2^{\mathrm{z}})!}} \\ = & \sum_{S_1^{\mathrm{z}}=\mathrm{Min}(-S_1, S_{\mathrm{tot}}^{\mathrm{z}}-S_2)}^{\mathrm{Max}(S_1, S_{\mathrm{tot}}^{\mathrm{z}}+S_2)} \sqrt{\begin{pmatrix} S_{\mathrm{tot}}+S_{\mathrm{tot}}^{\mathrm{z}} \\ S_1+S_1^{\mathrm{z}}\end{pmatrix}\begin{pmatrix} S_{\mathrm{tot}}-S_{\mathrm{tot}}^{\mathrm{z}} \\ S_1-S_1^{\mathrm{z}}\end{pmatrix}}\end{aligned}$$

B.2 $S = 1$ CSL wavefunction

The Schwinger boson language allows us to merge 2 $S = 1/2$ CSLs into a $S = 1$ liquid with chirality by a simple multiplication :

$$
\begin{aligned}
\psi_+^{\mathrm{S1CSL}}[a^\dagger, b^\dagger] &= \psi_+^{\mathrm{CSL}}[a^\dagger, b^\dagger]\psi_+^{\mathrm{CSL}}[a^\dagger, b^\dagger] \\
&= \sum_{\substack{\{z_1,\ldots,z_M\}\\ \{z'_1,\ldots,z'_M\}}} \prod_{i<j,1}^{M} (z_i - z_j)^2 \prod_{i<j,1}^{N-M} (z'_i - z'_j)^2 \prod_j G(z_j)G(z'_j) \\
&\qquad \times \prod_j \mathrm{e}^{-\frac{\pi}{2}(|z_j|^2+|z'_j|^2)}\; a^\dagger[\boldsymbol{z}]b^\dagger[\boldsymbol{z}^C]a^\dagger[\boldsymbol{z'}]b^\dagger[\boldsymbol{z'}^C] \\
&= \sum_{\substack{\{z_1,\ldots,z_M\\ z_{M+1}\ldots z_N\}}} \prod_{i<j,1}^{M} (z_i - z_j)^2 \prod_{i<j,M+1}^{N} (z_i - z_j)^2 \prod_{j=1}^{N} G(z_j) \\
&\qquad \times \prod_{j=1}^{N} \mathrm{e}^{-\frac{\pi}{2}|z_j|^2}\; a^\dagger[\boldsymbol{z}]b^\dagger[\boldsymbol{z}^C] \\
&= \sum_{\{z_1,\ldots,z_N\}} \mathscr{S}\left\{ \prod_{i<j,1}^{M} (z_i - z_j)^2 \prod_{i<j,M+1}^{N} (z_i - z_j)^2 \right\} \prod_{j=1}^{N} G(z_j) \\
&\qquad \times \prod_{j=1}^{N} \mathrm{e}^{-\frac{\pi}{2}|z_j|^2}\; a^\dagger[\boldsymbol{z}]b^\dagger[\boldsymbol{z}^C] \\
&= \sum_{\{z_1,\ldots,z_N\}} \mathrm{Pf}\left[\frac{1}{z_i - z_j}\right] \prod_{i<j,1}^{N} (z_i - z_j) \prod_{j=1}^{N} G(z_j)\, \mathrm{e}^{-\frac{\pi}{2}|z_j|^2} a^\dagger[\boldsymbol{z}]b^\dagger[\boldsymbol{z}^C]
\end{aligned}
$$

Here $\boldsymbol{z}^C$ denotes the set of sites complementary to $\boldsymbol{z} = \{z_1, \ldots, z_M\}$ and the notation $a^\dagger[\boldsymbol{z}]$ stands for

$$a^\dagger[\boldsymbol{z}] := a^\dagger_{z_1} \ldots a^\dagger_{z_M}$$

and analogously for $b^\dagger[\boldsymbol{w}]$.
In the step from line 2 to 3 we merged the two sets of sites $\boldsymbol{z}$ (M sites) and $\boldsymbol{z'}$ (N–M sites) each with double occupation *forbidden* into one list of N sites where (at most) double occupation *is* allowed. This does not cause problems, because even though a double occupation might now occur within the first M or the last $N-M$ sites, these configurations do not contribute since then at least one of the factors $(z_i - z_j)^2$ gives 0.
Since we already sum over all possible ways to pick N sites from the lattice allowing for double occurances, we can add a symmetrizer without changing the wavefunction except for an overall

factor $N!$, *i.e.*, we use the follwing property of symmetrization

$$\mathscr{S}: \sum_{\{z_1 \ldots z_N\}} \mathscr{S} f[\boldsymbol{z}] = N! \sum_{\{z_1 \ldots z_N\}} f[\boldsymbol{z}]$$

if $f[\boldsymbol{z}]$ is a symmetric function.

To obtain the final result, we used the identity [58]

$$\mathscr{S}\left\{ \prod_{i<j,1}^{M} (z_i - z_j)^2 \prod_{i<j,M+1}^{N} (z_i - z_j)^2 \right\} = \mathrm{Pf}\left[\frac{1}{z_i - z_j}\right] \prod_{i<j,1}^{N} (z_i - z_j) \tag{B.10}$$

which only holds in the case $M = N/2$. We do not attempt a proof here, but let us quickly check that the degree of the polynomials on both sides coincides. On the lhs, the braces contain polynomials with total degree $2 \times 2 \times M(M-1)/2 = 2M(M-1)$ (the symmetriser does not change this), while the rhs gives $N(N-1)/2 = M(2M-1)$ from the Jastrow-factor and $-M$ from the Pfaffian for a total of $M(2M-1) - M = 2M(M-1)$, so it does check out.

B.3 $S = 1$ CL wavefunction

We want to give the explicit form of the chirality liquid wavefunction and prove that it is real valued. Plugging in the $S = 1/2$ CSL into (3.12) we obtain

$$\hat{\Psi}^{\mathrm{S1CL}} = \sum_{\substack{\{z_i\},\{w_j\} \\ \{z'_i\},\{w'_j\}}} \prod_{i<j}^{M} (z_i - z_j)^2 (\bar{z}'_i - \bar{z}'_j)^2 \prod_{j=1}^{M} G(z_j) G(z'_j) \mathrm{e}^{-\frac{\pi}{2}(|z_j|^2)+|z'_j|^2} \prod_{k=1}^{M} a^\dagger_{z_k} a^\dagger_{z'_k} b^\dagger_{w_k} b^\dagger_{w'_k} \tag{B.11}$$

for the $S = 1$ CL creation operator where the sum runs over two sets $Z = \{z_1, \ldots, z_M\}$, $Z' = \{z'_1, \ldots, z'_M\}$ each containing $M = N/2$ distinct sites and each associated with its complementary set $W = \{w_j\}, W' = \{w'_j\}$ (thus $Z \cup W = Z' \cup W'$ exhaust the lattice and W, W' can be assumed to be in some standard order, because including all $M!$ orders in the sum would only contribute an overall factor $(M!)^2$ to the wavefunction).

Let us now consider one (fixed) configuration $\prod_k a^\dagger_{z_k} a^\dagger_{z'_k} b^\dagger_{w_k} b^\dagger_{w'_k}$ and assume $|Z \cap Z'| = d$, *i.e.*, d sites occur in both Z and Z' (since the number of $a^\dagger$ and $b^\dagger$ are the same it implies $W \cap W' = d$). Define $Z_{\mathrm{D}} = Z \backslash (Z \cap Z')$ and $Z'_{\mathrm{D}} = Z' \backslash (Z \cap Z')$. The key observation is now that exchanging sites between Z_{D} and Z'_{D} does not change the configuration $\prod_k a^\dagger_{z_k} a^\dagger_{z'_k} b^\dagger_{w_k} b^\dagger_{w'_k}$. Therefore the coefficient $c[\prod_k^M a^\dagger_{z_k} a^\dagger_{z'_k} b^\dagger_{w_k} b^\dagger_{w'_k}]$ can be written as

$$c[\prod_k a^\dagger_{z_k} a^\dagger_{z'_k} b^\dagger_{w_k} b^\dagger_{w'_k}] = \sum_{P \in S_{2(M-d)}/S_{M-d} \times S_{M-d}} P \prod_{i<j} (z_i - z_j)^2 (\bar{z}'_i - \bar{z}'_j)^2 \prod_{j}^{M} G(z_j) G(z'_j) \mathrm{e}^{-\frac{\pi}{2}(|z_j|^2)+|z'_j|^2} \tag{B.12}$$

where $S_{2(M-d)}/S_{M-d}\times S_{M-d}$ denotes all classes of permutations which exchange sites between Z_{D} and Z'_{D}. Such a permutation P is applied to $\prod_{i<j}(z_i-z_j)^2(\bar{z}'_i-\bar{z}'_j)^2$ in the natural way (*e.g.* $P_{(12)}\,(r_1-r_3)^2(\bar{r}_2-\bar{r}_3)^2=(r_2-r_3)^2(\bar{r}_1-\bar{r}_3)^2$). The factor $\prod_j^M G(z_j)G(z'_j)\mathrm{e}^{-\frac{\pi}{2}(|z_j|^2)+|z'_j|^2}$ is evidently real and invariant under any interchanges we might apply, so we do not have to worry about it. It is the other product which we must inspect more closely. But a short thought reveals that each permutation P in the sum has a (unique) complementary 'partner' Q, defined as the permutation which exchanges those sites which are left alone by P and vice versa. It has the properties:

$$PZ_{\mathrm{D}}\cap QZ_{\mathrm{D}}=PZ'_{\mathrm{D}}\cap QZ'_{\mathrm{D}}=\varnothing\;\Leftrightarrow\;PZ_{\mathrm{D}}=QZ'_{\mathrm{D}}\wedge PZ'_{\mathrm{D}}=QZ_{\mathrm{D}} \tag{B.13}$$

The sites in appear withoutZ_{D}, the ones in Z'_{D} with complex conjugation respectively, therefore (B.13) says that every z_k appearing in $P\prod_{i<j}(z_i-z_j)^2(\bar{z}'_i-\bar{z}'_j)^2$ will appear as $\bar{z}_k$ in $Q\prod_{i<j}(z_i-z_j)^2(\bar{z}'_i-\bar{z}'_j)^2$ and vice versa. But this means

$$P\prod_{i<j}(z_i-z_j)^2(\bar{z}'_i-\bar{z}'_j)^2=\overline{Q\prod_{i<j}(z_i-z_j)^2(\bar{z}'_i-\bar{z}'_j)^2} \tag{B.14}$$

Since we have identified pairs of complex conjugate summands in the sum (B.12) it follows that the whole sum must be real. Since the configuration $\prod_k^M a^\dagger_{z_k}a^\dagger_{z'_k}b^\dagger_{w_k}b^\dagger_{w'_k}$ we investigated was arbitary, it holds in general and thus $|\psi^{\mathrm{S1CL}}\rangle$ is real.

B.4 SU(2) level k anyons

In some models there exist fundamental excitations with exotic statistics described by a SU(2) level k algebras. Such an algebra consists of a set of 'fusion rules' which the result of all possible 2 quasi-particles merging operations.

Algraically, SU(2) level k works the following way: each particle can be thought to represent a spin $S=0,1/2,\ldots,k/2$. The fusion rules for a particle S_1 and S_2 are basically the decomposition of the product representation $S_1\otimes S_2$ with an artificial cap on the highest allowed spin

$$S_1\otimes S_2\rightarrow\bigoplus_{S=|S_1-S-2|}^{\mathrm{Min}(k-S_1+S_2,S_1+S_2)}S \tag{B.15}$$

Note the upper boundary, which would be just S_1+S_2 if we were considering normal SU(2) spins.

For the case of the simplest non-trivial example, $k=1$, we have 2 possible 'spins' $0,1$ but they are usually called 1 and σ. (1 because spin 0 is a singlet and as such the unit element of the tensor product operation). There are only 2 fusion rules:

$$1\times\sigma\rightarrow\sigma \tag{B.16}$$

$$\sigma\times\sigma\rightarrow 1 \tag{B.17}$$

Just like in the coupling of ordinary SU(2) representations, the order of the factors does not matter. The interpretation is, that annihilating 2 quasiparticles to the vacuum is always possible. This describes quasiparticles with Abelian statistics, in contrast to the algebra of SU(2) level 2 described next.

In the next level, $k = 2$, the possible spins are 0,1 and 2 which we label by $1, \sigma$ and τ respectively. They fuse like

$$1 \times \sigma \to \sigma \tag{B.18}$$
$$1 \times \tau \to \tau \tag{B.19}$$
$$\sigma \times \sigma \to 1 + \tau \tag{B.20}$$
$$\sigma \times \tau \to \sigma \tag{B.21}$$
$$\tau \times \tau \to 1 \tag{B.22}$$

The interesting rule is the third: it is not determined wether two σ-particles fuse to give a singlet 1 or a τ particle.

This is the algebra describing excitations in Pfaffian states like the one proposed for $\nu = 5/2$ in the fQHE, vortex core states of $p + ip$ superconductors or the NACSL and S2CL in our hierarchy. The connection is as follows: quasi-particles are represented by Majorana fermion operators η_j with (anti-)commutation relations

$$\{\eta_i, \eta_j\} = 2\delta_{ij} \tag{B.23}$$

They are the σs of the algebra. Quasi-particles are created in pairs η_{2k-1}, η_{2k} and each pair corresponds to a full Dirac fermion with creation and destruction operators

$$c_k^\dagger = \frac{1}{2}(\eta_{2k-1} + \eta_{2k}) \tag{B.24}$$
$$c_k = \frac{1}{2}(\eta_{2k-1} - i\eta_{2k}) \tag{B.25}$$

A Dirac fermion corresponds to the τ particle from above and the '1' we identify with the state with no Dirac-fermion present. The eigenstates of the $c_k^\dagger c_k$ span the Hilbert space. Given a fixed number of quasi-particles, say $2N$, the Hilbert space $\mathscr{H}_{2N}$ is therefore 2^N dimensional. Defining the operation

$$U_{ij} = \frac{1}{\sqrt{2}}[1 + \eta_i \eta_j] \tag{B.26}$$

one can show that they form a representation on $\mathscr{H}_{2N}$ of the braid group of N particles on a sphere. U_{ij} can therefore be interpreted as the operation of braiding two Majoranas, while, *e.g.* U_{ij}^2 corresponds to winding them around each other once. If there is 1 pair of quasi-particles, there is only one representation matrix, U_{12}, 2-dimensional and diagonal. But as soon as there are 2 pairs or more there are non-Abelian U_{ij} [35].

Take $N = 2$: with the pairing $(\eta_1, \eta_2), (\eta_3, \eta_4)$, U_{12} and U_{34} are diagonal (*i.e.*, Abelian) 4×4 matrices, while the other 4 matrices have *off-diagonal* entries, hence they do not commute with U_{12} and U_{34} (they are however not independent and we may choose one of them, say, U_{23}

as representative/generator). This is just what non-Abelian statistics is about: exchanging particles does not only give a phase factor, it rather rotates our state vector in the Hilbert space! 'Fusion' of quasi-particles j and k equates to applying the Dirac-fermion destruction operator

$$c_{jk} = \frac{1}{2}(\eta_j - i\eta_k) \tag{B.27}$$

to the system. As in the blocking mechanism described in section 2.2.5, by virtue of our basis states not being the natural basis for c_{jk}, the result is a superposition of a state with a Dirac-fermion present in orbital jk (corresponding to a τ) and no such Dirac-fermion (corresponding to the 'vacuum' 1).

We see now how non-Abelian statistics is essential here: this behaviour is only possible because winding quasi-particles can change their state and not only their phase.

B.5 $S = 2$ CL wavefunction

In analogy to the $S=1$ CSL, we would like to rewrite the $S=2$ CL in terms of renormalised spin flips. The Schwinger-boson form allows us to merge two $S = 1$ CSL wavefunctions by simple multiplication:

$$\begin{aligned}\psi^{\mathrm{S2CL}}(z_1,\ldots,z_N;w_1,\ldots,w_N) &= \psi_+^{\mathrm{S1CSL}}[\boldsymbol{z}]\,\psi_-^{\mathrm{S1CSL}}[\boldsymbol{w}] \\ &= \mathrm{Pf}\left[\frac{1}{z_i - z_j}\right]\mathrm{Pf}\left[\frac{1}{\bar{w}_k - \bar{w}_l}\right]\prod_{i<j}(z_i - z_j) \\ &\quad\times\prod_{k<l}(\bar{w}_k - \bar{w}_l)\prod_{i,k}G(z_i)G(\bar{w}_k)\,\mathrm{e}^{-\frac{\pi}{2}(|z_i|^2+|w_k|^2)}\end{aligned}$$

Here $\boldsymbol{z}$ and $\boldsymbol{w}$ are two lists of sites where (only) double occupation is allowed withing each. The creation operator for an $S=2$ CL is then

$$\hat{\Psi}^{\mathrm{S2CL}} = \sum_{\substack{\{z_1,\ldots,z_N\}\\ \{w_1,\ldots,w_N\}}} \psi^{\mathrm{S2CL}}(z_1,\ldots,z_N;w_1,\ldots,w_N)\; a^\dagger[\boldsymbol{z}]b^\dagger[\boldsymbol{w}] \tag{B.28}$$

and the state is obtained by applying this operator to the vacuum:

$$|\psi^{\mathrm{S2CL}}\rangle = \hat{\Psi}^{\mathrm{S2CL}}\,|0\rangle \tag{B.29}$$

Since both are bosonic in nature, it is no problem to substitute renormalised spin-flip operators $\tilde{S}^+$ for the $a^\dagger$s:

$$|\psi^{\mathrm{S2CL}}\rangle = \sum_{\{z_i\},\{w_j\}} \psi^{\mathrm{S2CL}}(z_1,\ldots,z_N;w_1,\ldots,w_N)\tilde{S}^+_{z_1}\ldots\tilde{S}^+_{z_N}\tilde{S}^+_{w_1}\ldots\tilde{S}^+_{w_N}\,|-2\rangle_N \tag{B.30}$$

The empty vacuum $|0\rangle$ is replaced by a 'vacuum' of completely down polarised spins $|-2\rangle_N = |2,-2\rangle^{\otimes N}$ and the renormalisation of spin-raising operators is given by

$$\tilde{S}^+_\eta = \sqrt{\frac{2+S^{\mathrm{z}}_\eta}{3-S^{\mathrm{z}}_\eta}}S^+_\eta$$

C Addenda: Entanglement spectrum analysis

C.1 Partial trace and reduced density matrix

A system S can be decomposed into subsystems A and B (*i.e.*, is bipartite), if it allows a description by product states

$$|\psi^{\mathrm{S}}_{jk}\rangle = |\phi^{\mathrm{A}}_{j}\rangle\,|\phi^{\mathrm{B}_k}\rangle \leftrightarrow \mathscr{B}_{\mathrm{S}} = \mathscr{B}_{\mathrm{A}} \times \mathscr{B}_{\mathrm{B}} \tag{C.1}$$

with $\mathscr{B}_{\mathrm{A}}$ and $\mathscr{B}_{\mathrm{B}}$ bases of the two subsystems. Given a density matrix ρ of the full system, we can perform a partial trace over, say, B to obtain a *reduced* density matrix on subsystem A (4.1)

$$\rho_{\mathrm{A}} = \mathrm{Tr}_B\rho = \sum_{|\phi^{\mathrm{B}}_k\rangle\in\mathscr{B}_{\mathrm{B}}} \langle\phi^{\mathrm{B}}_k|\rho|\phi^{\mathrm{B}}_k\rangle \tag{C.2}$$

Proposition 1 *ρ_A is again a density matrix, i.e., it is (i) hermitian, (ii) has unital trace and (iii) probabilistic eigenvalues* $\mathrm{e}^{-\xi/2}$, $\xi \in [0,\infty)$.

Proof—
(i) follows directly from $\rho^\dagger = \rho$
(ii)

$$\begin{aligned}
\mathrm{Tr}_{\mathrm{A}} &= \sum_{|\phi^{\mathrm{A}}_j\rangle\in\mathscr{B}_{\mathrm{A}}} \langle\phi^{\mathrm{A}}_j|\rho_{\mathrm{A}}|\phi^{\mathrm{A}}_j\rangle \\
&= \sum_{|\phi^{\mathrm{A}}_j\rangle} \langle\phi^{\mathrm{A}}_j| \sum_{|\phi^{\mathrm{B}}_j\rangle\in\mathscr{B}_{\mathrm{B}}} \langle\phi^{\mathrm{B}}_k|\rho|\phi^{\mathrm{B}}_k\rangle\,|\phi^{\mathrm{A}}_j\rangle \\
&= \sum_{|\psi^{\mathrm{S}}_{jk}\rangle} \langle\psi^{\mathrm{S}}_{jk}|\rho|\psi^{\mathrm{S}}_{jk}\rangle \\
&= \mathrm{Tr}_{\mathrm{S}}\rho = 1
\end{aligned} \tag{C.3}$$

(iii) Let $\rho = \sum_\alpha p_\alpha\,|\psi_\alpha\rangle\langle\psi_\alpha|$. Each $|\psi_\alpha\rangle\langle\psi_\alpha|$ can be written as

$$|\psi_\alpha\rangle\langle\psi_\alpha| = \sum_{i,j,j'} \bar{c}^{\alpha}_{ij} c^{\alpha}_{ij'}\,|\phi^{\mathrm{A}}_i\rangle\langle\phi^{\mathrm{A}}_i| \otimes |\phi^{\mathrm{B}}_j\rangle\langle\phi^{\mathrm{B}}_{j'}|$$

Therefore

$$\begin{aligned}\mathrm{Tr_B}\rho &= \sum_k \langle\phi_k^{\mathrm{B}}| \sum_{i,j,j'} \sum_\alpha \bar{c}_{ij}^\alpha c_{ij'}^\alpha \, |\phi_i^{\mathrm{A}} h\rangle\langle\phi_i^{\mathrm{A}}| \, |\phi_j^{\mathrm{B}}\rangle\langle\phi_{j'}^{\mathrm{B}}| \, |\phi_k^{\mathrm{B}}\rangle \\ &= \sum_{i,j,j',k} \sum_\alpha \bar{c}_{ij}^\alpha c_{ij'}^\alpha \delta_{jk}\delta_{j'k} \, |\phi_i^{\mathrm{A}}\rangle\langle\phi_i^{\mathrm{A}}| \\ &= \sum_i \left(\sum_k \sum_\alpha |c_{ik}^\alpha|^2 \right) |\phi_i^{\mathrm{A}}\rangle\langle\phi_i^{\mathrm{A}}| \end{aligned} \tag{C.4}$$

Therefore the eigenvalues λ_i of ρ_{A} are $\sum_k \sum_\alpha |c_{ik}^\alpha|^2 \geq 0$. Together with (ii) it follows $1 \geq \lambda_i \geq 0$, *i.e.*, they are probabilistic and can be written like $\lambda_i = \mathrm{e}^{-\xi/2}$.
This concludes the proof.

C.1.1 Alternative approach to ρ_{A}

In the literature one often finds the following way to define the reduced density matrix spectrum

$$|\psi\rangle = \sum_i \mathrm{e}^{-\xi_i/2} \, |i\rangle_A \, |i\rangle_B \tag{C.5}$$

From which the form (C.2) for ρ_{A} follows immediately. Being succinct and ostensibly clear, it lends itself to brief, to-the point introductions to the topic of entanglement spectra. However, we feel it requires some closer explanation.

A general state on a bipartite system with bases $\mathscr{B}_A = \{|i\rangle_A\}$ and $\mathscr{B}_B = \{|j\rangle_B\}$ is given by

$$|\psi\rangle = \sum_{ij} c_{ij} \, |i\rangle_A \, |j\rangle_B \tag{C.6}$$

where normalisation implies $\sum_{ij} |c_{ij}|^2 = 1$. Now one can define the states on B

$$\lambda_i \, |i\rangle_B = \sum_j c_{ij} \, |j\rangle_B \tag{C.7}$$

and again from normalisation we can infer

$$\lambda_i = \sqrt{\sum_j |c_{ij}|^2} \tag{C.8}$$

i.e., $\lambda_i \geq 0$. Since also $\sum_i \lambda_i^2 = 1$ it follows that we can set $\lambda_i = \mathrm{e}^{-\xi_i/2}$ for some $\xi_i \in [0, \infty)$, which brings us to (C.5).

a)

S^z_A	$\dim(\mathscr{H}_A^{S^z_A})$	$\Delta\xi$ shift
0	924	0.00
1	792	0.31
2	495	1.62
3	220	2.87

b)

S^z_A	$\dim(\mathscr{H}_A^{S^z_A})$	$\Delta\xi$ shift
0	1107	0.00
1	1016	0.17
2	784	0.70
3	504	1.57

Table C.1: $\Delta\xi$ shifts for a) $N = 12, S = 1/2$ and b) $N = 8, S = 1$ spins

C.1.2 Quantum number resolved spectra

If we can express the Hilbert space $\mathscr{H}_\mathrm{S}$ of the total system as a direct sum of product spaces $\mathscr{H}^{\boldsymbol{n}}_{\mathrm{A—B}}$ on the subsystems, *i.e.*,

$$\mathscr{H}_\mathrm{S}^{\boldsymbol{n}} = \bigoplus_{\boldsymbol{m}} \mathscr{H}_\mathrm{A}^{\boldsymbol{m}} \times \mathscr{H}_\mathrm{B}^{\boldsymbol{n}-\boldsymbol{m}} \tag{C.9}$$

where $\boldsymbol{n}$ is a set of quantum numbers that is conserved for all systems, then we can compute *quantum number resolved* reduced density matrices

$$\rho_\mathrm{A}^{\boldsymbol{n}} = \mathrm{Tr}_\mathrm{B}^{\boldsymbol{n}-\boldsymbol{m}}\, \rho^{\boldsymbol{n}}. \tag{C.10}$$

The trace is only over those states on B, which conserve the quantum numbers.

For instance given an $S^z_\mathrm{tot} = 0$ state $|\psi_{S^z_\mathrm{tot}=0}\rangle$ of N spins S on a lattice cluster, partitioned into subsystem A with M and B with $N - M$ spins, the Hilbert space $\mathscr{H}_\mathrm{S}^{S^z_\mathrm{tot}=0}$ of the total system decomposes into

$$\mathscr{H}_\mathrm{S}^{S^z_\mathrm{tot}=0} = \bigoplus_{k=-Ns}^{+Ns} \mathscr{H}_\mathrm{A}^{S^z_A=k} \times \mathscr{H}_\mathrm{B}^{S^z_B=-k} \tag{C.11}$$

and we can compute a reduced density matrix on A for each value of S^z_A. Since we do not include the full Hilbert space, of the original density matrix, it will *not* satisfy $\mathrm{Tr}_A^{S^z_A=k} \rho_\mathrm{A}^{S^z_A=k} = 1$. To obtain a proper density matrix we have to renormalise $\rho_\mathrm{A}^{S^z_A=k}$ with its trace.

Care must be taken when comparing levels for different S^z: since the subspaces $\mathscr{H}_{S^z}$ have different dimensions, the levels in their spectra carry different weight. The true difference between two levels $\xi_1^{S^z_1}$ and $\xi_2^{S^z_2}$ is therefore not $\Delta\xi = \xi_1^{S^z_1} - \xi_2^{S^z_2}$ but

$$\Delta\xi' = \xi_1^{S^z_1} - \xi_2^{S^z_2} + 2\ln(\frac{\dim \mathscr{H}_{S^z_2}}{\dim \mathscr{H}_{S^z_1}}) \tag{C.12}$$

C.2 Entspec: an implementation for symmetry resolved ES generation

We are given a state $|\psi\rangle$ in a product basis of the total system, the lattice specification (including the specification of subsystem A shape and those symmetries of A, which will still

give good quantum numbers after the partial trace over B, which are exactly those A has in common with B) and the bases for subsystems A and B, $\mathscr{B}_\mathrm{A}$ and $\mathscr{B}_\mathrm{b}$ respectively. We want to compute the spectrum of the reduced density matrix resolved into eigenvalues of symmetries on A.

This is done in 5 steps

1 ρ_A generation: rewrite $|\psi\rangle$ from a list into a matrix Ψ where rows are labeled by the states in $\mathscr{B}_\mathrm{A}$ and columns by the states in $\mathscr{B}_\mathrm{B}$. The reduced density matrix is then $\rho_\mathrm{A} = \Psi^\dagger\Psi$

2 Q-matrix generation: the Q-matrices are the projection matrices onto A-symmetry eigenspaces. For each symmetry A has in common with B and the total system, we compute the projection operator onto an eigenstate by looping through the configurations in $\mathscr{B}_\mathrm{A}$. In step j we choose a configuration ϕ_j from among those which we did not yet encounter. We apply the generator g of the symmetry until we return to ϕ. Each configuration $g^k\phi, k = 0, \ldots, K$ we look up in $\phi \in \mathscr{B}_\mathrm{A}$ and add an entry $\mathrm{e}^{i2\pi k/K}$ to column j row $g^k\phi$. This produces a projector for one symmetry only. It would be straightforward to handle several $g_1, g_2, \ldots$ however as long as they commute. We plan to include this feature into our program in the future.

3 symmetry projection: $\rho_\mathrm{A}^{\boldsymbol{g}} = Q_{\boldsymbol{g}}^\dagger \rho_\mathrm{A} Q_{\boldsymbol{g}}$.

4 diagonalise the $\rho_\mathrm{A}^{\boldsymbol{g}} \to \{\lambda_i\}_{\boldsymbol{g}}$

5 bin the λ_i, merging levels which are closer together than some desired precision (user specified with default value 10^{-9})

C.3 CSL on a cylinder

Just as one adapts a droplet CSL wavefunction to (quasi-)periodic boundary conditions by making the substitutions $Z \to \vartheta(Z|\tau)$ and $(z_i - z_j) \to \vartheta(z_i - z_j|\tau)$, with the 'wrapping function' $\vartheta(z|\tau)$ the odd Jacobi-theta function, we need to find an odd function suited to cylindrical boundary conditions (cbc). It need only be periodic in one direction now and the most natural choice having both properties is a Sin-function. We therefore write a lowest Landau level wavefunction $\phi[\boldsymbol{z}]$

$$\phi[\boldsymbol{z}] = \prod_{i<j}^{M} \sin(\pi(z_i - z_j)) \prod_{j}^{M} \mathrm{e}^{-\frac{\pi}{4}\mathrm{Im}[z_j]^2} \tag{C.13}$$

two of which we can combine just like with open or periodic boundary conditions to give a CSL wavefunction on the cylinder (4.9)

$$\psi_\mathrm{cyl}^\mathrm{CSL}[\boldsymbol{z}] = \mathrm{e}^{iKZ} \prod_{ij}^{M} \sin^2(\pi(z_i - z_j)) \prod_{j}^{M} G(z_j)\, \mathrm{e}^{-\frac{\pi}{2}\mathrm{Im}[z_j]^2}$$

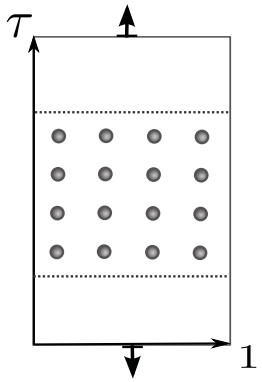

Figure C.1: One can obtain the CSL wavefunction for cylindrical boundary conditions by taking the torus version and sending the parameter $\tau \to i\infty$

where the factor π is included in the argument of the sine because our unit length is the circumference of the cylinder.

Substituting $z_j \to z_j + 1$ will leave the wavefunction unchanged with the exception of a phase e^{iK}, which can be set to equal the boundary phase:

$$\mathrm{e}^{iK} \stackrel{!}{=} \mathrm{e}^{i\phi_1} \Rightarrow K = \phi_1 \tag{C.14}$$

It is also possible to motivate (4.9) as a limit of the CSL on a torus when sending the parameter $\tau \to i\infty$ while keeping the total flux at $N\Phi_0$. As we see from (A.10), setting τ to be purely imaginary, $\vartheta(z|i\mathrm{Im}[\tau])$ will quickly approach $2\mathrm{e}^{-\pi\mathrm{Im}[\tau]/4}\sin(\pi z)$. This means for $\psi^{\mathrm{CSL}}_{\mathrm{torus}}$

$$\begin{aligned}
\psi^{\mathrm{CSL}}_{\mathrm{torus},\tau\to\infty} &= \mathrm{e}^{iKZ}\sqrt{2}^{M(M+1)+2}\mathrm{e}^{-\pi\mathrm{Im}[\tau](M(M-1)+2)/8}\sin(\pi(Z-Z_0))\sin(\pi(Z+Z_0)) \\
&\quad\times\prod_{i<j}\sin^2(\pi(z_i-z_j))\prod_j G(z_j)\mathrm{e}^{-\pi\mathrm{Im}[z_j]^2}\mathrm{e}^{-\pi\mathrm{Im}[z_j]\mathrm{Re}[z_j]} \\
&= \mathrm{e}^{iKZ}\sqrt{2}^{M(M+1)+2}\mathrm{e}^{-\pi\mathrm{Im}[\tau](M(M-1)+2)/8}\mathrm{e}^{-\pi\sum_j\mathrm{Im}[z_j]\mathrm{Re}[z_j]} \\
&\quad\times\prod_{i<j}\sin^2(\pi(z_i-z_j))\prod_j G(z_j)\mathrm{e}^{-\pi\mathrm{Im}[z_j]^2} \\
&\propto [\cos(2Z_0)-\cos(2Z)]\prod_{i<j}\sin^2(\pi(z_i-z_j))\prod_j G(z_j)\mathrm{e}^{-\pi\mathrm{Im}[z_j]^2}
\end{aligned} \tag{C.15}$$

The first part on the rhs is just the wavefunction up to normalisation, the second describes a liquid with more zeros than particles, *i.e.*, a CSL with one additional flux quantum.

D Group theory and Young tableaux

In this appendix we would like to give a brief review of the basic results in the theory of groups and their representations. A special focus will be on the beautiful and intuitive technique of Young tableaux that was invented to describe irreducible representations of the symmetric group. However, there is a deep connection between the representations of the symmetric group and the general linear group $\mathrm{GL}(V)$ (as well as its subgroups $\mathrm{U}(n)$ and $\mathrm{SU}(n)$) which manifests itself most visibly in the one-to-one relationship between highest weight labels and Young diagrams as well as the fact that Young tableaux can be used to decompose representations of $\mathrm{GL}(V)$ as well.

D.1 Definition, fundamental consequences

Definition 1 *A group is a pair $(G, \cdot)$ of a set of elements G, finite or infinite, with a multiplication operation '$\cdot$' defined on it:*

$$'\cdot' \,:\, G \times G \to G \tag{D.1}$$

such that the following three conditions are satisfied

$$\forall x, y, z \in G: \quad (x \cdot y) \cdot z = x \cdot (y \cdot z) = x \cdot y \cdot z \quad \textit{(associativity)} \tag{D.2}$$

$$\exists_1 e \in G : \forall x \in G: \quad x \cdot e = e \cdot x = x \quad \textit{(existence of unity)} \tag{D.3}$$

$$\forall x \in G : \exists_1 x^{-1} \in G: \quad x \cdot x^{-1} = x^{-1} \cdot x = e \quad \textit{(inverses)} \tag{D.4}$$

The cardinality $|G|$ of G is also called the order *of G.*

'$\exists_1$' stands for 'there is exactly one', i.e. it is the statement of uniqueness.

Definition 2 *A group G is called* abelian *or* commutative *if in addition to the basic group laws it also holds*

$$\forall x, y \in G: \; x \cdot y = y \cdot x \tag{D.5}$$

If it is clear which multiplication is meant, one omits the '$\cdot$' and just writes, e.g., xy instead of $x \cdot y$ and also refers to the set G alone as 'the group G'. Only if there is more than one multiplication operations and elements from different groups in one equation or the if there are 'multiplications' involved that are no real group operation (like the inner product of a vector

space or the cross-product '$\times$' of $\mathbb{C}^3$) does one mark them explicitly and we will keep with this convention in the following.

To name some example of groups there are the integer numbers $\mathbb{Z}$ with normal addition, which is a countably infinite abelian group, the set S_N of the permutations of N distinguishable items, which is a finite but non-abelian group or the set of invertible $n\times n$ matrices over $\mathbb{C}$, called $\mathrm{GL}(\mathbb{C}, n)$, which is uncountably infinite and also has the structure a complex manifold making it an example of a *Lie group*. The very simplest group is the *trivial group* $\{e\}$, containing only a single element.

Associativity

Associativity may look innocent enough at first glance, especially since one is very used to it, but it is quite a strong restriction on which structures of groups are possible and many properties can be deduced with its help. For example, the fact that for any $x \in G$ its inverse and the unit element e commute with it is a consequence of associativity: $xex^{-1} \overset{(D.3)}{=} xx^{-1} \overset{(D.4)}{=} e = exx^{-1}$ since x was arbitrary $\Rightarrow \forall x \in G : xe = ex$. A similar derivation shows $xx^{-1} = x^{-1}x = e$ so including the second equality in our above definition (D.3) was in fact redundant. The same can be said of the uniqueness we demanded: uniqueness of the unity also follows from existence of the inverse (and vice versa) due to associativity: let $a \in G$ be another element with $ax = xa = x\ \forall x \in G$ then multiplying with x^{-1} from, say, the right and using associativity we get $a = axx^{-1} = exx^{-1} = e$ proving that a is in fact identical with e. Similarly, if we have $y \in G : yx = e$ we can deduce $x^{-1} = (yx)x^{-1} = y(xx^{-1}) = y$, showing that there is really only one inverse.
Moreover, for all elements $x \in G$ the map f_x defined by

$$\begin{aligned} f_x : G &\to G \\ y &\mapsto xy \end{aligned} \tag{D.6}$$

is a bijection: if $y, y' \in G : f_x(y) = f_x(t') \Leftrightarrow xy = xy' \overset{x^{-1}\cdot}{\Leftrightarrow} y = y'$ and $\forall y \in G : f_x(x^{-1}y) = xx^{-1}y = y$ proving injectivity and surjectivity. Associativity comes in directly in the latter only, but we used it indirectly in showing injectivity via the commutativity of the inverse. Of course, reversing the order of multiplication in (D.6) defining $f'_x(t) := yx$ yields a bijective map as well.

Group table

For a finite group G, $|G| < \infty$, the information about its structure can be summarised in the *group table*. It is a square table, both rows and columns labelled by the group elements (in some arbitrary order) and the entry in row x and column y is given by $x \cdot y$. For example, the group table of S_3, the permutation group on 3 elements is given by:

	e	(123)	(132)	(12)	(13)	(23)
e	e	(123)	(132)	(12)	(13)	(23)
(123)	(123)	(132)	e	(13)	(23)	(12)
(132)	(132)	e	(123)	(23)	(12)	(13)
(12)	(12)	(23)	(13)	e	(132)	(123)
(13)	(13)	(12)	(23)	(123)	e	(132)
(23)	(23)	(13)	(12)	(132)	(123)	e

Here we use the cyclic notation of a permutation: e.g. (123) sends '1' to '2', '2' to '3' and '3' back to '1' closing the cycle. All permutations in S_N can be expressed in this way for arbitrary N. E.g. $(124)(35)(6) \in S_6$ is a 3-cycle on the letters 1,2 and 4, a 2-cycle on '3' and '5' and a 1-cycle, i.e. a fixed point, on '6'.
As one can see, the fact that (D.6) is bijective manifests itself through each element in G appearing exactly once in each row and column, which can serve either as a check of consistency or a way to speed up the computation of the group table.

Generators

Another concept which is very very important in group theory is the one of *generators* and *generating sets*.

Definition 3 *A set $S \subset G$ is said to be a* generating set *(for G) if every element in G may be written as a product of (finitely many) elements of S:*

$$\forall x \in G : \exists s_1, \ldots, s_k \in S : x = s_1 s_2 \ldots s_k \tag{D.7}$$

For instance, if we look at the group table of S_3 we see that for instance the three transpositions $t_1 = (12), t_2 = (13)$ and $t_3 = (23)$ generate the full group. This choice is not minimal however: Using only two transpositions, or one transposition and one 3-cycle also works.

Generating sets also provide a key to unlocking infinite groups: for those we of course cannot write down the full group table, but what we can do in many cases is find a finite generating subset. Accordingly, in that case G is called *finitely generated*. In fact, the finitely generated groups are the only infinite groups we can investigate in a meaningful way. The easiest example of such a group is $(\mathbb{Z}, +)$ again, where the generating set is simply $S_\mathbb{Z} = \{1\}$. Others are the free groups F_k on k generators $\{a_1, \ldots, a_k\}$ (consisting of all products of the generators were no factors of the form $a_j a_j^{-1}$ appear), but also the Lie groups like $\mathrm{GL}(V)$ are finitely generated if we understand this in an infinitesimal way and drop the limitation to finite products (since otherwise the resulting group would necessarily be countable).

One can take the notion of generators one step further: in general, we need only specify the set S and a suitable set of relations between the generators in it to define a group in an abstract sense.
Using again the example of S_3 with the above definition of the generators t_i, we only need to know that $t_i^2 = e$, $i = 1, 2, 3$ and $i \neq j \Rightarrow t_i t_j \neq t_j t_i$ to be able to deduce the full group table. Here is how: if we form $t_i t_j t_i$ for $i \neq j$ it holds

$$(t_i t_j t_i)^2 = t_i t_j (t_i t_i) t_j t_i = t_i t_j t_j t_i = \cdots = e$$

Therefore we must have $t_i t_j t_i = t_k$ for some k. Now, $k = i$ is ruled out by $e = t_i(t_i t_j t_i) = t_j t_i \neq e$ and $k = j$ by $t_j t_i \neq t_i t_j$ so the only possibility is for k to be the remaining third index. This implies

$$t_1 t_3 = t_2 t_1 = t_3 t_2 =: c$$
$$t_3 t_1 = t_1 t_2 = t_2 t_3 = c^{-1}$$

and thus c, c^{-1} are the only new elements, since all other products of generators can be reduced to one of e, t_1, t_2, t_3, c or c^{-1}.

Homomorphism

Frequently one is interested in maps between groups that are 'compatible' with the group structure, because they provide a means of analysing, classifying and comparing different groups.

Definition 4 *A map $\phi : G \to H$ between two groups G and H is called a **homomorphism** if*

$$\forall x, y \in G : \phi(x \cdot_G y) = \phi(x) \cdot_H \phi(y) \tag{D.8}$$

*A homomorphism of G into itself, i.e. if $H = G$, it is called an **endomorphism**. A very important class of homomorphisms are the bijective ones, called **isomorphisms**.*

Here we made it explicit that the multiplication on the lhs refers to the one of G while on the rhs it is the one defined on H.
Isomorphisms deserve special attention, because they are a 'generalisation the equality sign' for groups. With this we mean that to isomorphic groups $G \cong H$ are essentially the same even if they are not one and the same. I.e. given some realisation of G it might appear to differ from the one we are given of H, but the existence of an isomorphism means their group tables must be the same up to reordering of elements. If they are finitely generated infinite groups we may not be able to look at their group tables, but an isomorphism allows us to find two generating sets with the same algebraic behaviour. This remains true if G and H are uncountably infinite, e.g. realisations (properly called representations, D.2) of some Lie group in different dimensions.

Conjugacy Classes

Definition 5 *The* conjugacy class *of an element $c \in G$ is the G-subset $[c] = GcG^{-1}$ which is shorthand for*

$$[c] := \left\{x \in G | \exists t \in G : x = tct^{-1}\right\} \tag{D.9}$$

This does indeed define a classification of G which becomes clear when we consider the relation $\equiv$ defined by

$$x \equiv y :\Leftrightarrow \exists t \in G : x = tyt^{-1} \tag{D.10}$$

Using $t = e$ we see that it is reflexive, it is also symmetric because of the existence of inverses and above all it is transitive since from $x = tyt^{-1}$ and $y = szs^{-1}$ it follows $x = ts\,z\,s^{-1}t^{-1} = (ts)z(ts)^{-1}$ and thus $x \equiv z$.
This also implies that we can use any member $x \in [c]$ to generate the entire class via GxG^{-1} i.e. forming products with all elements in G and their inverses. This motivates the definition of the natural projection onto the factor set $G/\equiv$ (factor sets will be defined in the next section)

$$\begin{aligned}[.] : G &\to G/\equiv \\ x &\mapsto [x] = GxG^{-1}\end{aligned} \tag{D.11}$$

mapping x to its conjugacy class $[x]$.

Since it commutes with all elements in the group, the identity e is always in a class by itself. Similarly, if G is abelian all classes contain only single elements and the factor set $G/\equiv$ is isomorphic to G itself.

Subgroups

A notion of supreme importance is that of a subgroup.

Definition 6 *If a group G contains a subset $H \subseteq G$ that is algebraically closed under the multiplication of G and the inverse operation then H is called a* subgroup *of G.*

Every group trivially contains the subgroups $\{e\}$ and G itself. For a nontrivial example we can again turn to S_3: inspecting its group table we see that the first three elements, $e, (123)$ and (132) transform only among each other upon multiplication, which is exactly what is meant by algebraic closure. Thus they form a three-element abelian subgroup, called the *cyclic subgroup of order three* (also known as the *alternating group* A_3).

In general, if we have a homomorphism between two groups $\phi : G \to H$, both its *kernel* and its *image* form subgroups of G and H respectively: Let $x, y \in \ker\phi \subseteq G$ then: $\phi(xy) = \phi(x)\phi(y) = e^2 = e$ and thus $xy \in \ker\phi$. Similarly for the image $x', y' \in \mathrm{Im}\phi = \phi(G) \subseteq H$ there are $x, y \in G : x' = \phi(x)$ and $y' = \phi(y)$ thus $x'y' = \phi(x)\phi(y) = \phi(xy) \in \mathrm{Im}\phi$.

These relatively simple facts already lead to some interesting consequences: If two groups of the same order $|G| = |H|$ and G has no proper subgroup, then we immediately know that any homomorphism from one to the other is either an isomorphism or trivial. Similarly, if $|G| < |H|$ and H is the group without proper subgroup, then there can only be the trivial

homomorphism from G to H.

The notion of a *factor set* allows us to draw farther reaching conclusions about the relationship between groups and possible homomorphisms between them.

Definition 7 *Given a group G and a subgroup $H \subseteq G$ we can define the **factor set** $G/H = \{[x]_H | x \in G\}$ where*

$$[x]_H := \{y \in G | \exists h \in H : y = xh\} \tag{D.12}$$

This defines the *left factor sets*, which are the only ones we will be using, but it is of course possible to use the reverse order as well. The classes $[.]_H$ should not be confused with the conjugacy classes (which we denote by simple brackets $[.]$ without indices). This definition achieve a proper classification because the relation $x \sim_H y$ defined by (D.12) is indeed an equivalence. Since multplication with a fixed element x is injective for all $x \in G$ and therefore in particular all $x \in H$, the classes $[.]_H$ in the factor set necessarily all have the same size:

$$\forall x \in G : |[x]_H| = |H| \tag{D.13}$$

This definition holds for groups of all cardinalities. For finite groups however this lets us infer more: the existence of a homomorphism with trivial kernel $\phi : G \to H$, $\ker\phi = \{e\}$ implies that $|H|$ must be a multiple of $|G|$.

Normal subgroups

There is a special kind of subgroup which allows defining a group structure on the factor set.

Definition 8 *A subgroup $N \subseteq$ of a group G is called **normal** if $GN = NG$. This is shorthand set-notation for*

$$\forall x \in G : a, a' \in N : \; ax = xa' \tag{D.14}$$

In a somewhat imprecise way one can say that normal subgroups are those which 'commute' with the group. If we multiply (D.14) by x^{-1} from the left, we obtain $a' = x^{-1}ax$, which we recognize as the equivalence condition (D.10). This shows that a normal subgroup must contain complete conjugacy classes. This also works the other way around: if we can identify a collection of conjugacy classes that are closed under the group multiplication, they form a normal subgroup.

Consider two classes $[x]_N, [y]_N$ from the factor set $G/N = \{[c]_N | c \in G\}$ of G with respect to a normal subgroup N and take two representatives $x, x' \in [x]_N$ and $y, y' \in [y]_N$ repectively. Then it follows for the conjugacy classes of the product:

$$[x'y']_N = [xh\, yh']_N = [xy\, h''h']_N = [xy]_N \tag{D.15}$$

Where we have used in the first step that since they each come from the same class and in the second the normal subgroup property (D.14). But this implies that we can define a multiplication on G/N in well defined manner by simply defining the product of two classes

as the class of the product. With this multiplication, G/N is indeed a group: associativity follows from associativity of the G-product, the unit element is $[e]_N$, the class of the G-unit element, and the inverse of $[x]_N$ is simply $[x]_N^{-1} = [x^{-1}]_N$.

Again S_3 provides an illustrative example: the cyclic subgroup C_3 contains all the elements in the conjugacy classes $[e]$ and $[(123)]$ and nothing besides, so it is normal. The factor group is isomorphic to $S_2 = \{e, (12)\}$: $S_3/C_3 \cong S_2$. S_3 contains no other normal subgroup.

The (Cartesian) product $G \times H$ of two groups G, H is again a group if we define multiplication componentwise:

$$\forall (g,h),(g',h') \in G \times H : \; (g,h) \cdot (g',h') = (gg', hh') \tag{D.16}$$

D.2 Representations of finite groups

Definition 9 *A **r**epresentation of a group G is a homomorphism D from G into the group of invertible linear automorphisms of a vector space V, the **c**arrier space.*

$$D : G \to \mathrm{GL}(V) \tag{D.17}$$

$$g \mapsto D(g) \tag{D.18}$$

*D is called a **f**aithful representation if it is injective.*

Because it is usually clear which mapping D is meant, one often simply calls the carrier space V itself 'a representation'.

All linear maps can be associated with square matrices over the basis field V is defined over, therefore one usually thinks of a representation as a realisation of the group G with $n_V \times n_V$ matrices ($n_V = \dim V$) and therefore we will take $D(g)$ to denote a matrix. When applying a group operation g to an element $v \in V$ one also frequently omits the representation matrix and for brevity's sake writes directly gv instead of $D(g)v$.

The representation matrices $D(x)$, $x \in G$ are only determined up to a basis transformation: If the invertible matrix T effects a change to a new basis the representation matrices change like

$$D(x) \mapsto \tilde{D} = T^{-1} D(x) T \tag{D.19}$$

The two representations $D(x)$ and $\tilde{D}(x)$ are called *equivalent*.
If we can find a basis transformation such that the matrices $\tilde{D}(x)$ are, for all $x \in G$, of the form

$$\tilde{D}(x) = \left(\begin{array}{c|c} D_1 & R \\ \hline 0 & D_2 \end{array} \right) \tag{D.20}$$

we call the representation *reducible* and if the offdiagonal part R vanishes too, the representation is said to be *decomposable* because in that case the representation is clearly just a direct sum of two independent representations $D_1(G)$ and $D_2(G)$.

Irreducible representations

Definition 10 *A representation $D(G)$ of a group G is called* ***irreducible*** *if there is no basis transformation such that brings all matrices $D(G)$ simultaneously into the form (D.20).*

Finite groups have the neat property that reduciblity and decomposability are equivalent, i.e. a reducible representation always decomposes into direct some of irreducible ones which can be shown in the following way: given any inner product $\langle .,. \rangle$ on V we obtain a G-invariant one by averaging over the group

$$\langle v, w \rangle_G := \frac{1}{|G|} \sum_G \langle D(g)v, D(g)w \rangle \tag{D.21}$$

Now if V is not already irreducible, we can find a proper subrepresentation W. Then V decomposes into W and $W^\perp$, the orthogonal subspace to W with resp to $\langle .,. \rangle_G$. Because $\langle .,. \rangle_G$ is G-invariant it holds for all $v \in W$, $w \in W^\perp$ and $g \in G$

$$0 = \langle v, w \rangle_G = \langle gv, gw \rangle_G = \langle v', gw \rangle_G$$

proving that $G \cdot W^\perp \subseteq W^\perp$. But this means that the representation matrices $D(g)$ are all block-diagonal and thus decompose into a direct sum of two subrepresentations.

Constructing representations

There are other ways to construct new representations besides taking the direct sum. Given two representations D_1, D_2 on the spaces V_1 and V_2 respectively we can also form the product representation, i.e. the tensor product of all representation matrices

$$\begin{aligned} D : G &\to \mathrm{GL}(V_1 \times V_2) \\ x &\mapsto D_1(x) \otimes D_2(x) \end{aligned} \tag{D.22}$$

This representation lives on the carrier space $V = V_1 \times V_2$ and is in general reducible. It is the main purpose of this chapter to introduce methods how we can decompose it in the cases when $G = S_N$, the symmetric group, and $G = \mathrm{U}(n)$, the unitary group. However, we consider not only two- but in general N-fold tensor products ($V^{\otimes N}$).

The symmetric power $\mathrm{Sym}^N V$ of a vector space V are all elements in $V^{\otimes N}$ defined in the following way:

$$v \in \mathrm{Sym}^N V \;\Leftrightarrow\; \exists v_1, v_2, \ldots, v_N \in V : v = \mathscr{S}(v_1 \times v_2 \times \cdots \times v_N) \tag{D.23}$$

where we defined the symmetrisation operation

$$\mathscr{S}(v_1 \times v_2 \times \cdots \times v_N) := \sum_{P \in S_N} v_{P(1)} \times v_{P(2)} \times \cdots \times v_{P(N)} \tag{D.24}$$

The elements of $\mathrm{Sym}^N V$ are thus completely symmetric under all permutations. This property clearly survives addition of vectors and multiplication with scalars, i.e. $\mathrm{Sym}^N V$ is a vector space.
If $\{e_i,\, i = 1, \ldots, n_V\}$ is a basis of V, then a basis of $\mathrm{Sym}^N V$ is given by

$$\{\mathscr{S}(e_{j_1} \times \cdots \times e_{j_N}),\ 1 \le j_1 \le j_2 \le \cdots \le j_N \le n_V\}$$

and has a dimension of $(N + n_V - 1)!/n_V!(N-1)!$.

Similar to symmetrization, we define the outer or wedge product of N vectors

$$v_1 \wedge v_2 \wedge \cdots \wedge v_N := \sum_{P \in S_N} (-1)^{|P|}\, v_{P(1)} \times v_{P(2)} \times \cdots \times v_{P(N)} \tag{D.25}$$

where $|P|$ denotes the number of transpositions required to build the permutation P.

In analogy to symmetrization above, the outer power $\wedge^N V$ of a vector space V is given by all elements of the form $v_1 \wedge v_2 \wedge \cdots \wedge v_N$ in $V^{\otimes N}$. The basis

$$\{e_{j_1} \wedge \cdots \wedge e_{j_N},\ 1 \le j_1 < j_2 < \cdots < j_N \le n_V\}$$

in terms of V-basis vectors e_j has the dimension $n_V!/(n_V - N)!N!$. Note, that this is undefined for $N > n_V$, which reflects the fact, that we cannot antisymmetrize over more constituents (copies of V) than there are degrees of freedom (dimenson of V).

Schur's lemma

An extremely useful tool in representation theory is Schur's lemma. A succinct formulation is

Theorem 1 *Let A a homomorphism between two* irreducible *representations V and W of G. It holds*
(1) either A is an isomorphism or $A = 0$.
(2) if $V = W$, then $A = \xi\, \mathbb{1}_{\dim V}$ with $\xi \in \mathbb{C}$

Here '$V = W$' is shorthand for $\forall g \in G : D_V(g) = D_W(g)$.

Proof:
(1) We know that the subspaces $\mathrm{Ker}\, A \subseteq V$ and $\mathrm{Im}\, A \subseteq W$ are invariant under G. But being irreducible only they themselves and the trivial subspace $\{0\}$ can be invariant in V and W.
If $\mathrm{Ker}\, A = V$ then of course $\mathrm{Im}\, A$ is trivial: $A = 0$.
Otherwise $\mathrm{Ker}\, A$ is trivial and consequently $\mathrm{Im}\, A = W$, which implies that A is both injective and surjective, i.e. an isomorphism (of groups *and* vector spaces).

(2) In that case we can identify $V = W$ and consider the matrix of A in some basis. Because the underlying field $\mathbb{C}$ is algebraically closed, A must have at least one eigenvalue λ. But then $A - \lambda\, \mathbb{1}$ has a non-zero kernel, and using irreducibility again this must in fact comprise all of V. $\square$

In practical terms therefore, Schur's lemma is a statement about matrices that commute with all matrices of irreducible representations. If A satisfies

$$D^\lambda(g)A = AD^\mu(g)$$

for all $g \in G$ and two IRs λ, μ then $A = \xi \mathbb{1}_{\chi_\lambda(1)}$ if $\lambda = \mu$ and $A = 0$ otherwise.

Schur's lemma is invoked frequently in many proofs representation and character theory, but it find one of its most elegant applications in Yamanouchi's elegant construction of explicit representation matrices of the symmetric group, which we will sketch briefly in section D.3.

Characters

The goal of representation theory is to determine how many and what kind of (inequivalent) irreducible representations a group G can have. If $|G| < \infty$ this is achieved by help of the powerful method of group characters, of which we would like to introduce the basic notions and results.

Definition 11 *Given $g \in G$, its **c**haracter $\chi(g)$ in a representation $D(G)$ of G on the space V is defined as the trace of its representation matrix*

$$\chi(g) := \operatorname{Tr} D(g) \tag{D.26}$$

Since the trace operation is invariant under unitary transformations and one can show that all representations of finite groups are unitary, it follows that the character is a *class function*, i.e. must be the same for all elements of a conjugacy class:

$$\operatorname{Tr}[D(x)^\dagger D(g) D(x)] = \operatorname{Tr}[D(g)] \;\Rightarrow\; \chi(g) = \chi([g]) \tag{D.27}$$

This is important from a practical point of view, since it simplifies sums over G involving characters, but also because it implies that the number of conjugacy classes $k_G := |G/\equiv|$ is equal to the number of inequivalent irreducible representations.

In a unitary transformation, the character of the inverse element is the complex conjugate:

$$\chi(x^{-1}) = \bar{\chi}(x)$$

This also implies that classes containig both x and x^{-1} must have real character.

The following relations for characters of compound representations are quite useful:

Proposition 2 *Given two representation V, W of a group G it holds*

$$\begin{aligned}
\chi_{V\oplus W} &= \chi_V + \chi_W, \\
\chi_{V\otimes W} &= \chi_V \chi_W \\
\chi_{\wedge^2 V} &= \frac{1}{2}[\chi_V^2(g) - \chi_V(g^2)]
\end{aligned}$$

The first two are not very surprising and the third one can be shown by diagonalising g on $\wedge^2 V$. The eigenvalues are $\{\lambda_i\lambda_j \| i < j\}$, where λ_i are those on V,.
A very similar relationship holds for the characters of $\mathrm{Sym}^2 V$.

The central result of character theory are the criteria for reducibility and the decomposition of reducible representations it provides. This is summarized in the following two propositions.

Proposition 3 *The character χ (viewed as a vector in a k_G dimensional space) uniquely identifies an irreducible representation, in particular are two representations equivalent if and only if their characters are identical.*

The forward direction is clear, because as all representations of finite groups are unitary, transformations between equivalent ones are unitary operations, so they do not change the character. The reverse direction follows from the fact that the set of all matrices with the same character is connected with respect to unitary changes of basis.

If χ and χ' are two characters and thus two vectors in a k_G dimensional space we define their inner product as

$$\langle \chi, \chi' \rangle := \frac{1}{G} \sum_{[x]} k_x \chi([x^{-1}]) \chi'([x]) \tag{D.28}$$

where $k_x = |[x]|$.

Proposition 4 *The characters χ_λ of the irreducible representations V_λ of a finite group G form the basis of a k_G dimensional vector space and are* orthonormal *with respect to the inner product (D.28). This means it holds*

$$\langle \chi_\lambda, \chi_\mu \rangle = \delta_{\lambda\mu} \tag{D.29}$$

for all irreducible representations V_λ, V_μ.

Criteria for reducibility

Thus, given the character χ of some representation V, we easily see whether it is reducible by taking the scalar product with itself. For assume $V = \bigoplus_\lambda V_\lambda^{\oplus a_\lambda}$, then we have $\chi = \sum_\lambda a_\lambda \chi_\lambda$ and therefore if follows from (D.29)

$$\langle \chi, \chi \rangle = \sum_\lambda |a_\lambda|^2 \tag{D.30}$$

Thus, if and only if the 'square' of χ equals one is it irreducible, otherwise it is compound. Also, exploiting orthonormality once more, we can obtain the multiplicity a_λ of V_λ in V from

$$a_\lambda = \langle \chi_\lambda, \chi_{\mathrm{V}} \rangle \tag{D.31}$$

Since the represenation $D(G)$ is a homomorphism, the unit element of G must be mapped onto the unit element in the space of $\dim V \times \dim V$ matrices, i.e. the unit matrix $\mathbb{1}_{\dim} V$. This implies

$$\chi_{\mathrm{V}}(e) = \dim V \tag{D.32}$$

which will be useful later on when we derive *all* properties of the irreducible representations of the symmetric group S_N via their characters.

In what sense do characters provide all the information about a representation? Well, if take any element $g \in G$ of the group, we know all its eigenvalues of its representation matrix $D(g)$ if we know the characteristic polynomial and the coefficients of that we can obtain from the characters. The characteristic polynomial is defined $p[x] = \det(D(g) - x)$ and the coeffients a_i, $i = 0, .., n_V$ of the monomials x^i are

$$\begin{aligned}
a_{n_V} &= (-1)^{n_V} \\
a_{n_V - 1} &= \sum_j \lambda_j = \chi_{\mathrm{V}}(g) \\
a_{n_V - 2} &= \sum_{i \neq j} \lambda_i \lambda_j = \frac{1}{2} \left[\chi^2_{\mathrm{V}}(g) - \chi_{\mathrm{V}}(g^2) \right] \\
&\dots \\
a_{n_V - k} &= \sum_{j_1 \neq j_2 \neq \dots \neq j_k} \lambda_{j_1} \dots \lambda_{j_k} = \\
&\dots \\
a_0 &= \prod_j \lambda_j
\end{aligned}$$

So the entire characteristic polynomial is expressible via the characters of $g, g^2, \dots, g^m$, where m is the order of g. It is defined as the first natural number such that $g^m = e$. For finite $|G|$, m is obviously finite as well.

Group ring and regular representation

Given a finite group G we can built an *algebra* over some field F by using the group elements themselves as vectors. This is the motivation behind the following definition

Definition 12 *The **g**roup ring of G over a field F is the vector space*

$$FG = \mathrm{span}_F\, G$$

together with the multiplication inherited from G.

To become more familiar with this new structure, lets look at a general element from FG in the natural basis provided by G

$$x \in FG : x = \sum_{g \in G} \alpha_g \, g \tag{D.33}$$

The coefficients $\alpha_g \in F$ are the (unique) expansion coefficients in the natural basis. Given a second element $y = \sum_{g \in G} \beta_g \, g$ the ring operations '+' and '$\cdot$' can be written explicitly

$$x + y = \sum_g (\alpha_g + \beta_g) \, g \tag{D.34}$$

$$xy = x \cdot y = \sum_{g,h} \alpha_g \beta_h \, gh = \sum_g \left(\sum_h \alpha_{gh^{-1}} \beta_h \right) \, g \tag{D.35}$$

Clearly, $G \subset FG$, and thus FG provides a representation of the group G which is called the *regular representation*.
In the natural basis the representation matrices of group elements are $|G| \times |G|$ permutation matrices $D^{\mathrm{R}}(g)$, i.e. matrices which have exactly one entry '1' in each row and column and otherwise only '0's. Similar to the group table, we can label both rows and columns of these matrices by the elements of G. The entries in the hth row and h'th column of $D^{\mathrm{R}}(g)$ is given by

$$D^{\mathrm{R}}_{hh'}(g) = \delta_{h,gh'}$$

Where the Kronecker-delta is to be read the usual way: it is '0' unless $h = gh'$ is true, in which case it gives '1'.

Decomposing the regular representation

Since all its matrices are permutation matrices, the character of the regular representation is easily found to be

$$\chi_{\mathrm{R}}(g) = \begin{cases} |G| & \text{if } g = e \\ 0 & \text{otw.} \end{cases} \tag{D.36}$$

Every irreducible representation λ appears in the regular one: If λ is of dimension $n_\lambda = \chi_\lambda(e)$ its multiplicity is

$$a_\lambda = \langle \chi_\lambda, \chi_{\mathrm{R}} \rangle = \frac{1}{|G|} n_\lambda |G| = n_\lambda \tag{D.37}$$

Thus, each IR appears with a multiplicity equal to its dimension, which implies

$$|G| = \sum_\lambda n_\lambda^2 \tag{D.38}$$

where the sum extends over all k_G irreducible representations of G.

Especially for smaller groups, this allows a quick guess as to the dimensions of the IRs involved.
Let S_3 serve as an example again: It's regular representation is $3! = 6$ dimensional. There is only one way to write 6 as the sum of squares: $6 = 2 \times 1^2 + 2^2$. The two one-dimensional IRs are the trivial one, which every group has and which maps all $g \in G$ to the 1×1-matrix (1), and the alternating representation which maps $p \in S_3 \mapsto \mathrm{sgn}(p)$. The two-dimensional representation is called the *standard representation* V_3. It is faithful, and in a suitable basis the matrices of the two generators T_{12} and T_{23} are

$$T_{12} = \begin{pmatrix} 1 & 0 \\ 0 & -1 \end{pmatrix}, \quad T_{23} = \begin{pmatrix} -1 & \frac{\sqrt{3}}{2} \\ \frac{\sqrt{3}}{2} & -1 \end{pmatrix} \tag{D.39}$$

The easiest way to obtain the generators for general IRs of S_N is via Yamanouchi's construction (see D.3), but in this simple example they can be derived 'by hand': start with the natural representation which has a basis $\{|100\rangle, |010\rangle, |001\rangle\}$. T_{12} acts on this basis like $T_{12}|100\rangle = |010\rangle$, $T_{12}|010\rangle = |100\rangle$ and $T_{12}|001\rangle = |001\rangle$. The action of T_{23} can be obtained analogously. If we define the state $|u\rangle = 1/\sqrt{3}(|100\rangle + |010\rangle + |001\rangle)$ we see that it is invariant under both generators and thus forms the basis of the trivial representation U_3. If, in the remaining two-dimensional subspace, we choose the basis

$$|a\rangle = \frac{1}{\sqrt{6}}(|100\rangle + |010\rangle + 2|001\rangle)$$
$$|b\rangle = \frac{1}{\sqrt{2}}(|100\rangle - |010\rangle)$$

we see that T_{12} and T_{23} attain just the form (D.39).

Of course, S_3 is a very easy example, so let us consider S_4 to illustrate the full power of character theory.
S_4 has five classes and therefore we expect to find as many IRs. The order of S_4 is $4! = 24$ and there are two ways to write this as the sum of five squares

$$24 = 2 \times 1^2 + 4^2 + 2 \times 1^2 = 2 \times 1^2 + 2 \times 3^2 + 2^2$$

The first however is not possible, as it does not sum to 24. Even if it did, it would still not be possible because there are no other one-dimensional IRs besides the trivial U_4 and the alternating U_4'. This is due to the fact that one-dimensional representations are abelian and therefore unfaithful for a non-abelian group like S_4. But every unfaithful IR for a group comes from a non-trivial normal subgroup and S_4 contains only three of these: S_4 itself, the alternating group A_4 and $M := \{e\} \cup [(12)(34)]$. S_4 gives rise to the trivial representation U_4, A_4 to the alternating representation U_4' and M gives rise to a two-dimensional IR called W_4 which turns out to be isomorphic to V_3. Thus, S_4 has two one-dimensional, two (inequivalent) three dimensional and one two-dimensonal representations.

The characters of all five representations are determined as follows: $\chi_{U_4} = 1$ on all classes and $\chi_{U_4'} = +1$ for classes of even and -1 for classes of odd permutations. Similar to S_3,

the four-dimensional natural representation of S_4 decomposes into the trivial IR U_4 and the standard rep V_4, therefore $\chi_{V_4} = \chi_{\text{nat}} - \chi_{U_4}$. Multiplying χ_{V_4} (class-wise) by $\chi_{U_4'}$ we get a new character which we recognize as irreducible by taking the scalar-product with itself (see (D.30)). The character χ_{W_4} of the last remaining IR is easily determined by exploiting orthonormality. The complete character table of S_4 is then

size	1	6	8	6	3
class	$[e]$	$[(12)]$	$[(123)]$	$[(1234)]$	$[(12)(34)]$
U_4	1	1	1	1	1
U_4'	1	-1	1	-1	1
V_4	3	1	0	-1	-1
V_4'	3	-1	0	1	-1
W_4	2	0	1	0	-2

D.3 The symmetric group and Young tableaux

The quintessential finite groups are the symmetric groups S_N, consisting of all $|S_N| = N!$ permutations of N distinguishable things. We have already become familiar with them, their representations and subgroups up to $N = 4$. It can be shown, that *every* finite group arises as the subgroup of some S_N (Sydney's theorem, 2). It is because of this function as a role model for the analysis of finite groups, that they were intensily studied in the past and their properties like subgroups, characters and irreducible representations determined already a century ago in the works of Alfred Young and Issai Schur [83, 90]. It was Schur who discovered and Weyl who later explored in detail the intimate connection between the representations of the (finite) symmetric groups and those of the (continous) groups $\mathrm{GL}(V)$ and its subgroups $\mathrm{U}(n)$ and $\mathrm{SU}(n)$.
It is this connection which makes the symmetric group highly relevant in many-body physics, where Hamiltonians of N particles transforming like a representation of $\mathrm{SU}(n)$ often commute with the $\mathrm{SU}(n)$ Casimir-operators thus have total 'spin' (total highest weight) eigenstates which are also *symmetric* (bosons)or *antisymmetric* (fermions) in the full set of particle coordinates. This means the full wavefunction transforms like either the trivial or the alternating representation of S_N for particles in 3 dimensions. So one might at first glance hope to have to know only a very basic version of S_N representation theory. But while the full wavefunction always shows trivial or alternating behaviour under particle exchange, this is not true of either a subset of all particles or partial wavefunctions of incomplete sets of coordinates (regarding e.g. just spatial coordinates and not the spin). In both cases mixed symmetries corresponding to multi-dimensional irreducible S_N representations may occur.

The discovery of anyonic quasi-particle statistics in 2 dimensions in the context of the fractional quantum hall effect spawned much interest in the braid group which is a generalisation of the symmetric group where the condition $T_i^2 = 1$ on the $N-1$ canonical generators of S_N (the transpositions $(i, i{+}1)$) is dropped. While quite intriguing quasi-particle effects were uncovered and explained in terms of non-trivial representations of the braid group defined on

the internal Hilbert space of windings, the fundamental degrees of freedom of full many-body wavefunctions remain bosonic or fermionic.

Sydney's theorem

Theorem 2 *Every finite group G is isomorphic to a subgroup of the symmetric group $S_{|G|}$.*

Proof: The regular representation of G consists of $|G| \times |G|$ dimensional permutation matrices which can as well be interpreted as *natural* permutation matrices for elements from $S_{|G|}$. This identification provides an injective group homomorphism $\phi : G \to S_{|G|}$ whose image must therefore be a subgroup of $S_{|G|}$. □

Conjugacy classes

Every permutation can be expressed very succinctly in cycle-notation, where one groups together indices which are mapped one onto the other in a cyclic fashion, usually starting with the lowest index in the cycle. For instance (134) is a cycle on the three indices 1,3 and 4 where $1 \mapsto 3$, $3 \mapsto 4$ and $4 \mapsto 1$. (413) is the same cycle in non-canonical order. 1-cycles are also called fixed point (of the permutation) and are often omitted for brevity. A transposition for instance is thus a permutation consisting one 2-cycle and $N-2$ fixed points and is written simply as (ij).
A general permutation in S_N is made up from α_1 1-cycles, α_2 2-cycles, ..., α_N N-cycles where the multiplicities α_j obviously have to satisfy

$$\sum_j j\,\alpha_j \;=\; N \tag{D.40}$$

What does this have to do with the conjugacy classes? Well, given $p \in S_N$ we can constuct its class by taking the product $p' = qpq^{-1}$ for all $q \in S_N$.
If, say, $p(i) = j$, then $p'(q(i)) = qp(i) = q(j)$. There is thus the following intuitive rule

Proposition 5 *p' is obtained from p by replacing a k-cycle $(j_1 j_2 \dots j_k)$ by $(q(j_1)q(j_2)\dots q(j_k))$.*

But this means that the conjugacy-transformation does not change the cycle structure $\{\alpha_1, \dots, \alpha_N\}$.

Proposition 6 *The conjugacy class $[p]$ for $p \in S_N$ contains all $p' \in S_N$ that have the same cycle structure as p.*
If this structure is given by the cycle multiplicities $\alpha_1, \dots, \alpha_N$, then the size of $[p]$ is

$$n_p := |[p]| = \frac{N!}{\prod_{k=1..N} \alpha_k!\, k^{\alpha_k}} \tag{D.41}$$

Because the cycle frequency $(c) = (\alpha_1, \ldots, \alpha_N)$ *corresponds in a natural way to the integer partition*

$$(c) \mapsto (\mu) = (1, 1, \ldots, 1, 2, \ldots, 2, \ldots)$$

where '1' appears α_1 *times, '2'* α_2 *times and so on, the number of conjugacy classes in* S_N *is equal to the number of partitions of* N *into positive integers.*

Irreducible representations, characters, Young tableaux

In representation theory, the central quantities which neatly sums up the essence of the group (or the group table) and provides the information to e.g. decompose an arbitrary representation into its irreducible atoms is the character table.
How can obtain the simple characters of S_N? Since we know S_N must have as many irreducible representations as there conjugacy classes $[c]$, we can use positive integer partitions (μ) of N as labels for the IRs as well as the classes. But a labelling alone is of course not much use without having some procedure to compute the characters from the labels.

The connection between the integer partitions λ and the characters $\chi^{(\lambda)}_{(c)}$ is via the characters $\phi^{(\lambda)}$ of representations $\mathrm{Ind}_{H_\lambda}^{S_N} 1$ induced from the trivial representation of the subgroup $H_{(\lambda)} = H_{\lambda_1} \times H_{\lambda_1} \times \ldots H_{\lambda_k}$, defined as the direct product of symmetric groups constructed on the sets of indices $1, 2, \ldots, \lambda_1$; $\lambda_1, \ldots, \lambda_1 + \lambda_2$;...;$N - \lambda_k + 1, \ldots, N$ respectively.
For a general group G with subgroup H the character of the l-th class of G in $\mathrm{Ind}_H^G 1$ is $|G|h_c/|H|g_c$ where g_c is the size of class c in G and h_c the number of elements from the class which are also in H. Applying this to our case we have $|S_N| = N!$, $|H_\lambda| = \prod_j \lambda_j!$, if $p \in [c]$ then $g_c = n_p = N!/\prod_{k=1..N} \alpha_k!\, k^{\alpha_k}$ (cp. (D.41)) and finally

$$h_c = \sum_{\{\beta_j^l\}} \prod_j \frac{\lambda_j!}{\prod_l l^{\beta_j^l} \beta_j^l!}$$

where the sum extends over all nonnegative integer solutions β_j^l of the two conditions $\sum_l l\beta_j^l = \lambda_j$ and $\sum_j \beta_j^l = \alpha_l$. β_j^l is just the number of l-cycles in the subgroup H_{λ_j}, and for each subgroup we apply formula (D.41) with N and α_l replaced by λ_j and β_j^l.

Thus finally $\phi^{(\lambda)}_{(c)}$ is

$$\phi^{(\lambda)}_{(c)} = \frac{|S_N|h_c}{|H_\lambda|g_c} = \sum_{\substack{\alpha_1,\alpha_2,\ldots,\alpha_N \\ \sum_l l\beta_j^l = \lambda_j,\, \sum_j \beta_j^l = \alpha_l}} \prod_l \frac{\alpha_l!}{\prod_j \beta_j^l!} \tag{D.42}$$

The $\phi^{(\lambda)}_{(c)}$ are compound characters of S_N, but one can show (see,*e.g.* [91]) that they are linearly independent as λ varies over all integer partitions of N. Therefore, taking suitable linear combinations, we can obtain all simple characters $\chi^{(\lambda)}_{(c)}$ from the $\phi^{(\lambda)}_{(c)}$.
The way to find this linear combination is to construct polynomials

$$s_{(c)} := \prod_l s_l^{\alpha_l}, \quad \text{with} \quad s_l := \sum_{i=1}^{k} x_i^l$$

in the variables $x_1, \ldots, x_m$, where m, the number of variables, must be larger than k, the number of rows in (λ) but no larger than N.
The compound characters $\phi^{(\lambda)}_{(c)}$ appear as the coefficients of monomials $x^{\lambda_1}_{p(1)} x^{\lambda_2}_{p(2)} \ldots x^{\lambda_k}_{p(k)}$, $p \in S_N$ in $s_{(c)}$:

$$s_{(c)} = \sum_{(\lambda)} \phi^{(\lambda)}_{(c)} \sum_{p \in S_N} x^{\lambda_1}_{p(1)} \ldots x^{\lambda_k}_{p(k)},$$

Multiplying with the totally antisymmetric Jastrow-polynomial $J_m = \prod_{i<j\leq m}(x_i - x_j)$ gives Frobenius' famous formula

$$s_{(c)} J_m = \sum_{(\lambda)} \chi^{(\lambda)}_{(c)} \sum_{p \in S_N} (-1)^{|p|} x^{\lambda_1+m-1}_{p(1)} x^{\lambda+m-2}_{p(2)} \ldots x^{\lambda_m}_{p(m)} \tag{D.43}$$

where the simple characters $\chi^{(\lambda)}_{(c)}$ appear as coefficients on the rhs (for a lucid derivation see *e.g.* [91]).

We would like to briefly sketch how a graphical method for obtaining characters involving Young tableaux can be derived from (D.43) in a natural way. The full account can be found in [91]. Let us consider the class $(1, 1, \ldots, 1)$ of the identity element. The corresponding polynomial is

$$s_{(1^N)} = \left(\sum_i x_i \right)^N$$

Starting with the 'bare' Jastrow-factor

$$J_k = \prod_{i<j} (x_i - x_j) = \sum_{p \in S_N} (-1)^{|p|} \, x^{m-1}_{p(1)} x^{m-2}_{p(2)} \ldots x^1_{p(m-1)} x^0_{p(m)}$$

the idea is to built up the full rhs of Frobenius' formula by successively multiplying with $\sum_i x_i$ a total of N times. We want to arrive at the monomial $x_1^{\lambda_1+m-1} x_2^{\lambda_2+m-2} \ldots x_m^{\lambda_m}$ ($\lambda_j = 0$ if $j > k$). At all times during this stepwise process, the exponents of any intermediate monomial must all be different, because otherwise it would be annihilated by the sum over all permutations. But since we can raise the exponents by at most 1 in each step, it follows that at all times we must have multiplied with more x_1s than x_2s, more x_2s than x_3s and so on. The total number of ways in which we can do this is then the character $\chi^{(\lambda)}_{(1^N)}$. If for instance we want to know the character of the unit element of the representation $(\lambda) = (2, 1, 1)$ of S_4 we must in the end have raised the power of x_1 by 2, of x_2 by 1 and x_3 also by 1. The possible ways of doing this are (factors on the left are applied first):

$$x_1^2 x_2 x_3, \; x_1 x_2 x_1 x_3, \; x_1 x_2 x_3 x_1$$

Therefore this character is 3. We can depict these three different multiplication-orders graphically in the following way:

$$\begin{array}{|c|c|}\hline 1 & 2 \\ \hline 3 \\ \cline{1-1} 4 \\ \cline{1-1} \end{array} \quad , \quad \begin{array}{|c|c|}\hline 1 & 3 \\ \hline 2 \\ \cline{1-1} 3 \\ \cline{1-1} \end{array} \quad , \quad \begin{array}{|c|c|}\hline 1 & 4 \\ \hline 2 \\ \cline{1-1} 3 \\ \cline{1-1} \end{array} \tag{D.44}$$

The interpretation is straighforward: a number i in row j means that the i-th step is a multiplication with x_j. These patterns are called *Young tableaux*. Let us define them in general.

Definition 13 *A* ***Y****oung tableau (YT) is any filling of a Young diagram with indices* $1 \leq i_{jk} \leq N$.
The Young diagram *to the integer partition* $(\lambda) = (\lambda_1, \ldots, \lambda_k),\ \lambda_1 \geq \lambda_2 \geq \cdots \geq \lambda_k$ *is the visualisation of* (λ) *as* k *left aligned rows of boxes where row* j *has length* λ_j.
A standard YT *is a filling of the shape* (λ), $\sum_j \lambda_j = N$ *with the indices* $1, \ldots N$ *such that indices are strictly increasing in both rows and columns.*

The Young diagram of (λ) is usually referred to as the 'shape λ'.
The YT in D.44 are examples of *standard Young tableaux*, in this case on the shape $(2, 1, 1)$.
We can generalise from our simple example S_4, $\lambda = (2, 1, 1)$ and state

Proposition 7 *The dimension of the irreducible representation* $\lambda = (\lambda_1, \ldots, \lambda_k), \sum_j \lambda_j = N$ *of* S_N*, which equals the character* $\chi^{(\lambda)}_{(1^N)}$ *of the unit element, is just* N_λ*, the number of standard Young tableaux on* λ.

The graphical method of Young tableaux can be extended two work for any class $(c) = (1^{\alpha_1} 2^{\alpha_2} \ldots N^{\alpha_N})$, not only the class of the unity element.
Again multiplying the Jastor-polynomial J_m factor-by-factor with $s_{(c)} = s_1^{\alpha_1} s_2^{\alpha_2} \ldots s_N^{\alpha_N}$, the polynomial corresponding to (c), we see that we can now raise powers by more than 1: The s_2s raise it by 2, the s_3s by 3 and so on. It still holds however, that after each step monomials where two variables appear with the same power are killed by antisymmetrisation. The difference to the simple case $(c) = (1^N)$ is that now we do not have to raise the power of x_1 faster than x_2 faster than x_3 ... anymore precisely because we can use factors x_j^l, $l > 1$ from s_l to let x_j 'overtake' (a number of) variables x_i.
To make this clear, consider an intermediate monomial before step a

$$x_{j-a}^{\nu_{j-a}+m-(j-a)} x_{j-a+1}^{\nu_{j-a+1}+m-(j-a+1)} \ldots x_(j-1)^{\nu_{j-1}+m-j+1} x_j^{\nu_j+m-j}$$

somewhere into the process and assume it is well formed (i.e. $\nu_1 \geq \nu_2 \geq \cdots \geq \mu_m$). Multiplication with x_j^l raises the power of x_j by l. Regarding x_j's total new power we now assume

$$\nu_{j-\Delta-1} + m - (j - \Delta - 1) > \nu_j + m - j + l > \nu_{j-\Delta} + m - (j - \Delta)$$

Informally speaking, x_j overtakes the Δ variables $x_{j-\Delta}, \ldots, x_{j-1}$. The new monomial is of course not in standard order anymore, but there is a permutation $p \in S_N$ which will reorder it. In cyclic notation this permutation is

$$p = ((j - \Delta)(j - \Delta + 1) \ldots (j - 1)j)$$

and comes with a sign $(-1)^\Delta$. In terms ouf Young tableaux we can say we added l indices a to row j until its length surpassed row $j-1$ by 1, then continued there in the same fashion until we arrived in row $j-a$ where we added the remaining 'a's. This defines the following definitions

Definition 14 *A Young diagram where the rows are* not *left aligned and their length is not necessarily non-decreasing is called a* ***s****kew shape.*
A skew shape is ***c****onnected if in all its rows and columns there are at least 2 boxes.*

For example  is not connected while  is.

Definition 15 *We call the addition of l boxes 'a' to the rows $j, j-1, j-2$ of a (valid) shape μ and so on* ***r****egular if the final shape μ' is valid and if the skew shape $\mu' - \mu$ is connected.*

This leads to

Proposition 8 *The character $\chi^{(\lambda)}_{(c)}$ of the class (c) in the IR (λ) of S_N is*

$$\chi^{(\lambda)}_{(c)} = n^{\text{even}}(c,\lambda) - n^{\text{odd}}(c,\lambda)$$

where $n^{\text{even}}(c,\lambda)$ is the number of ways one can fill the shape λ with indices $(c) = (1^{\alpha_1} 2^{\alpha_2} \dots N^{\alpha_N})$ using an even *number of regular applications, and $n^{\text{odd}}(c,\lambda)$ the number of ways to do the same with an* odd *number of regular applications.*

Branching rules

A shape μ is contained in another shape λ, $\mu \subseteq \lambda$ iff for all rows j $\lambda_j \geq \mu_j$. The *difference* $\lambda - \mu$ is the skew shape with row lengths $\lambda_j - \mu_j$ where each row starts in column $\mu_j + 1$. For instance

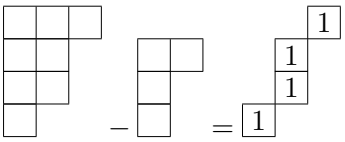

The difference of the sizes is the size of this skew shape: $|\lambda| - |\mu| = |\lambda - \mu|$.

It is not hard to see that we can built up all standard YT on a shape λ recursively by first building all YT on all shapes μ_r obtained from λ by removing a box from row r. To each std. YT on μ_r we then add a box 'N' in row r.

This implies for the number of std. YT on λ

$$N_\lambda = \sum_{\mu:|\lambda-\mu|=1} N_\mu \tag{D.45}$$

Interestingly, the same branching formula holds for the decomposition of $\text{Ind}_{S_{N-1}}^{S_N} U_N$ the representation of S_N induced from the trivial representation of $S_{N-1} \subset S_N$.

Young symmetrizers

Given a Young tableaux on the shape λ of type (1^N) we define the *row* and *column groups* R_T and C_T as all those $P \in S_N$ which permute boxes only within rows and columns respectively. Further we define symmetrization and antisymmetrization operations $a_T, b_T \in \mathbb{C}S_N$ by

$$a_T = \sum_{P \in R_T} P \tag{D.46}$$

$$b_T = \sum_{Q \in C_T} (-1)^Q Q \tag{D.47}$$

Multiplying these two operators we arrive at the *Young symmetrizer*

$$c_T = b_T \, a_T. \tag{D.48}$$

One can show that it holds

$$c_{T'} c_T = \begin{cases} N! c_T & \text{if } T' \geq T \\ 0 & \text{otw.} \end{cases} \tag{D.49}$$

where the order refered to is lexicographical: $T' \geq T$ if either $\lambda(T') > \lambda(T)$ or if, in case $\lambda(T') = \lambda(T)$, the first box in which they differ contains a higher number in T' than in T. This means the c_t are essentially idempotent (rescale with $1/\sqrt{N!}$) and therefore acts as a right-unit element left on the left ideal Ac_T:

$$\forall a \in Ac_T : \; ac_T = a \tag{D.50}$$

Furthermore c_T is a simple idempotent and the ideal Ac_T is minimal, *i.e.*, an IR of S_N. Let us prove this statement.

Assume, we find a subideal W of Ac_T. It must contain an idempotent, e_W, which generates W: $W = Ae_W$. Since $W \subseteq Ac_T$, it must hold by (D.50)

$$e_W c_T = e_W \tag{D.51}$$

As an element in A, e_W can be expanded in the natural basis of A (the one provided by S_N itself)

$$e_W = \sum_{g \in S_N} w_g \, g$$

Using the expansion $c_T = \sum_{R(T),C(T)} (-1)^q \, pq$ of c_T (D.51) the product reads

$$\left(\sum_{S_N} w_g \, g \right) \left(\sum_{R,C} (-1)^q \, pq \right) = \sum_{S_N,R,C} (-1)^q w_g \, gpq \stackrel{!}{=} \sum_{S_N} w_g \, g \tag{D.52}$$

i.e., we require $w_{gpq} = (-1)^q w_g$. In particular for $g = \mathrm{id}$ $w_{pq} = (-1)^q w_{\mathrm{id}}$. Also,

$$c_T e_W c_T = \sum_{S_N} w_g \, c_T g c_T = \sum_{S_N} w_g \, c_T c_{gT} \, g \tag{D.53}$$

where gT is the Young tableau obtained from T by applying permutation g (we used $gc_T = \sum_{R(T),C(T)}(-1)^q\, gpqg^{-1}g = \sum_{R(gT),C(gT)}(-1)^q\, p'q'\, g$). But it holds $c_T c_{gT} = 0$ unless $g = pq$, $p \in R(T), q \in C(T)$. Why is this the case? What we will show is that unless $g = pq$, gT will have two boxes in the same *row* which are in the same *column* in T. Assume there are no two such boxes, then all boxes in the first column of T must be in different rows in gT. We can therefore find a permutation $p_1 \in R(T)$ which brings these boses all to the first column (in $p_1 gT$). But the same must also hold for the boxes in the second column of T, *i.e.*, there is a $p_2 \in R(T)$ such that the boxes in the first two columns of $p_2 p_1 gT$ are the same as in T (they may not be in the same order though). We can continue this until after at most $l = \lambda(T)_1 - 1$ steps we equalized the contents of every column of $p_l \dots p_1 gT$ and T. We may then apply an element from $C(T)$ to bring all columns into the right order. In all we find

$$T = qp_l \dots p_1 gT = qpgT \Leftrightarrow pqT = gT$$

Therefore have proved the counterpositive must also be true: if $g \neq pq$ then there must be two boxes from the same column in T ending up in the same row in gT. But, rembering $c_T = a_T b_T$ this means we try to antisymmetrize on two symmetric indices which gives 0: $a_T b_T a_{gT} b_{gT} = a_T (b_T a_{gT}) b_{gT} = 0$. This concludes the proof.

The representations generated by the Young symmetrizers of all standard YT on a shape λ are all linearly independent. In fact, they sum directly and together span the space V_λ of all equivalent IRs λ. V_λ is also a two-sided ideal in A. This can be seen very easily: suppose there were a non-trivial x with $x \in Ac_T$ and $x \in Ac_{T'}$ for two standard YT on the same shape. Then $x = xc_T = xc_{T'} = xc_T c_{T'} = xc_{T'} c_T$. But the last two equalities cannot both be true as we have seen in the previous proof.

Young symmetrizers are the starting point for a construction of an explicit orthonormal basis $\{e_{TT'}\}$ of V_λ containing N_λ^2 elements each labelled by two standard YT on λ. The condition for orthonormality is

$$e_{TT'} e_{T''T'''} = \delta_{T'T''} e_{TT'''}. \tag{D.54}$$

Given this equation, we may compute the representation matrix of a permutation $g \in S_N$ in the IR λ via the formula

$$g_{TT'} e_{TT'} = e_{TT''} g e_{T'''T'} \tag{D.55}$$

As it turns out, we can find a basis with real coefficients by slightly extending the Young symmetrizers. They already satisfy $c_T c_{T'} = 0$ iff the permutation g taking T to T' cannot be written as $g = pq$ with $p \in R(T)$, $q \in C(T)$. Interestingly, we can define an *order* on the set of std. YT which respects this, *i.e.*, where $T' < T$ implies $c_T c_{T'} = 0$. The order is: $T' < T \Leftrightarrow$ the first box in which T and T' differ when read row-wise from top to bottom is larger in T.

To obtain a basis satisfying (D.54) we need to sandwich a suitable permutation between two a_T and $b_{T'}$ [92]:

$$e_{TT'} = \frac{1}{N_\lambda} a_T s_{TT'} b'_{T'} \tag{D.56}$$

where $b'_{T'}$ satisfies $b'_{T'} a_T = \delta_{TT'} b_T a_T$ and $s_{TT'} \in S_N$ is the permutation which takes the tableaux T' to T: $T = s_{TT'} T'$.

Yamanouchi construction

Computing the quantities defined above in practive for any S_N is very tedious even for relatively small N. Luckily, we do not actually need know the explicit form of the basis (D.54) to get the representation matrices of the corresponding IR λ. They can be obtained very elegantly using Yamanouchi's construction, which interprets the standart YT themselves as orthonormal basis states.

Let us briefly describe how it works. First up, it is clear that we need only find the matrices of a set of generators, and one chooses the transpositions $(12), (23), \ldots, (N-1N)$. Now assume we have the set of all std. YT of a shape λ. We will turn it into a list by requiring the following order: first collect together tableaux where the box N is in the same position. Within each of these collections form 'subcollections' of tableaux with the box $N-1$ in the same position. Continue in this fashion until each sub...subcollection contains only one YT. In effect we have now constructed the branching graph introduced in 5.11. Use lexicographical ordering on the paths of this graph.

Applying the Yamanouchi construction recursively, it is clear that the states, *i.e.*, tableaux, in each sub-collection at a level k with shape $\mu_k \subset \lambda$ form the basis of the irreducible representation labelled by μ_k. So if we can find the representation matrix D_{N-1} of $(N, N-1)$, all others follow by recursion.

Let us now state the procedure to determine D_{N-1}. Regarding the boxes 'N' and '$N-1$'in λ we can distinguish three cases:

- the boxes N and $N-1$ are in the same row. Then D_{N-1} is diagonal in these states with eigenvalue 1
- the box N is directly below $N-1$: D_{N-1} is again diagonal in these states, but with eigenvalue -1
- none of the above, *i.e.*, N is in row r of length λ_r, $N-1$ is in row $s \neq r$ of length $\lambda_s \neq \lambda_r$: then there are two collections of states which differ in N and $N-1$ being swapped. This means, removing both boxes N and $N-1$ one can reach the same subshape $\mu_{rs} = \mu_{sr} = \mu \subset \lambda$ with $|\mu| = N-2$ in two different ways. D_{N-1} will now have a diagonal and an off-diagonal block mixing these two collections of states. Each block is proportional to the unit matrix $\mathbb{1}_{N_\mu}$ with prefactors $\sigma_{rs,rs}$ on the diagonal and $\sigma_{rs,sr}$ on the off-diagonal which are given by

$$\sigma_{rs,rs} = \pm \frac{1}{\sqrt{1 + s_{NN-1}}} \tag{D.57}$$

$$\sigma_{rs,sr} = + \sqrt{\frac{s_{NN-1}}{1 + s_{NN-1}}} \tag{D.58}$$

where s_{NN-1} is the 1-norm distance between the boxes N and $N-1$, *i.e.*, the number of steps a rook (the chess piece) would have to take to get from box N to $N-1$:

This is in fact all one needs to know about the Yamanouchi's construction, yet if the reader is interested in the elegant and beautiful derivation, it can be found, *e.g.* , in [91].

D.4 The special unitary group SU(n)

In this section we will give short review of Lie groups and their relatives, the Lie algebras. Lie groups are infinite groups, which are at the same time differentiable manifolds. The 'mother' of all LGs is GL(n), the group of invertible automorphisms of an n-dimensional vector space, but it has many subgroups with more practical importance, *e.g.* in physics, like the symplecitc group SL(n), the unitary group U(n), the uni- modular group SU(n) or the orthogonal group O(n). These are in fact the 4 'classical' Lie groups (as opposed to the more 'exotic' exceptional Lie groups like E(8)) first fully analyzed by Weyl [85]. We will focus on the unimodular group SU(n), but the techniques shown here can easily be applied to the other examples.

Definition and Algebra

The group SU(n) is defined as the group of $n \times n$ matrices with entries in $\mathbb{C}$ with the following properities

$$A \in \mathrm{SU}(n) \Leftrightarrow A^\dagger A = A A^\dagger = \mathbb{1}_n \ \wedge \ \det A = 1 \tag{D.59}$$

From now on we will omit the index n on the unit matrix. That this defines a group follows from the properties of the † and det operations. Clearly, SU(n) is a subgroup of the unitary group.

Understanding the structure of a Lie group is next to impossible by only looking at the group itself, but luckily there is a closely related mathematical structure with nice properties, the Lie algebra. It is basically the tangent space of the unit-element in the Lie group. To find it in our case, we make the ansatz $A = 1 + iaX$ for a group element in the neighbourhood of $\mathbb{1}$, where a is a small real number. Using the defining relations of SU(n) then puts restrictions on the matrices X:

$$(1 - iaX^\dagger)(1 + iaX) \stackrel{!}{=} 1 + \mathrm{O}\left(a^2\right) \Leftrightarrow X = X^\dagger \tag{D.60}$$

$$\det 1 + iaX = 1 \Leftrightarrow \mathrm{Tr} X = 0 \tag{D.61}$$

So we see the tangent space of $\mathbb{1}$ is spanned by the set of traceless, hermitian matrices $X \in \mathbb{C}^{n\times n}$. It forms a group ring or algebra, *i.e.*, we can add and multiply matrices and there are inverses of addition but not in general of multiplication, and it is called the Lie algebra su(n). For any $X \in H_0$ it holds $\exp iX \in \mathrm{su}(n)$ because

$$\left(\mathrm{e}^{iX}\right)^\dagger = \mathrm{e}^{-iX} \text{ and } \det[\mathrm{e}^{iX}] = 1. \tag{D.62}$$

One says SU(n) is exponentially generated by its Lie algebra.

If we choose a basis $\{E_j\}$ in su(n), then the above looks

$$\forall A \in \mathrm{SU}(n) \exists \{x_j\} \in \mathbb{R} : \ A = \exp[-i \sum_j E_j x_j]$$

The E_j are also called (infinitesimal) generators of the group SU(n).

Introducing the Lie bracket as the commutator of X and Y:

$$\begin{aligned}[.,.] :&\mathrm{su}(n) \times \mathrm{su}(n) \to \mathrm{su}(n) \\ &X, Y \mapsto XY - YX\end{aligned} \tag{D.63}$$

one can express all relevant information about a Lie algebra through the commutation relations of the basis elements E_j:

$$[E_i, E_j] = c^{ijk} E_k$$

where we assume summation over repeated indices (on different levels). The numbers c^{ijk} are called the structure constants of the Lie algebra. They are of course dependent on the choice of basis, and choosing the basis properly can go a long way in helping to understand the structure of a Lie group, in our case su(n).

Standard basis of su(n)

We will no give a convenient basis of su(n). Define E_{ij} as the matrix with a '1' in the ith row and $j$the column if $i \neq j$. And if $i = j < n$ set E_{ii} to be the matrix with a '1' in position (i, i) and a '-1' in position $(i + 1, i + 1)$. These $n^1 - 1$ matrices obey the commutation relations

$$[E_{ij}, E_{kl}] = \delta_{jk} E_{il} \tag{D.64}$$

$$[E_{ii}, E_{jk}] = \delta_{ij} E_{ik} - \delta_{i+1j} E_{i+1k} - \delta ik E_{ji} + \delta_{i+1k} E(ji + 1) \tag{D.65}$$

all others are 0. In particular this is true of the ones between the diagonal matrices E_{ii}, which in fact form a maximal set of mutually commuting generators. Thus they from an Abelian subalgebra, the *Cartan algebra* of su(n). We can therefore use their eigenvalues to label the basis states in any representation of the algebra/group. The $n-1$ dimensional vector of eigenvalues, which are always integers, is called a *weight* of (this state) in the representation. Introducing lexicographical ordering on the weights of representations, each representation V is uniquely characterised by its highest weight $\boldsymbol{w}$. The heigest weight state $|\boldsymbol{w}\rangle$ is unique, *i.e.*, there is no other state in the representation with the same eigenvalues $\boldsymbol{w}^{\mathrm{z}} = \boldsymbol{w}$ of the Cartan generators. This uniqueness is in general not true for lower weight states. Only for SU(2), where the heigest weight is the spin and $\boldsymbol{w}^{\mathrm{z}}$ the z-component of spin, are all states in a representation unique. If we plot the weights of a represenation as points in an $n-1$dimensional space, we obtain the weight diagram of the su(n). It turns out that, after a suitable basis adaption, the weight diagrams of all su(n) have a high degree of symmetry. This comes from the subgroup decomposition property

$$\mathrm{SU}(n-1) \times \mathrm{U}(1) \subset \mathrm{SU}(n) \tag{D.66}$$

which tells us that, in the right basis, weight diagrams of su(n) are composed of stacked su($n-1$) diagrams. Of course we can only really do the plotting in case of $n \leq 4$. For $n = 2$, the weights are equidistant points on a line (corresponding as mentioned to the z-component of the spin, then the distance btw. each point is just 1). su(3) diagrams are made up of stacked su(2) diagrams and if the distance btw. neighbouring points is always the same (*e.g.* 1), they

will have $2\pi/3$ rotation symmetry. Using such su(3) weight diagrams to build those of su(4), we obtain 3dimensional diagrams with tetrahedral symmetry.

As we have mentioned, each point in such a diagram in general stands for multiple states, *i.e.*, the weights $\boldsymbol{w}^z$ do not provide a unique labelling. However, one can use the property (D.66) to find such a unique labelling [93]. The idea is to give each state additional labels coming from the the subalgebra su(k)-representations it is a part of. This provides an additional $\sum_j^{n-2} j$ labels bringing the total to $n(n-1)/2$, just as many as we need.

Gelfand and Tsetlin found an ingenious scheme how to obtain the matrices of the generators (D.65) in implicitly orthonormal bases represented by triangular ('Gelfand'-)patterns of $n-1$ rows with integers m_{ij} in them [71]. Here j is the row and i the column index and in row j there are $j-1$ entries. The top row entries $m_{in} = \boldsymbol{w}_i^z = w_i$ are just the weights, while the others satisfy the 'betweenness' condition

$$m_{ij} \geq m_{ij-1} \geq m_{i+1j}$$

Thus each Gelfand has $n(n-1)/2$ entries, which means they can be used to give a unique labelling of each state in a representation. In fact, one can interpret each row k as the weight of the state with respect to the subgroup/algebra su(k) $\subset$ su(n), which reveals that these patters are inspired by the subgroup decomposition we mentioned above. Gelfand and Tsetlin were now able to find analytic (if rather lengthy) expressions for the matrices E_{ij} in a basis of A nice, succinct introduction can be found in [73].

Connection to Young tableaux

Given an irreducible representation V of SU(n), the N fold tensor-product $V^{\otimes N}$ is again a representation, albeit not irreducible anymore, if SU(n) operates on $V^{\otimes N}$ like

$$A \in \mathrm{SU}(n), v = (v_1, \ldots, v_N) \in V^{\otimes N} : \; Av := (Av_1, \ldots, Av_N) \tag{D.67}$$

At the same time, it is clear that $V^{\otimes N}$ is also a representation of the permuation group S_N if we define

$$p \in S_N, v \in V^{\otimes N} : \; pv := (v_{p(1)}, \ldots, v_{p(N)}) \tag{D.68}$$

Now it is easy to see that the actions of SU(n) and S_N commute:

$$pAv = p(Av_1, \ldots, Av_N) = (Av_{p(1)}, \ldots, Av_{p(N)}) = A(v_{p(1)}, \ldots, v_{p(N)}) = Apv \tag{D.69}$$

What looks like a simple fact has far-reaching consequences, as Schur [84] first realized and Weyl [85] explored in detail (hence its name Schur-Weyl-duality). For assume we find an irreducible SU(n) representation $V_{\boldsymbol{w}}$ in $V^{\otimes N}$. Then for each $p \in S_N$ $pV_{\boldsymbol{w}}$ is an IR which is isomorphic to $V_{\boldsymbol{w}}$. $pV_{\boldsymbol{w}}$ can now either be identical with $V_{\boldsymbol{w}}$ or the two sum directly, *i.e.*, have no common vector except for 0. Assume there were such an element, say $w \neq 0$. Then there must be a $v \in V_{\boldsymbol{w}}$ s.t. $w = pv$ and

$$V_{\boldsymbol{w}} = \mathrm{SU}(n)w = \mathrm{SU}(n)pv = p\mathrm{SU}(n)v = pV_{\boldsymbol{w}}$$

where we have used that we can generate any representation (up to normalisation) by applying all group elements of SU(n). Therefore, if $V_{\boldsymbol{w}}$ and $pV_{\boldsymbol{w}}$ have one common element, they must necessarily coincide.

We can thus construct equivalent representations by applying permutation operations. It is not clear, whether this will give us all equivalent IRs contained in $V^{\otimes N}$ but we can definitely say that the subspace $V_{\boldsymbol{w}}^{\oplus a_{\boldsymbol{w}}}$ of all SU(n)- representations $V_{\boldsymbol{w}}$ is a representation of S_N.

If V is the fundamental representation of SU(n), *i.e.*, $V = \mathbb{C}^n$, and we represent it by a single box, $\square$, we can built IRs of SU(n) by applying the Young symmetrizer of the previous section to $V^{\otimes N}$ and obtain the decompostion into IR's of S_N labelled by a Young diagram λ which at the same time will be IR's of SU(n), labelled so far by $\boldsymbol{w}$. In fact, the highest weight $\boldsymbol{w}$ of an SU(n) is always an integer partition of at most $n-1$ rows, and since it must equal (λ) in this case, we se that Young symmetrizers of n or more rows give 0 $V^{\otimes N}$. This establishes an equivalence between highet weight and integer partitions which we can use to decompose tensor products of higher SU(n) IRs. The number of times a certain IR λ appears in $V_{\sigma}^{\otimes N}$ is given by the number of semi-standard YT on λ of type $(\sigma, \ldots, \sigma)$ (where σ is repeated N times) which obey the Littlewood-Richardson rule.

E Supplementaries to extended Young tableaux

E.1 Efficient graph iteration

The branching graph is the key datastructure for implementing fast Young tableaux generation, but the form presented in 5.5 is not yet sufficient to allow an efficient iteration over all paths through it. To achieve this we need to both add some additional information to the BG and use suitable datastructures to guide the iteration.

To illustrate: Taking the BG as it is, we could for instance perform a depth-first iteration: we use a size $N-1$ (= max. depth) array $c[.]$ recording to which child we descend to from the node $\mu_{c[d]}$ at each depth. In each step we then decend one level further down the graph until we reach the leaf and there, having found a new path, we add it to our result and backtrack to the closest node where we can descend in a different direction. Of course, we can easily, in addition to $c[.]$, also keep a record $l[.]$ of the labels encountered along the path or directly built the extended YT as we go along. The problem is however, that in all this we decend and backtrack step by step through the graph, which will take on average $\mathrm{O}(N)$ steps and this brings the total complexity to $\mathrm{O}(N\,N_\lambda)$.

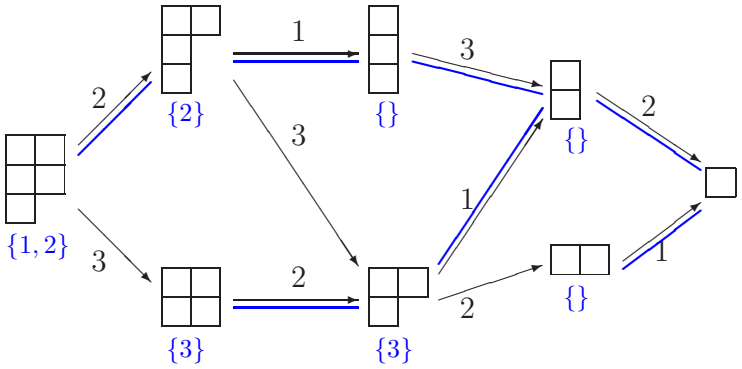

Figure E.1: To enable efficient graph iteration, we need to augment the ordinary branching graph with additional information: to each node we attach the potential backtracking- positions, *i.e.*, all nodes with more than one child (shown in the blue lists) lying on along the *leftmost path* descending from that node to the leaf (also marked in blue).

We can do better if we perform a precomputation before the iteration itself adding the following information to each node μ of the graph: from μ we follow the *leftmost path* (lmp) to the leaf and, while we descend, push on a *stack* K_μ all the nodes with more than one child, because only these will be potential candidates to backtrack to (see Fig. E.1). We also save $l_\mu[.]$, the label sequence along the lmp of μ and/or T_μ the 'incomplete' extended YT using indices $N-d(\mu), N-d(\mu)-1, \ldots, 1$ where $d(\mu)$ is the depth of node μ. We could of course also use the rightmost path.
Precomputation of the triple K_μ, l_μ, T_μ for all nodes of a BG for shape λ built from elementary shapes σ requires

$$\mathrm{C}_{\mathrm{pre}} = \mathrm{O}\,(N)\,\mathrm{O}\,(D_\lambda^\sigma) = \mathrm{O}\left(N^{k+1}/k^k\right) = \mathrm{O}\left(N^{k+1}\right) \tag{E.1}$$

steps where we used that the function D_λ^σ counting the number of shapes $\mu \subset \lambda$ obtainable from λ by regular removal of elementary tableaux σ is bounded from above by N^k/k^k (cp. next section).
We see it is only linearly more demanding (in N) than computing the basic branching graph and in particular still *polynomial* (in N).

We do not want to give the algorithm for efficient iteration in full detail, but let us at least describe the main steps, so that the idea becomes clear.
The ingredients are first the array $c[.]$, already known from the naive ansatz above and still needed to keep track of where we descend to from the node $\mu_{c[d]}$ lying at a depth d. Furthermore we introduce a stack K (the backtrack-stack) which will at all times contain the nodes on our current path where we could descend in a different direction, i.e. which have more than one child *and* have not yet been exhausted (i.e. $c[d]$ <#children of node $\mu(c[d])$). Flow control requires only a single 'while'-loop which is repeated as long as K is nonempty.
With these datastructures the iteration process works the following way:

0. assume we enter the loop with $c[.]$ completely filled and a complete extended YT (from initialisation or the previous pass)

i first, retrieve the uppermost element from K (removing it in the process)

ii if this is, say, j, increment $c[j]$ by one, reset $c[i] = 1$ for all $i > j$ and descend to $\mu(c[j+1])$ (the $c[j]+1$ th child of node $\mu(c[j])$)

iii update stack K: if $c[j]$ <#children of $\mu(c[j])$ $\rightarrow$ push j onto K again

iv in any case, push all backtrack positions indicated in $\mu(c[j+1])$ onto K (blue lists in Fig. E.1)

v obtain next extended YT: drop the indices $1, \ldots, N-j$ from the previous one and join remainder with the (incomplete) YT $T_{\mu(c[j+1])}$ that we added to $\mu(c[j+1])$ during the precomputation

Joining two parts of an extended YT can easily be done in O (1): we need only check wether $\mathrm{row}(N-j+1) > \mathrm{row}(N-j)$. If so, we merge the leftmost column of the remainder with the rightmost column of $T_{\mu(c[j+1])}$, if not, we simply concatenate. Strictly speaking this is true only for standard Young tableaux, where the number of boxes $|\sigma|$ in the elementary tableaux is equal to one. If we are considering tableaux with $|\sigma| > 1$, joining requires O ($|\sigma|$) time instead.

We should add, that this algorithm does not depend on the graph having only a single leaf. It will in fact work for any graph, where nodes have a (unique) depth.

In all, the algorithm sketched above needs O (1) (or O ($|\sigma|$) i.g.) steps to generate one path/extended Young tableaux, and thus the full iteration requires O ($|\sigma| N_\lambda$) time and O ($|\sigma| N\, N_\lambda$) memory. The memory requirements are dominated by the size of the resulting list of extended YT, but if we store only the momenta, memory requirment is down to O (N_λ).

E.2 Branching graph size

The time required to generate the basic branching graph for a shape λ built up from N elementary tableaux σ as well as augmenting it in preparation for efficient iteration is determined mostly by its size, i.e. the number of its nodes. This in turn is just D^σ_λ, defined as

$$\begin{aligned} D^\sigma_\lambda = &\#\text{diagrams } \mu \text{ with } \mu \subset \lambda \text{ and } \mu \text{ obtained from} \\ &\lambda \text{ by regular removal of one or more shapes} \sigma \end{aligned} \tag{E.2}$$

Our goal is now to find a good estimate for D^σ_λ.
Defining $D_\lambda := D^{\sigma=(1)}_\lambda$, we can use it as an upper bound on D^σ_λ, as the additional σ-dependent constraints in (E.2) serve only to *decrease* the number μ that are compatible.

But D_λ is easily expressed as the multiple sum

$$D_\lambda = \sum_{j_1 \le \lambda_1} \sum_{j_2 \le \mathrm{Min}(\lambda_2, j_1)} \cdots \sum_{j_k \le \mathrm{Min}(\lambda_k, j_{k-1})} 1 \tag{E.3}$$

where k is the number of rows in λ. This can be estimated from above by forgetting about $\mathrm{Min}(\lambda_i, j_{i-1})$ and bounding j_i just by j_{i-1} instead

$$D_\lambda \le \sum_{0 \le j_k \le j_{k-1} \le \cdots \le j_1 \le \lambda_1} 1 = \begin{pmatrix} \lambda_1 + k \\ \lambda_1 \end{pmatrix} \tag{E.4}$$

Two instances are of particular interest:
(a) $\lambda_1 = N, k = 1$ in which case the estimate gives almost the exact result ($D_\lambda = N$ compared to $\begin{pmatrix} N+1 \\ N \end{pmatrix} = N+1$) and
(b) $\lambda_1 = N/k =: m, k > 1, k|N$ where the above estimate gives the exact result. If $p_{<k;m}(n)$ is the number of integer partitions using at most m summands of size $\le k$ we have

$$D_{(m,\ldots,m)} = \sum_{j=1}^{N} p_{\le k;m}(j)$$

which leads to the same sum as in (E.4), proving that the bound (E.3) is exact and the number of nodes is really given by $(m+k)!/k!m!$.

For many other combinations of N and k (E.3) overestimates the size of the branching graph considerably. Take $\lambda = (N-k+1, 1, \ldots, 1)$ ('hook' shape). Assuming $N-k+1 > k$ the true value is $D_\lambda = (\lambda_1 - 1)^2 + (\lambda_1 - 1)(\lambda_1 - k + 1) \approx 2\lambda_1^2 - k\lambda_1 = \mathrm{O}\left(\lambda_1^2\right)$ independent of k (as long as it remains smaller than λ_1) while (E.3) yields $\mathrm{O}\left(\lambda_1^k\right)$.

It might well be possible to find a tighter bound, but (E.3) suffices for our purposes, as it already shows the polynomial dependance on N.

E.3 Momentum offset b_0

Given a tableaux T built from N elementary tableaux σ we may interpret it as pertaining to the product space $V_\sigma^{\otimes N}$ of any SU(n) where n is at least as large as the number of rows in T. We want to show here, that the momentum assigned to T (or rather its extended version $E(T)$, but they stand in 1-1 relation) via the sum (5.11) is independent of this interpretation, *i.e.*, n.

$$\begin{aligned}\sum_{c\in E(T)} b_c &= \sum_c (n-k_c)(\langle i\rangle_c - \frac{1}{2}) \\ &= n\left(\sum_c \langle i\rangle_c - \frac{1}{2}c_T\right) - \left(\frac{N(N+1)}{2}|\sigma| - \frac{1}{2}N|\sigma|\right) \\ &= n\left(\sum_c \langle i\rangle_c - \frac{1}{2}c_T\right) - \frac{1}{2}|\sigma|N^2\end{aligned}$$

where we defined c_T as the number of columns of $E(T)$ used the relations $c_T = \sum_c 1$, $\sum_c k_c = |\sigma|N$ and $\sum_c k_c \langle i\rangle_c = |\sigma|N(N+1)/2$. As a reminder, k_c is the number of boxes in column c of the extended tableaux $E(T)$ and $|\sigma|N$ is just the total number of boxes in $E(T)$ (and therefore also in T).

We see, that if we add the offset momentum number $b_0 = -(n-1)N^2/2$ we arrive at

$$b_0 + \sum_{c\in E(T)} b_c = n\left(\sum_c \langle i\rangle_c - \frac{1}{2}(c_T + |\sigma|N^2)\right) \tag{E.5}$$

and thus n cancels when computing the momentum $p_T = 2\pi/Nn(\sum_c b_c + b_0)$.

What still needs to be checked is whether the quantity in parenthesis in (E.5) is always an integer. To see that this is indeed the case, we need to analyze the relationship between N, c_T and $\sum_c \langle i\rangle_c$. Since in all columns of $E(T)$, the boxes are in sequence, $\sum_c \langle i\rangle_c$ is always either integer or half-integer. In fact we can express each summand as $\langle i\rangle_c = j_c + (k_c - 1)/2$, where j_c is number in the uppermost box. Therefore, $\langle i\rangle_c$ is half-integer, if and only if there is an

even number of boxes in column c. Now assume $\sum_c \langle i \rangle_c$ is half-integer. This means, we must have an *odd* number of columns with an even number of boxes. If now N is even, there is an even number of boxes left to be distributed over rows with an odd number of boxes in them. This means that this number of (odd-box-number) columns is even. Thus in this case $c_T/2$ is half-integer while $N^2/2$ is integer and in total sum (E.5) is of the form $n\times$integer. It is not hard to see that in the other three cases this holds as well (cp. Tab. E.1).

$\sum_c \langle i \rangle_c$	N	$\Rightarrow$	c_T	total
half-integer	even	$\Rightarrow$	odd	integer
”	odd	$\Rightarrow$	even	”
integer	even	$\Rightarrow$	even	”
”	odd	$\Rightarrow$	odd	”

Table E.1: The four possible parity combinations of $\sum_c \langle i \rangle_c$ and N. All lead to an integer value for the total momentum (E.5).

List of publications

publications

1. B. Scharfenberger, R. Thomale and M. Greiter *Fractional spin liquid hierarchy for spin S antiferromagnets*, arXiv:1105.4348, submitted to Phys. Rev. Lett.

2. B. Scharfenberger and M. Greiter *Momentum classification of SU(n) spin chains with arbitrary symmetric representations in terms of extended Young tableaux*, manuscript in preparation

3. B. Scharfenberger, R. Thomale and M. Greiter *Entanglement spectroscopy of antiferromagnetic states on a cylinder*, manuscript in preparation

conference proceedings

1. S. Rachel, D. Schuricht, B. Scharfenberger, R. Thomale, M. Greiter *Spontaneous Parity Violation in a Quantum Spin Chain*, J. Phys.: Conf. Ser. 200, 022049 (2010)

Bibliography

[1] X. G. Wen. Vacuum degeneracy of chiral spin states in compactified space. *Phys. Rev. B*, 40(10):7387–7390, Oct 1989. doi: 10.1103/PhysRevB.40.7387.

[2] D. C. Tsui, H. L. Stormer, and A. C. Gossard. Two-dimensional magnetotransport in the extreme quantum limit. *Phys. Rev. Lett.*, 48(22):1559–1562, May 1982. doi: 10.1103/PhysRevLett.48.1559.

[3] R. B. Laughlin. Anomalous Quantum Hall Effect: An incompressible quantum fluid with fractionally charged excitations. *Phys. Rev. Lett.*, 50(18):1395, May 1983.

[4] V. Kalmeyer and R. B. Laughlin. Equivalence of the resonating-valence-bond and fractional quantum Hall states. *Phys. Rev. Lett.*, 59(18):2095–2098, 1987.

[5] G. Vidal, J. I. Latorre, E. Rico, and A. Kitaev. Entanglement in quantum critical phenomena. *Phys. Rev. Lett.*, 90(22):227902, Jun 2003. doi: 10.1103/PhysRevLett.90.227902.

[6] Alexei Kitaev and John Preskill. Topological entanglement entropy. *Phys. Rev. Lett.*, 96 (11):110404, Mar 2006. doi: 10.1103/PhysRevLett.96.110404.

[7] Hui Li and F. D. M. Haldane. Entanglement spectrum as a generalization of entanglement entropy: Identification of topological order in non-abelian fractional Quantum Hall Effect states. *Phys. Rev. Lett.*, 101(1):010504, Jul 2008. doi: 10.1103/PhysRevLett.101.010504.

[8] Martin Greiter and Dirk Schuricht. Many-Spinon states and the secret significance of Young Tableaux. *Phys. Rev. Lett.*, 98(23):237202, 2007. doi: 10.1103/PhysRevLett.98.237202.

[9] K. v. Klitzing, G. Dorda, and M. Pepper. New method for high-accuracy determination of the fine-structure constant based on quantized Hall resistance. *Phys. Rev. Lett.*, 45(6): 494–497, Aug 1980. doi: 10.1103/PhysRevLett.45.494.

[10] S. M. Girvin and A. H. MacDonald. Off-diagonal long-range order, oblique confinement, and the fractional quantum Hall effect. *Phys. Rev. Lett.*, 58(12):1252–1255, Mar 1987. doi: 10.1103/PhysRevLett.58.1252.

[11] F. Wilczek. Magnetic flux, angular momentum, and statistics. *Phys. Rev. Lett.*, 48(17): 1144, April 1982.

[12] D. Arovas, J. R. Schrieffer, and F. Wilczek. Fractional Statistics and the Quantum Hall Effect. *Phys. Rev. Lett.*, 53(7):722, August 1984.

[13] Parsa Bonderson, Alexei Kitaev, and Kirill Shtengel. Detecting non-abelian statistics in the $\nu = 5/2$ fractional quantum hall state. *Phys. Rev. Lett.*, 96(1):016803, Jan 2006. doi: 10.1103/PhysRevLett.96.016803.

[14] V. J. Goldman and B. Su. Resonant tunneling in the quantum hall regime: Measurement of fractional charge. *Science*, 267(5200):1010–1012, 1995. doi: 10.1126/science.267.5200.1010.

[15] Moty Heiblum. arXiv:0912.4868.

[16] F. D. M. Haldane and E. H. Rezayi. Periodic Laughlin–Jastrow wave functions for the fractional quantized Hall effect. *Phys. Rev. B*, 31:2529, 1985.

[17] B. I. Halperin. Quantized Hall conductance, current-carrying edge states, and the existence of extended states in a two-dimensional disordered potential. *Phys. Rev. B*, 25(4):2185–2190, Feb 1982. doi: 10.1103/PhysRevB.25.2185.

[18] X. G. Wen. Gapless boundary excitations in the quantum Hall states and in the chiral spin states. *Phys. Rev. B*, 43(13):11025–11036, May 1991. doi: 10.1103/PhysRevB.43.11025.

[19] X. G. Wen and Q. Niu. Ground-state degeneracy of the fractional quantum Hall states in the presence of a random potential and on high-genus Riemann surfaces. *Phys. Rev. B*, 41(13):9377–9396, May 1990. doi: 10.1103/PhysRevB.41.9377.

[20] G. Moore and N. Read. Nonabelions in the fractional Quantum Hall Effect. *Nucl. Phys. B*, 360:362, 1991.

[21] Z Hiroi. *J. Phys. Soc. Jpn.*, 70:3377, 2001.

[22] A. Fukaya, Y. Fudamoto, I. M. Gat, T. Ito, M. I. Larkin, A. T. Savici, Y. J. Uemura, P. P. Kyriakou, G. M. Luke, M. T. Rovers, K. M. Kojima, A. Keren, M. Hanawa, and Z. Hiroi. Muon spin relaxation and susceptibility studies of the pure and diluted spin 1/2 kagomé-like lattice system $(cuxzn1-x)3v2o7(oh2)\ 2h2o$. *Phys. Rev. Lett.*, 91(20):207603, Nov 2003. doi: 10.1103/PhysRevLett.91.207603.

[23] J. Sirker, Zheng Weihong, O. P. Sushkov, and J. Oitmaa. $J1 - J2$ model: First-order phase transition versus deconfinement of spinons. *Phys. Rev. B*, 73(18):184420, May 2006. doi: 10.1103/PhysRevB.73.184420.

[24] Alexei Kitaev. Anyons in an exactly solved model and beyond. *Ann. of Phys.*, 321(1):2, January 2006.

[25] Hong Yao and Steven A. Kivelson. Exact chiral spin liquid with non-abelian anyons. *Phys. Rev. Lett.*, 99(24):247203, Dec 2007. doi: 10.1103/PhysRevLett.99.247203.

[26] N. Read and E. Rezayi. Beyond paired quantum Hall states: Parafermions and incompressible states in the first excited Landau level. *Phys. Rev. B*, 59(12):8084–8092, March 1999. doi: 10.1103/PhysRevB.59.8084.

[27] X.-G. Wen and A. Zee. Topological degeneracy of quantum Hall fluids. *Phys. Rev. B*, 58 (23):15717–15728, Dec 1998. doi: 10.1103/PhysRevB.58.15717.

[28] Michael Levin and Xiao-Gang Wen. Detecting topological order in a ground state wave function. *Phys. Rev. Lett.*, 96(11):110405, Mar 2006. doi: 10.1103/PhysRevLett.96.110405.

[29] R. Thomale, A. Sterdyniak, N. Regnault, and B. Andrei Bernevig. Entanglement gap and a new principle of adiabatic continuity. *Phys. Rev. Lett.*, 104(18):180502, May 2010. doi: 10.1103/PhysRevLett.104.180502.

[30] J. Reuther and P. Woelfle. J1-J2 frustrated two-dimensional Heisenberg model: Random phase approximation and functional renormalisation group. *Phys. Rev. B*, 81:144410, 2010.

[31] W. P. Su, J. R. Schrieffer, and A. J. Heeger. Solitons in Polyacetylene. *Phys. Rev. Lett.*, 42:1698, 1979.

[32] S. C. Zhang, T. H. Hansson, and S. Kivelson. Effective-field-theory model for the fractional Quantum Hall effect. *Phys. Rev. Lett.*, 62(1):82–85, Jan 1989. doi: 10.1103/PhysRevLett.62.82.

[33] X. G. Wen, Frank Wilczek, and A. Zee. Chiral spin states and superconductivity. *Phys. Rev. B*, 39(16):11413–11423, 1989.

[34] C.N. Yang. Concept of off-diagonal long range order and the quantum phases of liquid He and of superconductors. *Rev. Mod. Phys.*, 34(4), 1962.

[35] D. A. Ivanov. Non-Abelian statistics of half-quantum vortices in p-wave superconductors. *Phys. Rev. Lett.*, 86:268, 2001.

[36] N. Read and Dmitry Green. Paired states of fermions in two dimensions with breaking of parity and time-reversal symmetries and the fractional Quantum Hall effect. *Phys. Rev. B*, 61(15):10267–10297, Apr 2000. doi: 10.1103/PhysRevB.61.10267.

[37] Masaki Oshikawa and T. Senthil. Fractionalization, topological order, and quasiparticle statistics. *Phys. Rev. Lett.*, 96(6):060601, Feb 2006. doi: 10.1103/PhysRevLett.96.060601.

[38] Subir Sachdev. Quantum magnetism and criticality. *Nature Physics*, 4:173, Mar 2008.

[39] Cenke Xu and Subir Sachdev. Global phase diagrams of frustrated quantum antiferromagnets in two dimensions: Doubled chern-simons theory. *Phys. Rev. B*, 79(6):064405, Feb 2009. doi: 10.1103/PhysRevB.79.064405.

[40] Michael Hermele, T. Senthil, and Matthew P. A. Fisher. Algebraic spin liquid as the mother of many competing orders. *Phys. Rev. B*, 72(10):104404, Sep 2005. doi: 10.1103/PhysRevB.72.104404.

[41] A. Yu. Kitaev. Fault-tolerant quantum computation by anyons. *Ann. Phys.*, 303:2, 2002.

[42] M. Greiter and F. Wilczek. Exact solutions and the adiabatic heuristic for quantum Hall states. *Nucl. Phys. B*, 370:577, 1992.

[43] W. P. Su. Ground-state degeneracy and fractionally charged excitations in the anomalous quantum Hall effect. *Phys. Rev. B*, 30(2):1069–1072, Jul 1984. doi: 10.1103/PhysRevB.30.1069.

[44] S. A. Trugman and S. Kivelson. Exact results for the fractional quantum Hall effect with general interactions. *Phys. Rev. B*, 31(8):5280–5284, Apr 1985. doi: 10.1103/PhysRevB.31.5280.

[45] X. G. Wen. Chiral luttinger liquid and the edge excitations in the FQH states. *Phys. Rev. B*, 41:12838, 1990.

[46] Xiao-Gang Wen. Topological order and edge structure of $\nu = 1/2$ quantum Hall state. *Phys. Rev. Lett.*, 70(3):355–358, Jan 1993. doi: 10.1103/PhysRevLett.70.355.

[47] R. A. Webb F. P. Milliken, C. P. Umbach. Indications of a Luttinger liquid in the fractional quantum Hall regime. *Solid State Comm.*, 97(4):309, 1995.

[48] A. M. Chang, L. N. Pfeiffer, and K. W. West. Observation of chiral Luttinger behavior in electron tunneling into fractional Quantum Hall edges. *Phys. Rev. Lett.*, 77(12):2538–2541, Sep 1996. doi: 10.1103/PhysRevLett.77.2538.

[49] X. G. Wen. Theory of the edge states in fractional quantum Hall effects. *Int. J.Mod. Phys. B*, 6:1711, 1992.

[50] Andreas M. Läuchli, Emil J. Bergholtz, Juha Suorsa, and Masudul Haque. Disentangling entanglement spectra of fractional quantum Hall states on torus geometries. *Phys. Rev. Lett.*, 104(15):156404, Apr 2010. doi: 10.1103/PhysRevLett.104.156404.

[51] C. L. Kane and E. J. Mele. Quantum spin Hall effect in graphene. *Phys. Rev. Lett.*, 95 (22):226801, Nov 2005. doi: 10.1103/PhysRevLett.95.226801.

[52] B. Andrei Bernevig and Shou-Cheng Zhang. Quantum spin Hall effect. *Phys. Rev. Lett.*, 96(10):106802, Mar 2006. doi: 10.1103/PhysRevLett.96.106802.

[53] Markus Koenig et al. Quantum spin Hall insulator state in hgte quantum wells. *Science*, 318(5851):766, 2007. doi: 10.1126/science.1148047.

[54] Liang Fu and C. L. Kane. Topological insulators with inversion symmetry. *Phys. Rev. B*, 76(4):045302, Jul 2007. doi: 10.1103/PhysRevB.76.045302.

[55] H. Zhang, C.X. Liu, X.L. Qi, X. Dai, F. Zhong, and S.C. Zhang. Topological insulators in Bi_2Se_3,Bi_2Te_3 and Sb_2Te_3 with a single dirac cone on the surface. *Nat. Phys.*, 5:438, May 2009. doi: 10.1038/NPHYS1270.

[56] R. B. Laughlin and Z. Zou. Properties of the chiral-spin-liquid state. *Phys. Rev. B*, 41 (1):664–687, Jan 1990. doi: 10.1103/PhysRevB.41.664.

[57] M. Greiter. S=1 spin liquids: Broken discrete symmetries restored. *J. Low Temp. Phys.*, 126(3/4):1029, February 2002.

[58] Martin Greiter and Ronny Thomale. Non-abelian statistics in a quantum antiferromagnet. *Phys. Rev. Lett.*, 102:207203, 2009.

[59] Eduardo Fradkin, Chetan Nayak, Alexei Tsvelik, and Frank Wilczek. A Chern-Simons effective field theory for the Pfaffian quantum Hall state. *Nuclear Physics B*, 516(3):704 – 718, 1998. ISSN 0550-3213. doi: DOI:10.1016/S0550-3213(98)00111-4. URL `http://www.sciencedirect.com/science/article/pii/S0550321398001114`.

[60] T. H. Hansson, V. Oganesyan, and S. L. Sondhi. Superconductors are topologically ordered. *Ann. Phys.*, 313:497, 2004.

[61] V. E. Korepin. Universality of entropy scaling in one dimensional gapless models. *Phys. Rev. Lett.*, 92(9):096402, Mar 2004. doi: 10.1103/PhysRevLett.92.096402.

[62] Bill Sutherland. Model for a multicomponent quantum system. *Phys. Rev. B*, 12(9): 3795–3805, Nov 1975. doi: 10.1103/PhysRevB.12.3795.

[63] Ian Affleck. Exact critical exponents for Quantum Spin chains, non-linear σ-models at $\theta = \pi$ and the Quantum Hall Effect. *Nucl. Phys. B*, 265:409, 1986.

[64] Ian Affleck, D. P. Arovas, J. B. Marston, and D. A. Rabson. SU($2n$) quantum antiferromagnets with exact C-breaking ground states. *Nuclear Physics B*, 366(3):467 – 506, 1991. ISSN 0550-3213. doi: DOI:10.1016/0550-3213(91)90027-U.

[65] Z. N. C. Ha and F. D. M. Haldane. Squeezed strings and Yangian symmetry of the Heisenberg chain with long-range interaction. *Phys. Rev. B*, 47(19):12459–12469, May 1993. doi: 10.1103/PhysRevB.47.12459.

[66] Martin Greiter, Stephan Rachel, and Dirk Schuricht. Exact results for su(3) spin chains: Trimer states, valence bond solids, and their parent hamiltonians. *Phys. Rev. B*, 75(6): 060401, Feb 2007. doi: 10.1103/PhysRevB.75.060401.

[67] Daniel P. Arovas. Simplex solid states of $SU(N)$ quantum antiferromagnets. *Phys. Rev. B*, 77(10):104404, Mar 2008. doi: 10.1103/PhysRevB.77.104404.

[68] U. Schollwöck. The density-matrix renormalization group. *Rev. Mod. Phys.*, 77(1):259–315, Apr 2005. doi: 10.1103/RevModPhys.77.259.

[69] Paulo H. Acioli. Review of quantum Monte Carlo methods and their applications. *Journal of Molecular Structure: THEOCHEM*, 394(2-3):75 – 85, 1997. ISSN 0166-1280. doi: DOI:10.1016/S0166-1280(96)04821-X. Proceedings of the Eighth Brazilian Symposium of Theoretical Chemistry.

[70] Rodney Bartlett. Many-body perturbation theory and Coupled Cluster theory for electron correlations in molecules. *Ann. Rev. Chem. Phys*, 32:359, 1981.

[71] I.M. Gelfand and M.L. Tsetlin. *Doklady Akad. Nauk SSSR*, 71:825,1017, 1950.

[72] G.E. Baird and L.C. Biedenharn. On the representation of the semisimple Lie groups II. *J.Math.Phys.*, 4(12):1449, 1963.

[73] J. Paldus. Group theoretical approach to the configuration interaction and perturbation theory calculations for atomic and molecular systems. *J.Chem.Phys.*, 61(12):5321, 1974.

[74] S. Rettrup. Direct evaluation of elements of the representation matrices of the spin permutation group for transpositions. *Chem.Phys.Lett*, 47:59, 1977.

[75] P.J. Ruttink. On the evaluation of CI matrix elements for a canonically ordered basis. *Theor.Chem. Acta*, 49:223, 1978.

[76] J. Paldus and P.E.S. Wormer. Configuration interaction matrix elements. II. Graphical approach to the relationship between unitary group generators and permutations. *Int. J. Quantum Chem.*, 16(6):1321–1335, 1980.

[77] S. Rettrup. Direct evaluation of spin representation matrices and ordering of permutation-group elements. *Int. J. Quantum Chem.*, 29(1):119–128, 1986.

[78] W. Wu and Q. Zhang. The orthogonal and the natural representation for symmetric groups. *Int. J. Quant. Chem.*, 25:3737–3747, 1992.

[79] P.A.M. Dirac. Quantum mechanics of many-electron systems. *Proc.R.Soc.A*, 123:714, 1929.

[80] T. Yamanouchi. *Proc. Phys. Math. Soc. Jpn.*, 19:436, 1937.

[81] T. Yamanouchi. *Proc. Phys. Math. Soc. Jpn.*, 20:547, 1938.

[82] E. Schrödinger. Exchange and Spin. *Proc.R.Irish Acad. A*, 47:39, 1941.

[83] Alfred Young. On quantitative substitutional analysis. *Proc. London Math. Soc.*, 33: 97–146, 1900.

[84] Issai Schur. über die rationalen Darstellungen der allgemeinen linearen Gruppe. In *Sitzungsberichte Akad. Berlin*, pages 58–75, 1927.

[85] Hermann Weyl. *The Classical Groups. Their Invariants and Representations.* Princeton mathematical series ;. Princeton University Press, Princeton, N.J., 1939.

[86] F.D.M. Haldane. Exact Jastrow-Gutzwiller resonant-valence-bond ground state of the spin-1/2 antiferromagnetic Heisenberg chain with $1/r^2$ exchange. *Phys.Rev.Lett.*, 60:1529, 1988.

[87] B.S. Shastry. Exact solution of an S=1/2 Heisenberg antiferromagnetic chain with long-ranged interactions. *Phys.Rev.Lett.*, 60:639, 1988.

[88] A. M. Perelomov. On the completeness of a system of coherent states. *Theoret. Math. Phys.*, 6:156, 1971.

[89] Vadim Kalmeyer and R. B. Laughlin. Theory of the spin liquid state of the Heisenberg antiferromagnet. *Phys. Rev. B*, 39(16):11879, 1989.

[90] Issai Schur. über die Darstellung der symmetrischen und der alternierenden Gruppe durch gebrochene lineare Substitutionen. *Journal. f. die reine u. angewandte Mathematik*, 139: 155–250, 1911.

[91] Morton Hamermesh. *Group theory and its application to physical problems.* Dover books on physics. Dover, New York, NY, 1. publ. edition, 1989.

[92] H. Boerner. *Representations of groups.* Holland, Amsterdam, 1963.

[93] L.C. Biedenharn. On the representation of the semisimple Lie groups. I. The explicit construction of invariants for the unimodular unitary group in n dimensions. *J.Math.Phys.*, 4(3):436, 1963.